

UNDERSTANDING AND DESIGNING HYDROCOLLOID PARTICLES FOR THE STABILISATION OF FOAMS: A MICROSTRUCTURAL APPROACH

Amy Louise Ellis

A thesis submitted to
The University of Birmingham
for the degree of
DOCTOR OF PHILOSOPHY

School of Chemical Engineering
College of Engineering and Physical Sciences
The University of Birmingham
2019

UNIVERSITY OF
BIRMINGHAM

University of Birmingham Research Archive

e-theses repository

This unpublished thesis/dissertation is copyright of the author and/or third parties. The intellectual property rights of the author or third parties in respect of this work are as defined by The Copyright Designs and Patents Act 1988 or as modified by any successor legislation.

Any use made of information contained in this thesis/dissertation must be in accordance with that legislation and must be properly acknowledged. Further distribution or reproduction in any format is prohibited without the permission of the copyright holder.

Abstract

Consumer and Government awareness of obesity related illnesses has progressively increased over the past decade. This has directed the focus of research in the food industry towards healthier product formulations. Aerated products, in particular, are gaining attention, these are often high in fat content as oil droplets provide structural stability as well as desirable sensory attributes. Suspensions of microgel particles, known as fluid gels, have shown promising behaviour in the search for fat replacements as their structures can be designed to mimic those of the fat droplets they are replacing. However, their behaviour when aerated has not yet been explored. Therefore, the ultimate goal of this research is to develop and apply hydrocolloid fluid gel technology to create fat-free aerated products.

The focus of this thesis is directed towards gaining an understanding, on a microstructural level, of the performance of fluid gels in foams, with the aim of designing stable edible foams. Firstly, fluid gel/surfactant systems were characterised and aerated, with a relationship determined between particle microstructure and foam properties. Once aerated, the confinement of particles in foam channels provided localised plugs to drainage. The high volume fraction of particles and their ability to interact resulted in the continuous phase behaving as a network of particles with a finite yield stress. Foam half-life was ultimately dependent upon this; stability considerably increased as the yield stress became larger than the gravitational stress acting inside the foam channels. Yield stress was manipulated by changing the concentration of agar, which increased both the fluid gel particle modulus and volume fraction.

This concept was further explored by changing the microstructure through sugar addition. The change in solvent availability affected fluid gel gelation and, subsequently, particle size and material properties. As previously observed in this thesis, foam half-life was ultimately dependent upon fluid gel yield stress. However, at low particle phase volumes, particle size began to directly influence liquid drainage.

In the final chapter, the potential to surface activate kappa carrageenan fluid gel particles was explored. The hydrophobicity of particles was modified by electrostatically binding an ionic surfactant, lauric arginate, onto their surface. Particles subsequently adsorbed at the a/w interface providing enhanced foam stability. The rate of disproportionation and liquid drainage in foams was lowest when an intermediate concentration of surfactant was used, a result of optimum adsorption to bubble interfaces. At high concentrations of surfactant, large aggregates formed which were unable to adsorb to the interface. This modification of kappa carrageenan particles provides a much more versatile ingredient for food microstructure design.

Acknowledgements

Firstly, I would like to thank my supervisor, Prof. Ian Norton, for providing me with this opportunity. I thank Ian for all his supervision and supporting me throughout my PhD, whilst continually challenging me to develop my skills as a researcher. I would also like to express thanks to my supervisor, Dr. Tom Mills, for his continual support, guidance and enthusiasm for trips to America over the past three years. Finally, thank you to my supervisor, Dr. Abigail Norton-Welch, who's guidance and encouragement throughout my PhD has been instrumental.

I thankfully acknowledge the financial support from the EPSRC and Rich Products Corporation, as well as their permission to publish research articles and this thesis. I am very grateful of the support given to me by those at Rich Products Corporation. In particular, my thanks goes to Mike Piatko and Shawn Campbell for the many useful discussions over the past three years and to all those who helped me in the laboratory during my visits to Buffalo. I always felt so welcome when visiting and have so many great memories of my time there. With this, I'd like to give a special thanks to Mike Piatko, whose passion and enthusiasm for research I will always remember.

I have been fortunate enough to be surrounded by a network of excellent scientists during my time in the microstructure research group, whose expertise and assistance have helped contribute to the success of my research. I am grateful to all of you, in particular, a special thanks goes to Dr. Aris Lazidis for all his help and motivation. I thank my friends at the University of Birmingham for sharing all the joyful, as well as tough, moments of my PhD. I've also been lucky enough to have amazing housemates who made sure there was

never a dull moment. Thank you to all of you for giving me so many happy memories that I will treasure forever.

Last but not least, I would like to thank my family; I can't thank them enough for their continual love and support, as well as always being on hand with a fun distraction. Finally, thank you to Harry for all the adventures we've shared over the past three years and for your constant encouragement and belief in me.

Table of Contents

Abstract i
Acknowledgements iii
Table of Contents v
List of Figures ix
List of Tables xiv
Nomenclature xv
Chapter 1: INTRODUCTION 1
1.1 Context for this study 2
1.2 Relevance to Rich Products Corporation 4
1.3 Objectives 5
1.4 Thesis layout 6
1.5 Publications and presentations 8
1.5.1 Publications 8
1.5.2 Presentations 8
Chapter 2: LITERATURE REVIEW 9
2.1 Introduction 10
2.2 Food hydrocolloids 11
2.2.1 Agar 14
2.2.2 Carrageenan 15
2.3 Fluid gels 18
2.3.1 Fluid gel formation 19
2.3.2 Effect of hydrocolloid concentration 21
2.3.3 Fluid gel particle-particle interactions 23
2.4 Foams 25
2.4.1 Foam structure 25
2.4.2 Methods of foam formation 27
2.4.3 Surfactants 30
2.4.4 Foam (in)stability 31
2.4.4.1 Liquid drainage 32
2.4.4.2 Disproportionation 33
2.4.4.3 Coalescence 35
2.4.5 Particle stabilisation of foams 36
2.4.5.1 Hydrophobic particles 36

2.4.5.2 Biopolymers in foams 40
2.4.5.3 Hydrophilic particles 41
2.4.5.3.1 Hydrophobic modification of hydrophilic particles 43
2.4.5.4 Microgels at the a/w interface 45
Chapter 3: AGAR FLUID GELS AND THE STABILISATION OF THEIR FOAMS 59
3.1 Background 60
3.2 Materials and Methods 61
3.2.1 Materials 61
3.2.2 Preparation of agar fluid gels using a rheometer 61
3.2.3 Preparation of agar fluid gels using pin stirrer 61
3.2.4 Preparation of foams and determination of foam overrun 62
3.2.5 Determination of foam half-life 62
3.2.6 Rheological methods 63
3.2.7 Surface tension measurements 63
3.2.8 Imaging fluid gel particles 63
3.2.9 Texture Analysis 64
3.2.10 Micro Computed Tomography (Micro-CT) 64
3.3 Results and Discussion 65
3.3.1 Preparation and characterisation of agar fluid gels 65
3.3.2 Rheological properties 70
3.3.3 Foaming capabilities 74
3.3.4 Foam stability mechanism 75
3.3.5 Fluid gel thixotropy 79
3.3.6 Effect of pin stirrer exit temperature 82
3.4 Conclusions 89
Chapter 4: THE EFFECT OF SUGARS ON AGAR FLUID GELS AND THE STABILISATION OF THEIR FOAMS 94
4.1 Background 95
4.2 Experimental 96
4.2.1 Materials 96
4.2.2 Preparation of agar fluid gels using pin stirrer 96
4.2.3 Preparation of agar fluid gels using a rheometer 96
4.2.4 Optical microscopy 97
4.2.5 Texture analysis of quiescent agar gels 97
4.2.6 Bulk rheology 97
4.2.7 Aeration 98

4.2.8 Foam liquid drainage measurements 98
4.3 Results and Discussion 99
4.3.1 Effect of sugar on gelation 99
4.3.2 Effect of sugar on microstructure 103
4.3.3 Effect of sugar on quiescent agar gels 108
4.3.4 Bulk rheological properties 110
4.3.5 Foam capabilities and stability 114
4.3.6 Effect of particle size on foam drainage 116
4.4 Conclusions 122
Chapter 5: THE HYDROPHOBIC MODIFICATION OF KAPPA CARRAGEENAN MICROGEL PARTICLES FOR THE STABILISATION OF FOAMS 127
5.1 Background 128
5.2 Materials and methods 129
5.2.1 Materials 129
5.2.2 Preparation of fluid gel 129
5.2.3 Preparation of κC fluid gel-LA complexes 129
5.2.4 Zeta potential measurements 129
5.2.5 Turbidity measurements 130
5.2.6 Rheology 130
5.2.7 Surface tension 130
5.2.8 Aeration 131
5.2.9 Liquid drainage and foam structure measurements 131
5.2.10 Optical microscopy 132
5.2.11 Confocal microscopy 132
5.3 Results and Discussion 133
5.3.1 Production and characterisation of kappa carrageenan fluid gels 133
5.3.2 Complex formation through surfactant binding 136
5.3.3 Surface activity 142
5.3.4 Aeration of surface-activated κC fluid gels 143
5.3.5 Foam stability mechanism 147
5.3.6 κC fluid gels with non-ionic surfactant 153
5.4 Conclusions 155
Chapter 6: CONCLUSIONS AND FUTURE RECOMMENDATIONS 160
6.1 Conclusions 161
6.1.1 The formation and aeration of agar/Tween20 fluid gels 161
6.1.2 Understanding the addition of sugar in agar/Tween 20 fluid gels 162

6.1.3 The hydrophobic modification of kappa carrageenan fluid gel particles 163
6.2 Recommendations for future work 164

List of Figures

Figure 1.0.1: Schematic representation of the microstructural approach to food formulation engineering. *4*

Figure 2.1: Schematic representation of the viscosity dependence of polysaccharide solutions at dilute and concentrated regions. Image adapted from Clegg (1995). *12*

Figure 2.2: Comparison of the textures exhibited from a range of hydrocolloid gels. Image adapted from Phillips and Williams (2009). *13*

Figure 2.3: The chemical structure of agarose: a linear polymer composed of repeating units of agarobiose. Image adapted from Araki (1956) and Fernández Farrés (2015). *14*

Figure 2.4: The gelation mechanism of agarose; upon cooling of random agarose coils in solution (A), symmetric and antisymmetric double helices form (B_1 and B_2), which aggregate together to give the structures in C and then D. Image from Medin (1996). *15*

Figure 2.5: The gelation mechanism of κ-carrageenan. Upon cooling a hot solution of κ-carrageenan, random coils undergo a coil-to-helix conformational transition. Double helices form which then aggregate together in the presence of cations to form the final gel structure. Figure adapted from Alba and Kontogiorgos (2015). *17*

Figure 2.6: A gellan gel formed under quiescent conditions (left) and under shear to form a fluid gel (right). Image from Norton (2016). *19*

Figure 2.7: Viscosity as a function of temperature during fluid gel production, at various shear rates. A constant cooling rate of 0.5 °Cmin^{-1} was used for all fluid gels. Image from Gabriele et al. (2009). *21*

Figure 2.8: Yield stress dependence on pin stirrer exit temperature for fluid gels at 0.5%, 1% and 2% κC. Samples were tested as initial fluid gels (open symbols) and 24 h after shearing (closed symbols). Linear fits are shown with equal fits for each series. Figure from Garrec (2013). *24*

Figure 2.9: A photograph of the bubbles comprising an aqueous foams. Bubbles lower down the foam are spherical whereas towards the top, the foam is drier and bubbles are more polyhedral in shape. Image adapted from Larson (1999). *27*

Figure 2.10: Images of bubbles created by different foaming techniques. Image adapted from Weaire (1999). *28*

Figure 2.11: An example of surfactant behaviour at an air/water interface at a concentration above the surfactant CMC. Free monomers and micelles reside in the bulk solution, whilst an adsorbed monolayer of surfactant molecules assembles at the interface. *30*

Figure 2.12: Liquid drainage through a Plateau border. Gravity and capillary forces causes thinning of the films, whilst the Gibbs-Marangoni effect acts to reduce this. *33*

Figure 2.13: (Above) positioning of a particle at a planar gas/water interface with a contact angle of <90° (left), =90° (middle) and >90° (right). (Below) positioning of particles at the curved interface; particles with a contact angle of <90° (left) reside largely in the aqueous phase, whilst those with a contact angle of >90° (right) remain largely in the gas phase. Image adapted from Binks (2002). *38*

Figure 2.14: A representation of the two mechanisms of foam stabilisation available to biopolymer particles, along with the pathways for protein and polysaccharides to reach them based on their surface activity. Image from Ellis and Lazidis (2018). *41*

Figure 2.15: (Left) normalised liquid fraction (ε') as a function of time at a fixed position inside the foam, for SDS foams at various concentrations of laponite particles (c_L). At c_L = 16 g/L, the times t_l and t_u are indicated. (Right) yield stress as a function of time for two laponite concentrations and two values of gap height between rheometer plates (mimicking confinement). Image adapted from Guillermic et al. (2009). *43*

Figure 3.1: Viscosity profiles during fluid gel production at different agar concentrations. *66*

Figure 3.2: Micrographs of 1% agar with Tween 20 fluid gels produced in (a) a rheometer with vane geometry and (b) in a pin stirrer, using phase contrast microscopy. *69*

Figure 3.3: Storage modulus (G') as a function of stress during oscillatory strain sweeps of agar fluid gels produced on both the rheometer and pin stirrer, 48 hours after production. Yield stress was calculated as the stress required to decrease G' from the LVR by 5%. *70*

Figure 3.4: Viscosity profiles of agar fluid gels produced at different concentrations, 48 hours after production. The viscosity curves of 2.5% and 3% agar overlap and are therefore highlighted for clarity. *71*

Figure 3.5: (a) Storage (G') and loss (G'') moduli as a function of applied oscillatory strain of agar fluid gels, 48 hours after production. (b) Storage modulus as a function of stress during oscillatory strain sweeps of agar fluid gels, 48 hours after production. *73*

Figure 3.6: Foam half-life measurements as a function of agar concentration of aerated agar fluid gels with 0.5% Tween 20. ..... *75*

Figure 3.7: Yield stresses of agar fluid gels as a function of half-life measurements of their foams. *77*

Figure 3.8: Micro-CT images of aerated 3% agar with Tween 20 fluid gels (a) 30 min after aeration and (b) 6 days after aeration. (c) Still of a video showing the microstructure of aerated 1% agar fluid gel and the plugging of particles in foam channels, observed using phase contrast microscopy. *78*

Figure 3.9: Thixotropic loop tests conducted on an agar fluid gel (1.5% agar) and a weak quiescently set gel (0.3% agar). Shear stress was plotted as a function of shear rate. Shear rate was increased from 0.1 s^{-1} to 500 s^{-1} (forward curves unfilled symbols) and decreased backwards (filled symbols) with no hold. 81

Figure 3.10: Storage modulus as a function of stress during oscillatory strain sweeps of 3% agar with 0.5% Tween 20 fluid gels produced at different pin stirrer exit temperatures, 48 hours after production. 85

Figure 3.11: Thixotropic loop tests conducted on 3% agar with 0.5% Tween 20 fluid gels produced at different pin stirrer exit temperatures. Shear stress was plotted as a function of shear rate. Shear rate was increased from 0.1 s^{-1} to 500 s^{-1} (forward curves unfilled symbols) and decreased backwards (filled symbols) with no hold. 86

Figure 3.12: Micrographs of 3% agar with 0.5% Tween 20 fluid gels produced at different pin stirrer exit temperatures (a) 5 °C, (b) 12.5 °C and (c) 20 °C, using phase contrast microscopy. 87

Figure 4.1: Viscosity profiles during fluid gel preparation of 1% agar fluid gels + 0.5% Tween 20 with 0% (square), 20% (circle), 40% (triangle up) and 60% (triangle down) of (a) glucose, (b) fructose and (c) sucrose. The temperature was decreased from 70 °C to 5 °C at a cooling rate of 2 °C min^{-1}, under a fixed applied shear of 500 s^{-1}. The inset graphs focus on the region between 20 °C and 40 °C for the three lower concentrations of sugar, where viscosity was normalised at 40 °C. This allows the ordering transition and its onset temperature to be observed more clearly. 103

Figure 4.2: Overlapping histograms showing particle size distributions for 1% agar fluid gels + 0.5% Tween 20 with 0%, 20%, 40% and 60% of (a) glucose, (b) fructose and (c) sucrose. Measured from micrographs using ImageJ software. 107

Figure 4.3: Optical micrographs of diluted 1% agar fluid gels + 0.5% Tween 20 with 0% (a), 20% (b), 40% (c) and 60% (d) sucrose, using phase contrast microscopy. 108

Figure 4.4: Initial Young's modulus of quiescently set 1% agar gels + 0.5% Tween 20 when compressed to 50% strain at a rate of 1 mms^{-1} as a function of sugar concentration. This reflects fluid gel particle stiffness. Measurements were conducted at 25 °C. 110

Figure 4.5: Rheological measurements of 1% agar + 0.5% Tween 20 fluid gels as a function of sugar concentration (glucose, fructose and sucrose). (a) shear viscosity at a shear rate of 1 s^{-1} measured from a flow curve (0.1 s^{-1} to 500 s^{-1}) and (b) storage modulus (G') from the LVR region of a strain controlled amplitude sweep. Measurements were carried out using a serrated parallel plate 48 h after production at 25 °C. 112

Figure 4.6: Yield stress of 1% agar + 0.5% Tween 20 fluid gels as a function of sugar concentration. Yield stress was measured as a 5% decrease in G' during an amplitude sweep conducted 48 h after production at 25 °C. 114

Figure 4.7: Foam half-life as a function of agar fluid gel yield stress for 1% agar + 0.5% Tween 20 with glucose, fructose and sucrose at various concentrations. The concentration of sugar to which each data point corresponds to can be determined from Figure 4.6. 116

Figure 4.8: Optical micrographs and corresponding particle size distributions for 1% agar fluid gels with 0.5% Tween 20 and 20% sucrose added post-production (a) and pre-production (b). 118

Figure 4.9: Liquid drainage profiles of aerated 1% agar + 0.5% Tween 20 fluid gels with 20% sucrose added pre-production (unfilled symbols) and post-production (filled symbols). Liquid content is shown over 12 h from initial foaming at sensor 3 in the column (positioned half way down the foam). Every 4th data point is sampled for clarity. 121

Figure 5.1: Schematic of foam column and electrodes of the Krüss DFA100LCM..... 132

Figure 5.2: Viscosity profiles during the production of a 1% kappa carrageenan fluid gel with different concentrations of LA. The temperature was lowered from 70 °C to 5 °C at a cooling rate of 2 °Cmin^{-1}, under an applied shear rate of 500 s^{-1}. 134

Figure 5.3: (Above) the interaction between lauric arginate and ideal κC fluid gel particles (formed in the presence of sufficient K^+ ions for complete gelation). (Below) the formation of a κC:LA aggregated system due to insufficient K^+ ions available during gelation...... 135

Figure 5.4: (a) Confocal micrograph of diluted 1 wt% κC fluid gel particles at natural pH (6.8) dyed with rhodamine B. (b) Zeta potential measurements of diluted 1 wt% κC fluid gel (▫) over a pH range and of LA at natural pH (■). 136

Figure 5.5: Zeta potential measurements of κC fluid gel particles as a function of increasing LA concentration. Concentration is calculated as wt% of the total solution. 138

Figure 5.6: (a) Photographs of κC + LA fluid gels at various LA concentrations. (b) Absorbance of the same solutions, measured using a UV-Vis spectrophotometer. 139

Figure 5.7: (a) Shear viscosity of 1 wt% κC fluid gel mixed with LA at 0.025% (▫), 0.05% (○), 0.075% (△), 0.1% (▽), 0.15% (◇) and 0.2% (×). (b) Storage modulus (▫) and loss modulus (■) of 1 wt% κC fluid gel mixed with LA as a function of LA concentration. 141

Figure 5.8: Surface tension measurements as a function of LA for pure LA solutions (□) and κC-LA complexes (■)...... 143

Figure 5.9: (a) Foam air fraction measurements for aerated κC-LA complexes (■) and pure LA solutions (□), as a function of LA concentration. Arrow indicates the CMC of LA. (b) Foam half-life measurements for aerated κC-LA complexes (■) and pure LA solutions (□), as a function of LA concentration. 146

Figure 5.10: (a) Optical micrograph of aerated 0.2% LA solution. (b) optical micrograph of aerated 1 wt% κC + 0.075% LA fluid gel complexes. (c) Optical

micrograph of aerated 1 wt% κC + 0.075% LA fluid gel complexes at a higher magnification. (d) Confocal micrograph of aerated 1 wt% κC + 0.075% LA fluid gel complexes dyed with rhodamine B. 148

Figure 5.11: (a) Mean bubble area of aerated κC-LA complexes as a function of time after aeration, LA concentrations of 0.025% (—◆—), 0.05% (—●—), 0.075% (—▲—), 0.1% (—▼—) and 0.15% (—■—). (b) Fraction of liquid content remaining 4 h after aeration in aerated κC-LA complexes as a function of LA concentration. Measurements were recorded at sensor 3 in a Krüss foam column (positioned half way down the foam)..... 152

Figure 5.12: (a) Foam air fraction measurements and (b) foam half-life measurements for 1 wt% κC + Tween 20 fluid gel complexes (■) and pure Tween 20 solutions (□), as a function of Tween 20 concentration. Arrow in (a) indicates the CMC of Tween 20. (b) Inset is an optical micrograph of aerated 1 wt% κC + 0.075% Tween 20 fluid gel. 154

List of Tables

Table 2.1: Fluid gel volume fraction and particle modulus as a function of κC concentration. Figure adapted from Garrec (2013). *22*

Table 2.2: Solubility mole fractions of commonly used gases in aeration at equilibrium (at 20 °C and atmospheric pressure). Data from Gevantman (2000)..... *35*

Table 3.1: The effect of Tween 20 addition on the gelation temperatures and material properties upon storage of fluid gels at different agar concentrations. Initial Young's modulus was measured from quiescently set gels. *67*

Table 3.2: Surface tension and foam overrun measurements of agar fluid gels with 0.5% Tween 20 at various agar concentrations. *74*

Table 3.3: Hysteresis loop area and yield stress values determined from model-fitting thixotropic loops shown in Figure 3.9. The correlation coefficients were ≥ 0.9997. ..... *82*

Table 3.4: Rheological data determined from Figure 3.10 and 3.11 (G' and yield stress from amplitude sweeps and hysteresis loop area from thixotropic tests) of agar fluid gels produced at different pin stirrer exit temperatures, together with their foam half-life measurements. *84*

Table 4.1: Viscosity of glucose, fructose and sucrose solutions at 70 °C of concentrations 10-60 wt%. Figure adapted from Telis et al. (2007)..... *104*

Table 4.2: Properties of 1% agar + 0.5% Tween 20 fluid gels with sucrose added pre- and post-production, as well as their properties once aerated. *119*

Nomenclature

C*	Critical concentration
G’	Elastic or storage modulus
G’’	Viscous or loss modulus
κC	Kappa carrageenan
T_{exit}	Pin stirrer exit temperature
T_m	Transition midpoint temperature
CMC	Critical micelle concentration
LMW	Low molecular weight
a/w	Air/water
γ	Surface tension
θ	Contact angle
γ_{pa}	Particle/air surface energy
γ_{pw}	Particle/water surface energy
γ_{aw}	Air/water surface energy
E	Interfacial elasticity
Ψ_p	Volume fraction of particles
λ	Confinement parameter
SDS	Sodium dodecyl sulfate
TTAB	Tetradecyltrimethylammonium bromide
CAPB	Cocamidopropyl betaine
LA	Lauric arginate
GRAS	Generally regarded as safe
$m_{fluidgel}$	Mass of fluid gel
m_{foam}	Mass of foam
LVR	Linear viscoelastic region
p	Fluid density
g	Gravity
d	Bubble radius
σ_y	Yield stress

n(e-OH)	Number of equatorial hydroxyl groups
MBA	Mean bubble area
t_A	Time for adsorption
t_{CR}	Time for interface creation

Chapter 1: INTRODUCTION

1.1 Context for this study

Bubbles are a food ingredient associated with indulgence and luxury; this has led to their use in a wide range of products, from aerated chocolate to vegan meringue. Increasing our understanding of their formation and evolution provides a versatile method for food microstructure engineering. Furthermore, their presence delivers a positive sensory experience to the consumer; examples include the incorporation of air to deliver creaminess in products such as whipped cream and mousses and the carbonation of soft drinks to provide the desired "fizziness". As well as providing a sophisticated mouthfeel, the addition of air has been recognised as a strategy to help control eating habits through improving satiation (the ability to control food intake); increasing the volume of food whilst maintaining the energetic content imparts a greater sense of fullness upon the consumer (Arboleya et al., 2014).

However, foams are thermodynamically unstable systems with structures that evolve over time through three main instability mechanisms (Weaire & Hutzler, 2001); typically, liquid drainage and disproportionation act synergistically to cause the coalescence of air cells and the ultimate collapse of the foam (Saint-Jalmes, 2006). In order to control foam stability and reduce the effects of these three pathways, the air/water interface requires stabilisation. In many aerated emulsions, such as whipped dairy cream and dessert toppings, this is done through the adsorption of a layer of partially crystalline fat droplets, termed Pickering stabilisation (Rousseau, 2000). The effectiveness of the adsorbed layer is heightened under conditions which enable particle aggregation, leading to the formation of a partial network throughout the continuous phase (Dickinson et al., 2004; Dickinson et al., 2002; Du et al., 2003). However, diets high in fat, especially the saturated

kind, can lead to high cholesterol and increase the risk of heart disease (NHS, 2018). Consequently, there has been Government and consumer pressure to reduce the levels of fat in food products.

The ability of hydrocolloids to structure water has often been utilised in fat replacement techniques in the food industry. For example, xanthan gum has been used as polymeric thickener in mayonnaise products (Katzbauer, 1998), whilst phase separated mixtures of maltodextrin and gelatin are used in low-fat spreads (Chronakis & Kasapis, 1995). The development of fluid gels has increased this functionality. A fluid gel is defined as a suspension of gelled particles dispersed in a non-gelled continuous phase (Norton, Foster, & Brown, 1998) and their structures can be designed to fulfil a range of structural requirements (Fernández Farrés, Moakes, & Norton, 2014). For example, they have the potential to replace a significant proportion of fat in emulsion based foods when designed to mimic the structural characteristics of the oil droplets (Norton & Norton, 2010). Furthermore, as many hydrocolloids can be classified as vegan, utilising fluid gel technology when designing these reduced fat systems is of high interest to the food industry as the demand for vegan products mounts (Mori, 2016).

In order to design products with new ingredients, the microstructural approach to food formulation engineering is typically applied. This pathway, represented schematically in Figure 1.0.1, recognises that the consumer response to a product is largely a function of its material properties. These properties are dependent upon its microstructure, which are determined from the ingredients and processing conditions used. This approach helps to bridge the gap between fundamental science and industrial application.

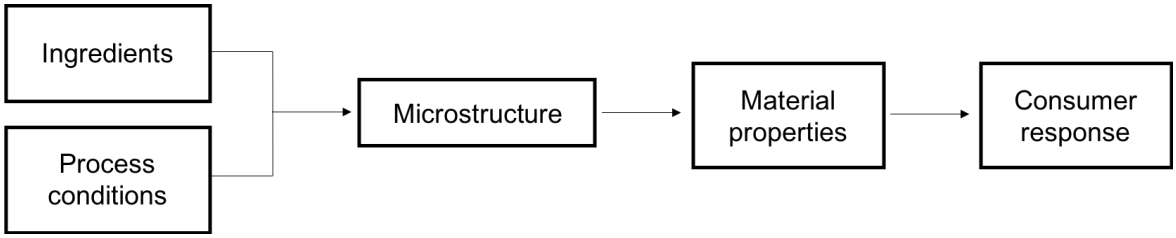


Figure 1.0.1: Schematic representation of the microstructural approach to food formulation engineering.

1.2 Relevance to Rich Products Corporation

Rich Products Corporation, the industrial collaborator in this study, is a privately held, multinational food products business headquartered in Buffalo, New York, USA. The company was founded in 1945 from the development of the world's first non-dairy whipped topping based on soybean oil. They are now a leading global supplier to the foodservice, in-store bakery, retail and industrial marketplaces, employing more than 10,000 associates worldwide. Over 4000 products across categories such as bakery, cooking creams and significant to this project, toppings and icings, are sold across 100 countries.

One of Rich Products Corporation's key products, whipped toppings, are often high in fat and sugar content. Fat delivers desirable sensory attributes and mouthfeel (Drewnowski, 1997), as well as the stabilisation of the air cells (Allen, Murray, & Dickinson, 2008) and sugar provides taste, texture and structure (Coultate, 2009). However, there has been recent Government and consequently consumer pressure to reduce the fat and sugar content in foods. As stated in Section 1.1, diets high in fat can increase cholesterol levels and the risk of heart disease (NHS, 2018), whilst a high sugar diet can cause obesity, which can lead to heart disease and type 2 diabetes (NHS, 2017). Therefore, in order to allow the continued consumption of foods such as these, the levels of fat and sugar need to be lowered. However, low-fat alternative products are often not well received by

consumers, due to a noticeable difference in mouthfeel. This highlights the importance of the relationship between ingredients, microstructure, material properties and the ultimate consumer response of a product, as shown in Figure 1.1. It has been reported that hydrocolloid fluid gels can be tailored to mimic fat droplets in emulsion based foods (Norton & Norton, 2010). For this reason, the aeration of fluid gels and the characterisation of their properties will be explored in this thesis. A strong focus is placed on improving the stabilisation of foams using fluid gel particles as a reasonably long life-time is required for this type of product e.g. its structure needs to be upheld when on top of a cake. In addition, this can prove a useful tool for scientists in other fields, as well as in the food industry, looking to engineer stabilised foams with novel ingredients. The effect of sugar on the microstructure of the system will also be investigated to provide an understanding of its influence on the final material properties. At the end of this study, the preparation of hydrocolloid fluid gels was successfully scaled-up to pilot plant scale at Rich Products Corporation, Buffalo and their potential commercialisation as a fat-free product is currently being explored.

1.3 Objectives

The ultimate goal of this research is to develop and apply hydrocolloid fluid gel technology to create fat-free aerated products. The focus is directed towards gaining understanding, on a microstructural level, of the performance of fluid gels in foams. As this project is industrially sponsored, the objectives of the company must be considered. For example, the hydrocolloids studied are non-animal based, to allow the potential commercialisation of a vegan product. The hydrocolloid investigated most intensively is agar. This is because of its unique gelling hysteresis, allowing fluid gels to be further

processed during manufacturing e.g. pasteurisation. In order to address the main scope of this research, the key research objectives are:

- To expand the knowledge and understanding of the effect that processing conditions have upon fluid gel material properties.
- To investigate and characterise the behaviour of hydrocolloid fluid gels mixed with a non-ionic surfactant (Tween 20) when aerated, and in particular to correlate their properties before aeration e.g. rheology, particle confirmation and after aeration e.g. foam ability and stability.
- To describe the effect that sugar has upon both the fluid gel and foam microstructure.
- To determine the foam stabilisation pathway and use this knowledge to improve the functionality of the particles e.g. by modifying their surface activity to improve stability.

1.4 Thesis layout

This thesis follows the alternative thesis format of the University of Birmingham where results chapters (Chapters 3-5) are presented in a form that is published in peer-reviewed journals.

Chapter 2: This chapter outlines the theoretical background knowledge of hydrocolloids, fluid gels and liquid foams, as well as providing a comprehensive review of the relevant published literature. Parts of Section 2.4 (Foams) was published in a book chapter titled: "Foams for food applications" in the book *Polymers for Food Applications* (Ellis, A. L., & Lazidis, A. 2018).

Chapter 3: This is the first of the results chapters and explores the production and characterisation of agar fluid gels, in order to advance the understanding from previous

literature. The properties of agar fluid gels at different concentrations were examined before and after aeration to predict foaming characteristics. The results of this allowed the foam stabilisation mechanism to be proposed. Finally, their advantages over quiescently set gels for this application were studied and discussed. The majority of this chapter was published under the title “Stabilisation of foams by agar gel particles” (Ellis et al., 2017).

Chapter 4: This chapter, published as “The effect of sugars on agar fluid gels and the stabilisation of their foams” (Ellis et al., 2019), investigates the effect of sugars on the microstructure of agar fluid gels and their foaming properties. Initially, the influence of sugars upon the gelation of agar fluid gels was studied to provide a foundation for exploring subsequent material properties, such as bulk rheology and trends in foam ability and stability. Finally, the manipulation of particle size through processing parameters was presented to provide further discussion on the mechanism of foam stability.

Chapter 5: This chapter focuses on hydrophobically modifying fluid gel particles by electrostatically binding a cationic surfactant, in order to facilitate their adsorption at the air-water interface to provide long-term foam stability. This work has been published under the title: **“**The hydrophobic modification of kappa carrageenan microgel particles for the stabilisation of foams” (Ellis et al., 2019).

Chapter 6: In this final chapter, the conclusions of this work are summarised, together with suggestions for future work.

1.5 Publications and presentations

1.5.1 Publications

- Ellis, A. L., Mills, T. B., Norton, I. T., & Norton-Welch, A. B. (2019). The hydrophobic modification of kappa carrageenan microgel particles for the stabilisation of foams. *Journal of Colloid and Interface Science, 538*, 165-173.
- Ellis, A., Mills, T., Norton, I., & Norton-Welch, A. (2019). The effect of sugars on agar fluid gels and the stabilisation of their foams. *Food Hydrocolloids, 87*, 371-381.
- Ellis, A. L., & Lazidis, A. (2018). Foams for food applications. In T. Gutiérrez (Ed.), *Polymers for Food Applications*: Springer Publishing.
- Ellis, A. L., Norton, A. B., Mills, T. B., & Norton, I. T. (2017). Stabilisation of foams by agar gel particles. *Food Hydrocolloids, 73*, 222-228.

1.5.2 Presentations

- Ellis, A., Mills, T., Norton, I., & Norton-Welch, A. Hydrocolloid fluid gel systems for the stabilisation of foams, *13th International Hydrocolloids conference*, Canada, 2016.
- Ellis, A., Mills, T., Norton, I., & Norton-Welch, A. Stabilisation of foams by agar fluid gels, *EPSRC CIM in Food 2nd Annual conference*, Birmingham, 2017.
- Ellis, A., Mills, T., Norton, I., & Norton-Welch, A. Stabilisation of foams by agar fluid gels, *UK Colloids*, Manchester, 2017.
- Ellis, A., Mills, T., Norton, I., & Norton-Welch, A. The role of hydrocolloid partilces in the stabilisation of foams, *14th International Hydrocolloids conference*, China, 2018.

Chapter 2: LITERATURE REVIEW

Parts of Section 2.4 published in: Ellis, A. L., & Lazidis, A. (2018). Foams for food applications. In T. Gutiérrez (Ed.), *Polymers for Food Applications*: Springer Publishing.

2.1 Introduction

The aim of this chapter is to provide a comprehensive review of the relevant literature. Firstly, the solution behaviour of hydrocolloids is described, with particular emphasis on the physical and chemical properties of specific food hydrocolloids used throughout this thesis, including gelation mechanisms. The fundamentals of fluid gels are then discussed, highlighting production methods and gelation. Finally, research into the effect of processing parameters on material properties is outlined, focusing on the ability to manipulate certain functionalities.

The next part of the literature review concentrates on liquid foams, initially, their structural properties and methods of formation. The structure of the gas/liquid interface and its role in the collapse of foams via the three main instability mechanisms is identified, providing the motivation behind the considerable research into foam stability. The role of particles in foams is then examined in relation to hydrophobicity, with particular attention focused towards particles used to stabilise foams in the food industry. Finally, research into the modification of hydrophilic particles for foam stabilisation is reported, highlighting the gap of such methods utilised in the food industry.

2.2 Food hydrocolloids

The term 'hydrocolloid' is used to describe a range of biopolymers (polysaccharides and proteins) that display colloidal behaviour in water (Phillips & Williams, 2009). They are utilised in a variety of industrial sectors in food, personal care and medicinal products (Cassiday, 2012; Nishinari & Doi, 2012; Thomas, 2008). In the food industry, hydrocolloids are commonly used to perform a number of functions, including thickening and gelling of aqueous solutions, stabilising foams, emulsions and dispersions, enhancing texture and controlling flavour release (Williams & Phillips, 2000). This thesis concerns the foaming behaviour of polysaccharides, as such they will form the main focus of this section, whilst foams will be discussed in detail in Section 2.4.

Polysaccharides are complex carbohydrates originating from botanical, algal and microbial sources, consisting of repeating monosaccharide units bound by glycosidic linkages (Rees, 1969). Their high molecular weight and hygroscopic character results in their ability to form dispersions in water, which exhibit colloidal behaviour. The viscosity of a polysaccharide solution is determined by a combination of polymer concentration, intrinsic viscosity and chain interactions (Morris, 1994). The intrinsic viscosity of a polymer is primarily determined by polymer shape and size. Most polysaccharides exist in solution as disordered coils (Harding, 1997). In dilute conditions, polymer chains are able to move independently of each other as single entities. Solution viscosity increases gradually with polymer concentration until a critical concentration (C*) is reached (Morris et al., 1981). Above this concentration, polymer chains are forced to occupy less volume leading to an overlap of hydrodynamic radii and the eventual formation of entangled networks. Solution viscosity therefore increases more rapidly beyond C*. This behaviour is represented in Figure 2.1 and is often utilised in the food industry as

hydrocolloids are commonly used as thickeners. Polymer solutions exhibit Newtonian behaviour below C*, but non-Newtonian behaviour above it (Williams & Phillips, 2000). The concentration range for which this regime occurs is dependent on the hydrocolloid.

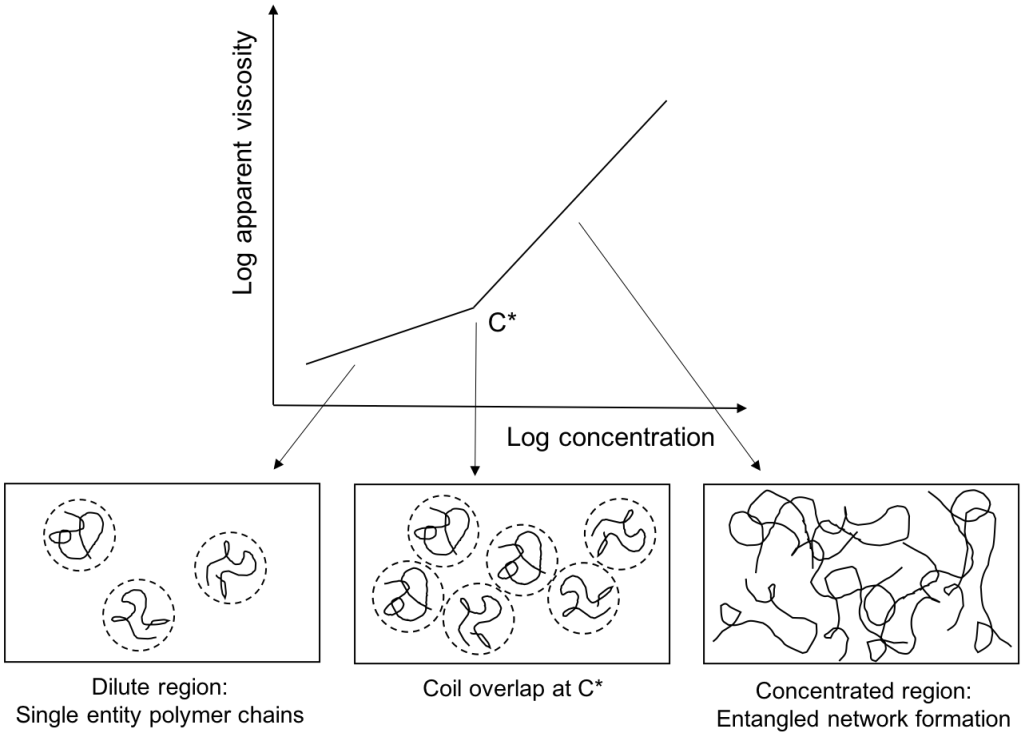


Figure 2.1: Schematic representation of the viscosity dependence of polysaccharide solutions at dilute and concentrated regions. Image adapted from Clegg (1995).

Although all hydrocolloids thicken aqueous dispersions, not all gums form gels (Saha & Bhattacharya, 2010). The gelation of most polysaccharides (i.e. the formation of an ordered, continuous network) can occur under certain conditions. The aggregation of inter-chain linkages into junction zones provides the foundation of the gel network (Oakenfull & Glicksman, 1987). These junction zones are often formed through physical interactions, such as hydrogen bonds and crosslinking (Nishinari, Zhang, & Ikeda, 2000). Gelation may only occur above a critical minimum concentration specific to each hydrocolloid and is often categorised into thermally reversible (cold-set and heat-set gelation) and thermally irreversible (ionotropic gelation). Thermally irreversible gels, e.g.

alginate, are often used in food products subjected to a high temperature process e.g. baking or sterilisation (Williams, Phillips, & de Vries, 2004). Gelation and gel properties can be tailored for specific applications, such as food or personal care products, by the choice of hydrocolloid and the environmental conditions. Figure 2.2 displays the mechanical properties of common hydrocolloid gels, which are dependent on molecular structure, side groups and chain conformation (Phillips & Williams, 2009). For example, xanthan gum forms short ordered sequences resulting in a soft and flexible gel texture (Lundin & Hermansson, 1995), whereas those which form longer and more rigid conformations, such as agar and kappa carrageenan, produce gels that are firmer and more brittle (Mitchell, 1976). The gelation of agar and carrageenan will be discussed in more detail as these polysaccharides are the focus of this thesis.

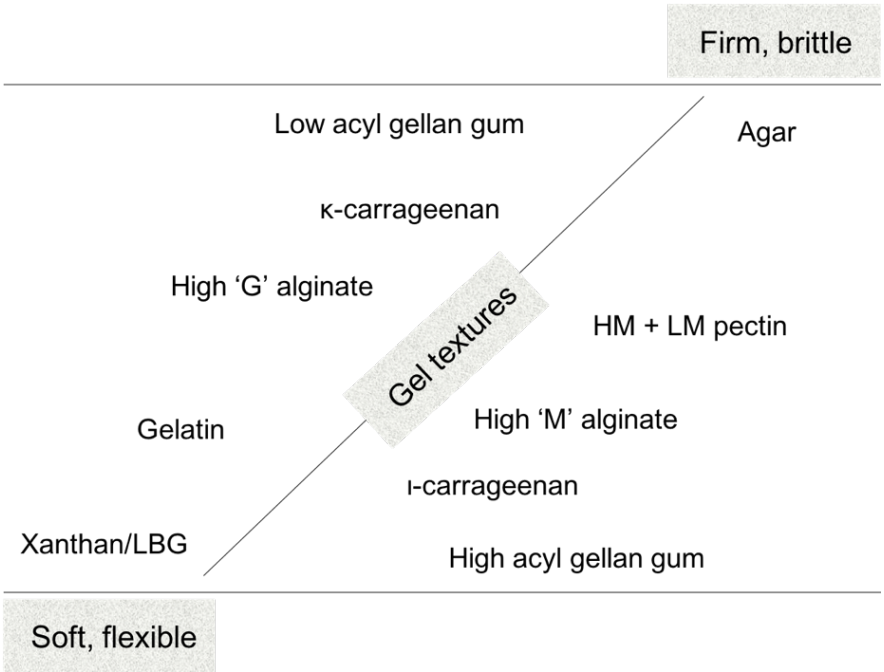


Figure 2.2: Comparison of the textures exhibited from a range of hydrocolloid gels. Image adapted from Phillips and Williams (2009).

2.2.1 Agar

The polysaccharide agar is comprised of both neutral agarose and charged agaropectin fractions in proportions that vary depending on the seaweed from which they originate, as well as the production process (Araki, 1956). Agarose, consisting of repetitive units of D-galactose and 3-6,anyhydro-L-galactose (Figure 2.3), provides the main structure of agar and its gelling capability. The role of agaropectin is not as well understood, although recent work by Nishinari and Fang (2017) reported that it may enhance gelation rather than inhibit it.

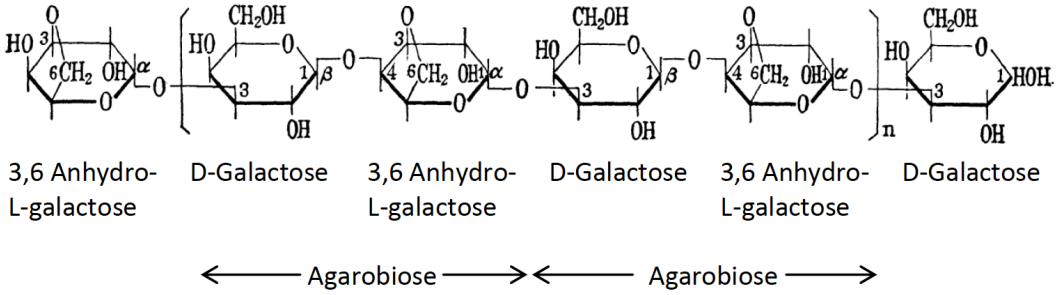


Figure 2.3: The chemical structure of agarose: a linear polymer composed of repeating units of agarobiose. Image adapted from Araki (1956) and Fernández Farrés (2015).

The gelation mechanism as described by the Domain model (Arnott et al., 1974) states that agarose molecules exist as random coils in solution, which undergo a coil-to-helix transition as the temperature is lowered. The helices, which are stabilised by hydrogen bonds with water (Foord & Atkins, 1989), then aggregate together and form a wider 3D network when linked through junction zones. Gelation occurs exclusively by hydrogen bonding. The gelling process is represented schematically in Figure 2.4. Agarose molecules as random coils can be seen (A), which upon cooling close to the gelation temperature undergo a coil-to-helix transition forming both double helices B_1 (antisymmetric) and B_2 (symmetric). The aggregation of helices then result in structures C and D. Both routes (B_1 and B_2) can co-exist, where one or the other dominates

depending on the cooling speed (Armisén & Gaiatas, 2009). The requirement of no additional ingredients for gelation has led to the use of agar gel in a wide variety of applications, from food products to cell culture (Armisén & Gaiatas, 2009). A further property which is exploited in the food industry is its very high gelling hysteresis i.e. the difference between its gelling temperature (≈ 38 °C) and its melting temperature (≈ 85 °C). This is considerably higher than most other gelling polysaccharides, which have an average hysteresis of ≈ 12 °C (Phillips & Williams, 2009). This is beneficial for products which need to be more heat-resistant e.g. pasteurisation.

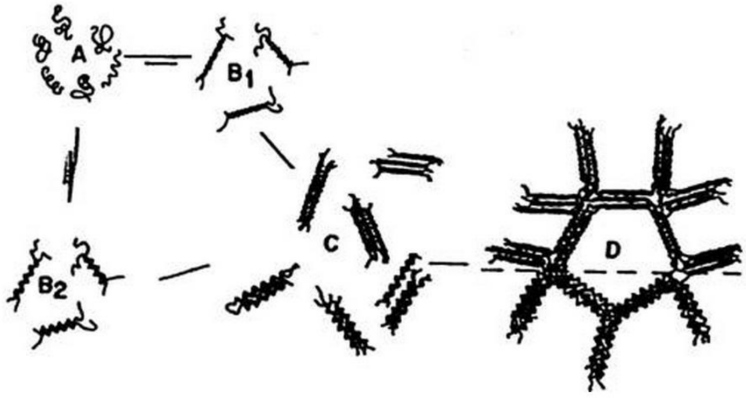


Figure 2.4: The gelation mechanism of agarose; upon cooling of random agarose coils in solution (A), symmetric and antisymmetric double helices form (B_1 and B_2), which aggregate together to give the structures in C and then D. Image from Medin (1996).

2.2.2 Carrageenan

Carrageenan, originating from seaweed (red algae), consists of repeating galactose and 3,6-anhydrogalactose units. Three main types of carrageenan were defined by Rees and co-workers (Anderson, Dolan, & Rees, 1965; Rees, 1963) as lambda (λ), kappa (κ) and iota (ι). These are categorised by their chemical structure and differ in 3,6-anhydrogalactose and ester sulphate content. This leads to very different thickening and gelling properties, which can be utilised in a wide variety of applications. For example, iota carrageenan interacts with calcium ions producing a soft and elastic gel, whereas

kappa carrageenan (κC) interacts with potassium ions forming a firm and brittle gel. Both are used as gelling agents in the food industry and therefore provide a range of structural requirements. κC for example, is now being utilised as a functional additive in the production of vegan cheese (Błaszak, Gozdecka, & Shyichuk, 2018). In contrast, λ-carrageenan does not gel but increases viscosity and improved mouthfeel in certain beverages (Blakemore & Harpell, 2010). With a recent Ipsos Mori poll reporting a 350% increase in people identifying as vegans over the past decade (Bixler, 2017), the demand to replace gels sourced from meat (e.g. gelatin) with those originating from plant-based material, such as carrageenan and agar is only going to increase as the trend in vegetarianism and veganism continues to rise.

The gelation mechanism of carrageenans was established by Morris et al., (1980) using calorimetric and chiroptical evidence to be similar to that of agar, i.e. molecular ordering of random coils to helical domains followed by the aggregation of these domains. In contrast to agar, the negatively charged sulphate groups of carrageenans result in electrostatic repulsion and as a result, only small clusters of helices (called domains) are formed through interchain interactions. The presence of cations enables further association of these domains by supressing the electrostatic repulsion resulting in a cohesive gel network (as seen in Figure 2.5). The extent of molecular ordering and final gel strength is therefore dependent upon the ionic environment of the aqueous solution. For example, κC binds monovalent ions, particularly K^+ ions, whereas ι-carrageenan binds divalent ions, in particular Ca^{2+} ions (Hermansson, Eriksson, & Jordansson, 1991; Janaswamy & Chandrasekaran, 2002; Norton et al., 1983; Rochas & Rinaudo, 1984). The

lower charge density of κC is also reflected in a greater ease of aggregation and gel formation at lower concentrations.

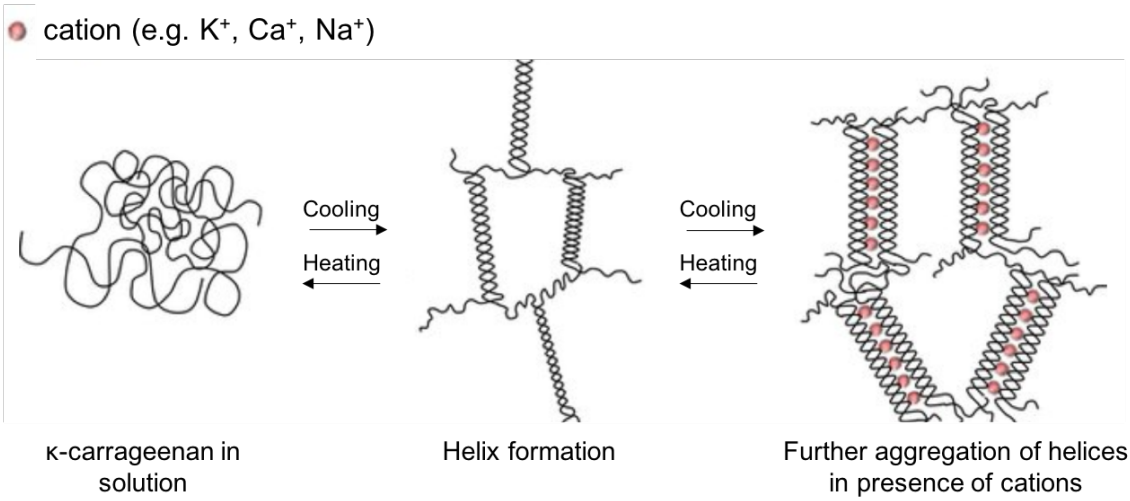


Figure 2.5: The gelation mechanism of κ-carrageenan. Upon cooling a hot solution of κ-carrageenan, random coils undergo a coil-to-helix conformational transition. Double helices form which then aggregate together in the presence of cations to form the final gel structure. Figure adapted from Alba and Kontogiorgos (2015).

2.3 Fluid gels

In order to expand the functionality of hydrocolloid gels, the microstructural engineering approach led to the development of fluid gels (Brown, Cuttler, & Norton, 1990). A fluid gel is defined as a suspension of microgel particles in a non-gelled continuous phase. Their structures can be designed to meet a wide range of functionalities (Fernández Farrés et al., 2014). For example, fluid gel particles can be designed to mimic the structural characteristics of oil droplets for potential fat replacement in products such as mayonnaise (Bialek, Jones, & Norton, 2000; Norton & Norton, 2010). Fluid gels are formed by applying a constant shear to a biopolymer solution undergoing gelation, confining gelation to particulates (Brown, Cuttler, & Norton, 1990). This results in a pourable and spreadable gel, as seen in Figure 2.6. It is important to note the difference in production between a fluid gel formed from shear throughout gelation compared to a sheared gel which is a quiescently formed gel subjected to mechanical break-up (Garrec & Norton, 2012). A sheared gel would result in the production of larger more inhomogeneous particles and would exhibit more syneresis than fluid gels, which is not desirable. The fluid gel approach was first applied to thermally set gels such as agar, gellan and kappa carrageenan. These fluid gels were prepared by shearing a hot solution of biopolymer whilst cooling (Garrec & Norton, 2012; Norton, Jarvis, & Foster, 1999; Sworn, Sanderson, & Gibson, 1995). More recently, fluid gels have also been prepared with biopolymers undergoing irreversible ionic gelation e.g. alginate fluid gels set with calcium ions (Hedges & Norton, 1991; Fernández Farrés et al., 2014), this results in thermally stable fluid gels. In addition, thermally stable whey protein fluid gels have also been prepared, by shearing protein solutions undergoing irreversible denaturation upon heating (Moakes, Sullo, & Norton, 2015b). The material properties of fluid gels can be

controlled by manipulating the material (hydrocolloid and salt concentration), as well as the processing conditions (shear rate and cooling profiles), which will be discussed in the following Section.

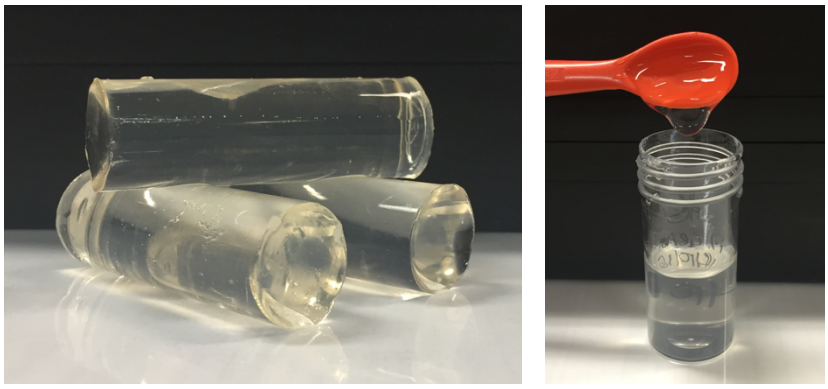


Figure 2.6: A gellan gel formed under quiescent conditions (left) and under shear to form a fluid gel (right). Image from Norton (2016).

2.3.1 Fluid gel formation

This section will focus on fluid gels produced from thermally set polysaccharides, in particular agar and kappa carrageenan. The mechanism of fluid gel formation was first described by Norton et al. (1999) when studying agar fluid gels, as a nucleation and growth process; firstly, the applied shear results in the separation of initial gel nuclei that form, which limits molecular ordering (gelation) to discrete particles. The initial gel nuclei then grow to an equilibrium particle size dictated by the applied shear rate. This ordering can be observed by a steep increase in viscosity, measured using a rheometer, at a temperature close to the gelation temperature for the specific biopolymer. Disordered chains make the particles appear "hairy", but as the system is cooled further, these disordered chains integrate within the particles making them smoother. Fluid gels then need to be stored at a temperature sufficiently lower than this, in order to stop any molecular re-ordering, which may result in the loss of a particulate structure. Norton et al. (1999) observed a considerable increase in elastic modulus when agarose fluid gels

were re-cooled from 50 °C compared to 5 °C indicating a change to a more quiescently set gel structure.

Processing conditions, such as the cooling rate and shear rate have a limited effect on the formation of particles and their subsequent properties. For example, at high cooling rates the aggregation rate can dominate over the break up controlled by shear rate and large irregular gel particles will form. At lower cooling rates, more closely matched to the rate of conformational ordering and in the order usually used during production processes, the shear rate has a stronger influence and smaller more homogenous particles are formed (Gabriele, 2011). Under this regime, the shear rate (up to a certain size) can control particle size. Previous research demonstrated the difficulty in accurately measuring fluid gel particle sizes due to the close proximity of the gel particle refractive index to that of the water continuous phase. However, Gabriele, Spyropoulos, and Norton (2009) used viscosity measurements to infer changes in particle size and interactions whilst producing κC fluid gels using a rheometer. Their results can be seen in Figure 2.7, where a sudden increase in viscosity at ≈ 35 °C (corresponding to molecular ordering) occurred for fluid gels produced at all shear rates. A larger increase in viscosity was observed for the fluid gel produced at the lowest shear rate (0.5 s^{-1}), which begins to decrease again once the maximum viscosity was reached. This was attributed to the breakdown of larger particles, which had grown through interactions between remaining disordered polymer chains. The authors concluded that increasing the applied shear rate resulted in smaller particles with lower bulk viscosities. However, changes in viscosity above 200 s^{-1} were minimal, shear rate therefore has less of an effect on particle size and interaction in this range; a concept initially discussed by Norton et al., (1999).

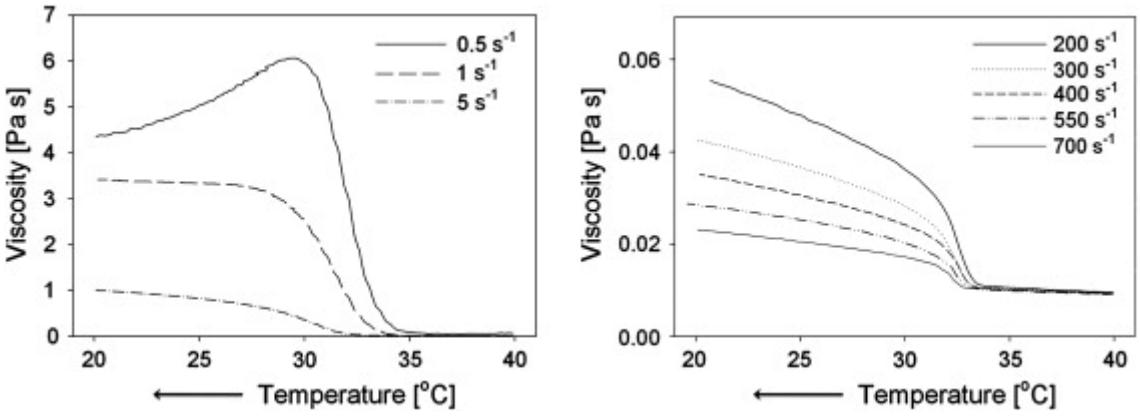


Figure 2.7: Viscosity as a function of temperature during fluid gel production, at various shear rates. A constant cooling rate of 0.5 °Cmin^{-1} was used for all fluid gels. Image from Gabriele et al. (2009).

2.3.2 Effect of hydrocolloid concentration

The effect of modifying hydrocolloid concentration on fluid gel material properties is two-fold; firstly it increases the particle volume fraction and secondly, it increases individual particle modulus. Garrec, Guthrie, and Norton (2013) explain the increase in volume fraction as a result of a higher number of particles. This was expected from a more rapid gelation, as previously indicated by studying agarose fluid gels (Norton et al., 1998). Table 2.1 shows results from Garrec (2013), who studied the effect of κC concentration on fluid gel material properties. An increase in both fluid gel particle volume fraction and particle modulus can be seen. Particle modulus was inferred by measuring the Young's modulus of quiescently cooled bulk gels at the same concentration of fluid gel; Frith et al., (2002) reported that the internal particle polymeric network and therefore the stiffness of individual particles is equivalent to that of their quiescently cooled counterparts. Volume fraction was calculated by centrifuging fluid gels and quiescent gels, where the former indicated fluid gel solid contents and the latter, gel deformation under centrifugation. This method relied on the assumption that an equivalent fraction of fluid is released from fluid gels and quiescently cooled bulk gels

under centrifugation. Fluid gel particle compressibility and, therefore, volume fraction were only approximate.

Table 2.1: Fluid gel volume fraction and particle modulus as a function of κC concentration. Figure adapted from Garrec (2013).

Concentration of κC (wt%)	Fluid gel particle volume fraction	Approximate particle Young's modulus (kPa)
0.5	0.46	2.6 ± 0.4
1	0.65	26.1 ± 3.3
2	0.76	66.5 ± 5.5

Particle volume fraction is a key parameter in determining the behaviour of a material. At low phase volumes, the suspension will act as a highly aggregated suspension dominated by colloidal forces (Moakes, Sullo, & Norton, 2015a). At higher volume fractions, particles behave as soft microgels and the rheology is dependent on particle elastic modulus as well as particle-particle interactions (Fernández Farrés et al., 2014; Gabriele et al., 2009). For example, Adams, Frith, and Stokes (2004) studied the rheological behaviour of high phase volume suspensions of agar microgels at various concentrations. Microgels at concentrations of 0.5-5 wt% agar were produced via a water-in-oil emulsion route resulting in a range of particle moduli from 2.4 kPa to 185 kPa. Upon increasing the particle modulus in suspensions with maximum packing, the storage modulus (G') increased by two orders of magnitude. In addition, the suspension containing the particles of the highest modulus also exhibited a considerably higher viscosity. The rheological properties of agar microgel suspensions at high volume fractions are therefore dictated by the deformability (or modulus) of the particles.

2.3.3 Fluid gel particle-particle interactions

Another way to tune the properties of fluid gels is by altering the interactions between particles. Garrec (2013) described κC fluid gel particles as "hairy" and to investigate potential interactions between particles, studied their thixotropic behaviour. A hysteresis in shear stress was observed between a shear rate ramp up and down. This indicated that the rate of structure breakdown was greater than that of rebuilding, suggesting that particles were initially aggregated together and once broken upon shear, these interactions did not immediately re-from. Oscillatory rheological data established a dependence of these particle-particle interactions on κC concentration. Strain sweeps were conducted on fluid gels at three different concentrations. The strain required to initiate flow (characterised by a 5% decrease in G') was observed to decrease at higher concentrations, due to an increased particle modulus (i.e. softer particles deform to greater strains). However, once flow was initiated, the particles at higher κC concentration had a weaker dependence on strain, implying enhanced interparticle structuring i.e. particle-particle interactions. It was concluded that the formation of these interactions and aggregation between particles was caused by long-range inter-particle ordering facilitated by the presence of disordered chains at the surface of particles.

Another way to manipulate the material properties of fluid gels is through altering the bridging between particles by controlling the temperature at which shear is stopped during formation. Garrec et al. (2013) prepared κC fluid gels in a pin stirrer where the exit temperature of the fluid gel could be altered to change the temperature at which shear is stopped and therefore the ratio of sheared to quiescent cooling. Typically T_{exit} was maintained at 5 °C , in order to ensure all molecular ordering took place within the pin

stirrer ($T_m \approx 35$ °C). The transition midpoint temperature, T_m , is the temperature at which the coil-to-helix transition is in dynamic equilibrium. Below this temperature, the helix growth process is favoured over its decay. Therefore, increasing T_{exit} (closer to T_m) results in an increase in the number of disorder-order events taking place quiescently. This was reflected in an observed increase in fluid gel G' and yield stress due to quiescent ordering causing bridging between particles. The dependence on yield stress can be seen in Figure 2.8. However, after the fluid gels were sheared, their yield stress showed no dependence on T_{exit}, suggesting that they were now structurally similar and the quiescent ordering can be irreversibly broken with shear. By manipulating T_{exit}, a range of material properties can be delivered, varying from that of a fluid gel to that of a quiescently cooled gel.

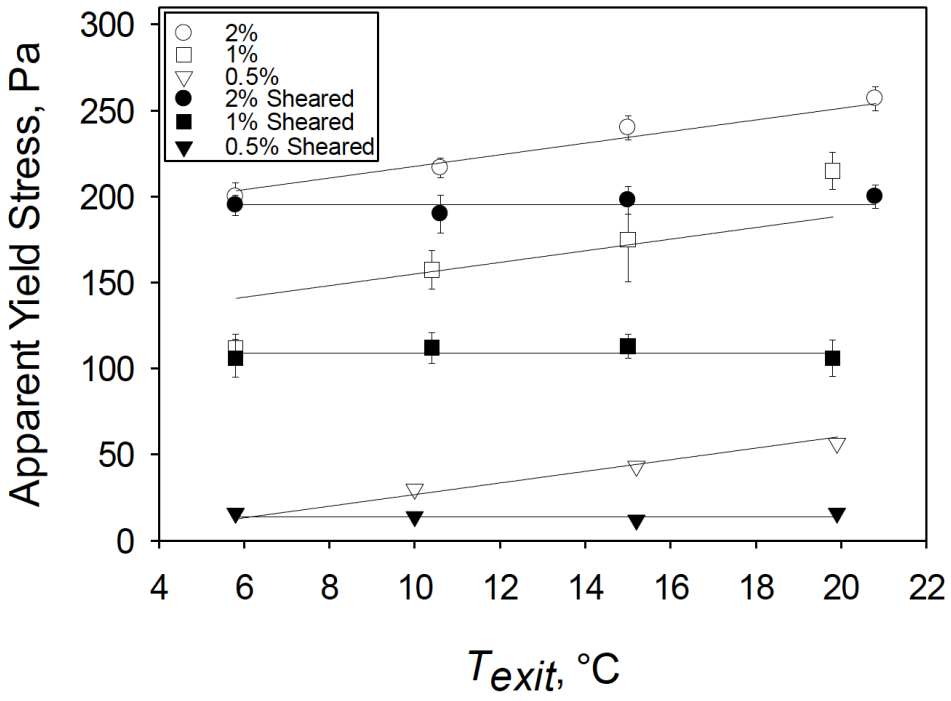


Figure 2.8: Yield stress dependence on pin stirrer exit temperature for fluid gels at 0.5%, 1% and 2% κC. Samples were tested as initial fluid gels (open symbols) and 24 h after shearing (closed symbols). Linear fits are shown with equal fits for each series. Figure from Garrec (2013).

2.4 Foams

The aeration of foods is utilised in a wide range of products and applications, from aerated chocolate to vegan meringue, as increased understanding has helped to exploit the novelty and versatility of bubbles as food ingredients. The incorporation of air into food products not only reduces the cost and calorific content of products but provides a luxurious texture desirable to consumers (Stanley, Goff, & Smith, 1996). For example, whipped cream and mousses acquire a creaminess, whilst the carbonation of soft drinks delivers the desired "fizziness" and solid products such as crisps, develop a light and crisp texture. Introducing a gas phase into a food matrix not only affects texture but also appearance, colour and physical properties. In addition, air cells in liquid foam precursors can be used to manipulate the structural properties of products such as bread and meringue during the cooking process. As well as advances in foam formulation, processing methods have continued to be developed, for example, microfluidics devices are being developed currently for the production of microbubbles, which are thought to have exciting practical applications in the food industry as fat-replacers and texture modifiers (Rovers et al., 2016). This chapter will first introduce the basic concepts of foams in terms of structure, production and stability, before exploring the use of particles, focusing on biopolymer particles to stabilise foams.

2.4.1 Foam structure

A foam is a colloidal dispersion where a gas, usually air, is distributed throughout a solid or aqueous continuous phase (Walstra, 2003). This thesis will focus on aqueous foams and so they will provide the basis of this literature review. Foams typically consist of polydispersed, macroscopic (>10 μm) bubbles, the size of which controls the transparency of the foam. Foams possess interesting mechanical, frictional and

rheological properties, which enable them to display a wide range of behaviour (Pugh, 2016). One such factor which influences foam properties is the ratio of gas to liquid. A wet foam consists of spherical bubbles separated by thin liquid films and can exhibit elastic properties under low shear but liquid-like properties upon higher shear. A drier foam, however, contains bubbles that are no longer spherical and tends to behave like a solid with a high shear modulus (Pugh, 2016). A wet foam will evolve with time as liquid starts to drain under gravity, eventually leaving behind polyhedral bubbles resembling a dry foam (Bergeron & Walstra, 2005). Although there is no clear boundary to distinguish whether a foam is dry or wet, it is generally believed that a foam with a gas fraction around 0.63 (the limit for randomly packed spheres) is a wet foam, while a gas fraction of 0.8 or higher constitutes a dry foam (Bergeron & Walstra, 2005). The difference in structures can be seen in Figure 2.9, where a drier foam exists towards the top of the foam but due to the drainage of liquid through the interstitial space, bubbles lower down the foam resemble that of a wet foam. The interstitial space (i.e. the liquid volume) can be described by (i) *films*, which form between two adjacent bubbles and are bounded by almost planar bubble faces (ii) *channels* (*or Plateau borders*), where three films meet and (iii) *nodes,* where four channels intersect (Koehler, Hilgenfeldt, & Stone, 2000).

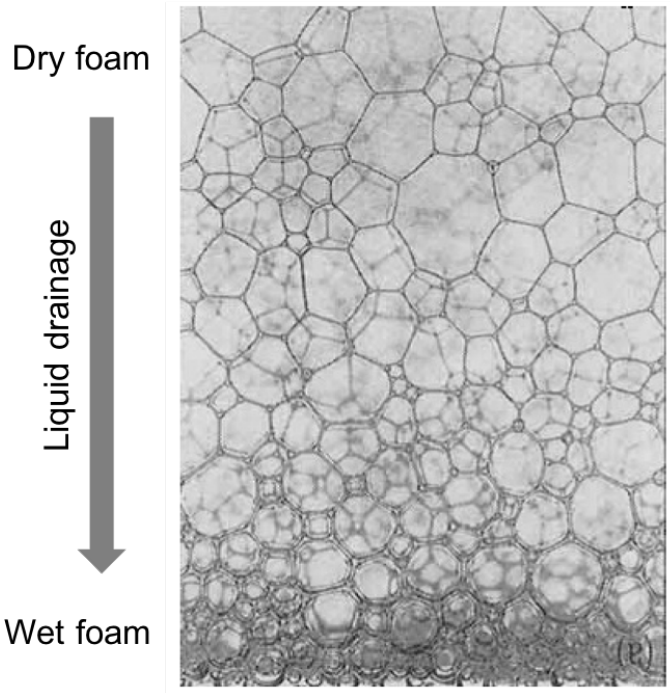


Figure 2.9: A photograph of the bubbles comprising an aqueous foams. Bubbles lower down the foam are spherical whereas towards the top, the foam is drier and bubbles are more polyhedral in shape. Image adapted from Larson (1999).

2.4.2 Methods of foam formation

There are a number of methods for generating foams that can be categorised into either the entrapment of air bubbles from the atmosphere (e.g. shaking, sparging, stirring etc.) or introducing gas bubbles by physical (e.g. nucleation) or chemical methods (e.g. by-product of a chemical reaction). Foam generation is typically a non-equilibrium process, where the foam microstructure is dependent on parameters, such as velocity, time, viscosity, surfactant type and diffusion rate. Bubble size and distribution in particular, is heavily influenced by the foaming method. For example, Weaire (1999) compared bubble size distributions of foams generated using common production methods (Figure 2.10). Gas sparging typically produces small bubbles which are monodispersed (under suitable conditions), whilst nucleation of gas in beverages for example, produces fairly large polydisperse bubbles.

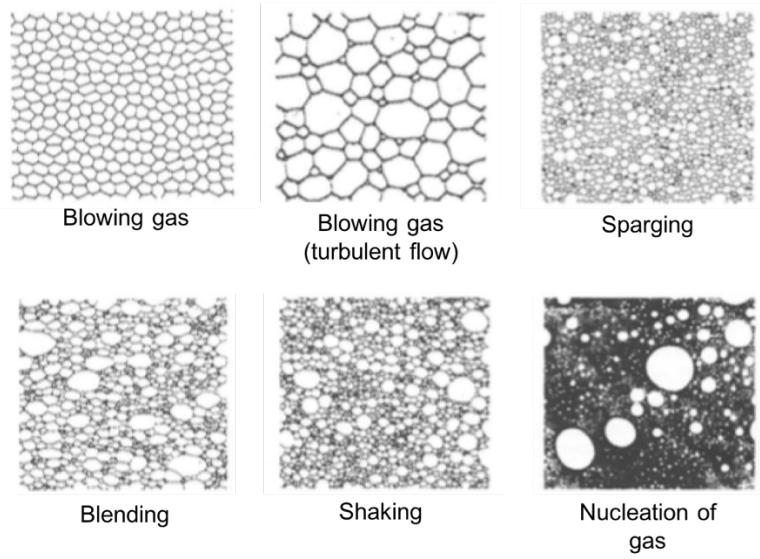


Figure 2.10: Images of bubbles created by different foaming techniques. Image adapted from Weaire (1999).

The most common method of foaming, especially in the food industry is mechanical agitation. This involves forcing liquid around an external gas, typically air, resulting in its entrapment, by methods such as whipping and shaking. According to Bergeron and Walstra (2005), the following cycle repeatedly takes place during the aeration process:

1. Bubbles are generated by the entrapment of gas.
2. Surfactant molecules diffuse and adsorb to the newly formed interface.
3. Bubbles break up and re-form.
4. Bubbles start to coalesce due to poor coverage by surfactant until system reaches a steady state.

The main processing parameters that effect the foam microstructure are mixing speed, mixing time and the type and geometry of the whisk. This technique is relatively easy and inexpensive and is particularly efficient for high viscosity systems. However, it can lead to the formation of large bubbles with wide size distributions. The difficulty in producing small bubbles stems from the opposition to the break-up of large bubbles into smaller bubbles by an increase in Laplace pressure (Pugh, 2016). However, in recent years,

research into these types of foaming processes has increased. High-speed rotatory mixers for example, have been designed to more effectively entrain gas to generate smaller bubbles with narrow size distributions (Pugh, 2016).

Bubbles can also be created as a by-product of a chemical reaction. For example, sodium bicarbonate reacts with cream of tartar (acid) in the presence of water, forming the CO_2, bubbles in a cake mixture. Another common example is the metabolism cycle of yeast in bread dough; CO_2 is produced from the fermentation of sugars when starch is broken down, creating small bubbles throughout the dough (Campbell & Mougeot, 1999). Currently in the food industry, attention has been focused on producing monodispersed, micron-sized bubbles using microfluidic devices. This involves the co-injection of gas and liquid simultaneously into narrow hydrophilic channels, producing so-called microbubbles. It is anticipated that these microbubbles will have novel applications as fat-replacers and texture modifiers in the food industry (Rovers et al., 2016).

Gas sparging has become a popular method of aeration in laboratories due to the relatively small and monodispersed bubbles it can generate (Bisperink, Ronteltap, & Prins, 1992). Typically, gas is injected through small capillaries inside the liquid, bubbles subsequently form and detach from the end of the capillary (Weaire, 1999). Processing parameters, such as the size and distance between capillaries, together with the flow rate of gas, need to be controlled in order to manipulate bubble size. For example, if the capillaries are too close or the flow rate is too high, bubbles will immediately coalesce (Camarasa et al., 1999). This method works best in low viscosity liquids and is commonly seen in practice at coffee shops, where milk is frothed by injecting steam through a nozzle.

2.4.3 Surfactants

At a gas-liquid interface, interactions between molecules, such as hydrogen bonds and Van der Walls, result in a force with inward direction causing instability and quick collapse of bubbles (Saint-Jalmes, 2006). Surface-active molecules (surfactants) are used to provide greater stability by adsorbing at the interface and lowering the surface tension. They adsorb at an interface by positioning themselves partly in the hydrophilic phase (liquid) and partly in the hydrophobic phase (gas), due to their amphiphilic nature. For example, the surface tension of pure water (72.8 mNm^{-1}) can be reduced to ≈35 mNm^{-1} by a good surfactant (Pugh, 2016). The surface tension of a solution reduces proportionally to the surfactant concentration up to its critical micelle concentration (CMC). Above the CMC, surfactant molecules form micelle structures in the bulk solution, which are in equilibrium with free monomers, as well as those adsorbed at the interface (Möbius, Miller, & Fainerman, 2001). This can be seen in Figure 2.11.

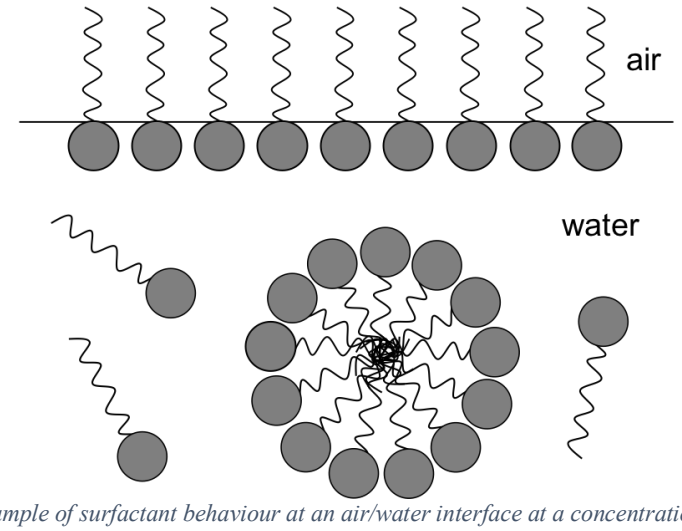


Figure 2.11: An example of surfactant behaviour at an air/water interface at a concentration above the surfactant CMC. Free monomers and micelles reside in the bulk solution, whilst an adsorbed monolayer of surfactant molecules assembles at the interface.

Low molecular weight (LMW) surfactants are soap-like substances where the hydrophobic part is typically an aliphatic chain, whilst the hydrophilic part can be more diverse (Fennema, 1996). They are categorised depending on the charge of the head group

into ionic (cationic, anionic or ampholyte) and non-ionic surfactants. The most commonly used LMW surfactants in foods are phospholipids (lecithin), mono- and diglycerides (glycerol monostearate); polysorbates (tweens), sorbitan esters (spans) and sucrose esters (Bos & van Vliet, 2001). Ionic LMW surfactants are more of a challenge to use in food products due to their instability to environmental conditions such as salt concentration and pH. However, the small size and good mobility of LMW surfactants results in their fast adsorption to newly formed interfaces during foam generation, which is advantageous compared to larger polymeric surfactants, for example. The most common polymeric surfactants are proteins, they have a more complex structure and adsorb to an interface due to their need to expose and spread their hydrophobic regions (Dickinson, 1998). Polymeric surfactants tend to be less sensitive to environmental conditions, however their increased size, poor solubility and insufficient amphiphilic character can limit their surface-activity (Dickinson, 2003).

2.4.4 Foam (in)stability

Foams are thermodynamically unstable systems that are constantly re-arranging to form lower energy structures (Weaire & Hutzler, 2001). The lifetime of foams is typically in the range of minutes or hours compared to equivalent emulsion systems, which can be stable for months (Walstra, 1989). There are three main mechanisms which drive the evolution of foam structure over time and lead to its eventual collapse:

1. **Liquid drainage**: the flow of liquid through the volume of the foam due to gravity.
2. **Disproportionation**: the diffusion of gas between bubbles of different internal pressures causing larger bubbles to grow in size and smaller bubbles to decrease in size.

3. **Coalescence**: the rupturing of a film between neighbouring bubbles.

2.4.4.1 Liquid drainage

Liquid drainage can be defined as the flow of liquid through a volume of foam. Liquid begins to drain from the top of the foam through the network of interconnected Plateau borders and nodes, as seen in Figure 2.12. The main driving force is gravity and capillary pressure, which causes thinning of the channels (Guillermic et al., 2009). This is, however, slightly restored by the surface tension gradient along the air/water (a/w) interface, known as the Gibbs-Marangoni effect. The balancing of these effects results in a steady-state flow. There are several models and approaches, which attempt to describe drainage, in general all indicate that the density and viscosity of the bulk phase are important factors in controlling the rate at which it takes place (Bickerman, 1973; Weaire, 1999). Recently, the viscosity of the bulk phase has been altered through cleverly manipulating the microstructure of the foam through the addition of suspended particles of polymeric or inorganic origin. For example, Carn et al., (2009) defined a new strategy of modifying liquid drainage using a much lower concentrated system than is typically used to alter viscosity. Aggregated silica nanoparticles were used to act as liquid-traps in the foam microstructure; their high internal porosity and hydrophilic character resulted in a considerable reduction in drainage.

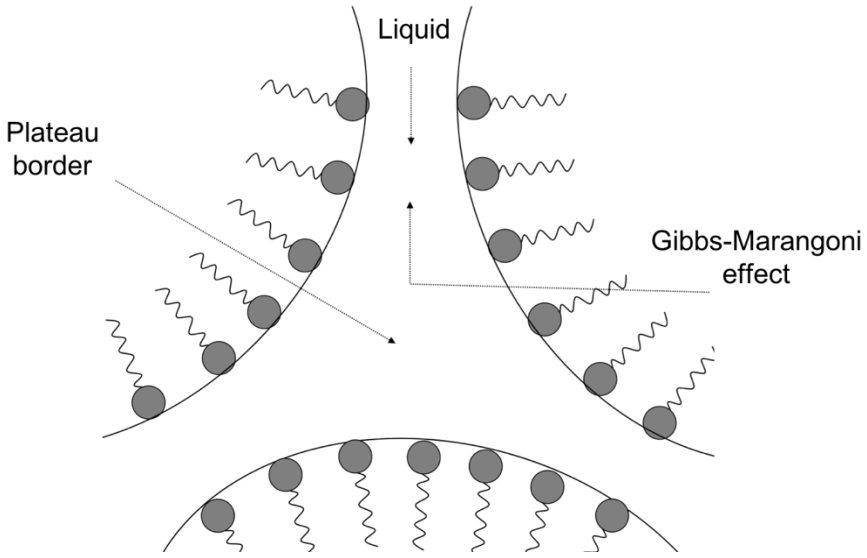


Figure 2.12: Liquid drainage through a Plateau border. Gravity and capillary forces causes thinning of the films, whilst the Gibbs-Marangoni effect acts to reduce this.

In addition, the type of surfactant can affect the extent of liquid drainage. As mentioned earlier, as liquid drains through the foam channels, there is a surface tension gradient at an interface caused by the shear stress applied on the layer of adsorbed surfactants. Surfactants will move against the direction of drainage to counteract the surface tension gradient, the process of which is called the Gibbs-Marangoni mechanism (Garrett, 1993). More mobile, low molecular weight (LMW) surfactants are more efficient in diffusing to the area and restoring the presence of fluid in the channels (Wilde et al., 2004). The process of drainage can be further complicated by disproportionation occurring simultaneously as the two process often re-enforce each other.

2.4.4.2 Disproportionation

Disproportionation can be defined as the movement of gas from regions of high concentrations to low concentrations via diffusion, leading to the continual coarsening of bubbles. The pressure inside bubbles is expressed by the Youngs-Laplace equation, which defines the pressure over a curved surface (the capillary pressure) (Pugh, 2016). A foam typically contains polydispersed bubbles and therefore regions of different Laplace

pressure and solubility of gas. As a result of the higher internal pressure of smaller bubbles, coupled with the increase in gas solubility in the aqueous phase with pressure, gas tends to diffuse from smaller to larger bubbles via the aqueous phase. Smaller bubbles therefore decrease in size, whilst larger bubbles grow. As such, coarsening of the bubbles is a self-accelerating process. Disproportionation is very similar to Ostwald ripening in emulsion systems, however it occurs on much quicker time scales due to the higher interfacial tension of gas-water interfaces compared to oil-water interfaces and the higher solubility of gas molecules (Ettelaie & Murray, 2015).

The rate of bubble coarsening is strongly influenced by the solubility of the gas that is dispersed in the liquid continuous phase; the more soluble a gas is, the faster it can diffuse through a bubble (if a pressure gradient exists) accelerating the disproportionation process. The solubility of common gases used for aeration in the food industry can be seen in Table 2.2. The life-time of a foam can be manipulated by altering the gas used. For example, a 1 mm radius bubble containing carbon dioxide gas in water will disappear in approximately 4 seconds, whilst the same size bubble of nitrogen will have a lifetime of ≈ 3 minutes (Fennema, 1996). This is utilised in the production of Guinness where the bubbles are composed of nitrogen gas, resulting in a longer lasting foam (Hildebrand, 1981).

Table 2.2: Solubility mole fractions of commonly used gases in aeration at equilibrium (at 20 °C and atmospheric pressure). Data from Gevantman (2000).

Gas	Mole fraction solubility
CO_2	7.07×10^{-4}
N_2O	5.068×10^{-4}
O_2	2.501×10^{-5}
N_2	1.274×10^{-5}

Another way to control the rate of coarsening is through modifying the a/w interface and therefore the permeability of the film. For example, polymeric surfactants, such as proteins will provide a thicker adsorbed layer than LMW surfactants, which will help to reduce the extent of disproportionation. Increasing the interfacial elasticity of the films can also provide stability; polymeric surfactants and strongly adsorbed particles can create a strong film with a high surface dilatational modulus (*E)*, providing a barrier to coarsening (Blijdenstein, De Groot, & Stoyanov, 2010). *E* describes the ability of the fluid to restore the surface tension during stress. If $E>\gamma/2$, coarsening due to gas diffusion can be theoretically stopped (Garrett, 1993).

2.4.4.3 Coalescence

The rupture of the film between two neighbouring bubbles leads to their coalescence into one larger bubble (Bergeron & Walstra, 2005). The main driving force for coalescence is the reduction in total surface area of the foam, since this is thermodynamically favourable (Weaire & Hutzler, 2001). The mechanism leading to coalescence is dependent on the film characteristics and the type of surfactant present. For example, when films are thin, Van der Waals attractions cause films to become close until they rupture (Fennema, 1996). This usually only occurs at the top of the foam, as the presence of drainage in the bulk of the foam usually prevents films from becoming this thin. In the case of thick films,

colloidal interactions are less evident and have little significance (Fennema, 1996). Typically, the surface dilatational modulus is substantial and film rupture is difficult. The presence of particles in a foam can also lead to coalescence. For example, hydrophobic particles (contact angle $\theta > 90°$) can cause film rupture if the film is thin enough for the particles to bridge the surfaces of two bubbles.

2.4.5 Particle stabilisation of foams

Particles can provide stabilisation in aqueous foams by slowing down the effects of coarsening, drainage or coalescence. The three effects are often coupled and in many cases act simultaneously, enhancing one another. The mechanism of stabilisation provided by particles depends on their hydrophobicity and therefore their presence in the bulk phase or at the a/w interface. Particles made from most food-based materials are often not able to stabilise foams on their own through adsorption to the interface, mostly due to limitations in size and hydrophobicity (Lazidis et al., 2017). However, hydrophilic particles can aid in foam stability by remaining in the continuous phase and creating a weak gel network with a finite yield stress (Dickinson et al., 2004; Zúñiga & Aguilera, 2008).

2.4.5.1 Hydrophobic particles

Hydrophilic particles can provide stability in foams by altering the continuous phase and primarily slowing drainage. In order to also tackle disproportionation and bubble coalescence, particles require a degree of surface-activity to manipulate the interface. Hydrophobic particles have therefore been utilised, as their adsorption to the a/w interface can provide a barrier against disproportionation. This stabilisation effect was first observed in emulsions and termed Pickering stabilisation (Pickering, 1907). Research

into particle-stabilised foams first focused on inorganic particles, such as silicas, as a result of their well-defined shape and narrow size distributions (Binks & Horozov, 2005; Gonzenbach et al., 2006). It was established that small particles of moderate hydrophobicity could most efficiently provide stability through adsorption the a/w interface. If particles are too hydrophobic, they can protrude the a/w interface causing film rupture and subsequent coalescence. If particles have an intermediate hydrophobicity and they are partially wetted, they can accumulate on the bubble surface providing a strong barrier to shrinkage and coalescence (Binks, 2002). In addition, partial coagulation or gelling of a film of particles has been found to be advantageous for stability, as this can provide a sufficiently high elastic modulus to prevent bubble shrinkage during disproportionation (Murray & Ettelaie, 2004).

The key parameter that determines the ability of solid particles to attach to an a/w interface is their wettability, as defined by the three-phase contact angle (θ). This is the angle formed between tangents of the solid surface and the liquid-gas interface (Hunter et al., 2008). A representation of contact angles for particles of different hydrophobicity is illustrated in Figure 2.13. The contact angle is related to the particle/air (γ_{pa}), particle/water (γ_{pw}) and particle air/water (γ_{aw}) surface energies by the Young's equation (Equation 2.1). Therefore, particles that are able to wet both air and water interfaces equally ($\gamma_{pa} = \gamma_{pw}$) will have a contact angle of 90°.

$$cos\theta = (\gamma_{pa} - \gamma_{pw})/\gamma_{aw} \quad (2.1)$$

When the contact angle is close to 90°, the particles have the tendency to reside on the interface and reduce the surface energy (Binks, 2002). The monolayer of adsorbed particles is curved in such a way that a larger proportion of their surface is located either in the liquid or gas phase. When the contact angle measured into water is smaller than 90°, the particles are partially wetted and partially hydrophobic, resulting in the formation of air cells in a water phase. However, when the contact angle is greater than 90°, the particles are strongly hydrophobic and non-wetted. A large proportion of the individual particles therefore reside in the gas phase, resulting in the potential rupturing of films. Strongly hydrophobic particles are therefore ineffective as foam stabilisers. A contact angle of around 70° is most effective for particle stabilisation of foams (Pugh, 2016).

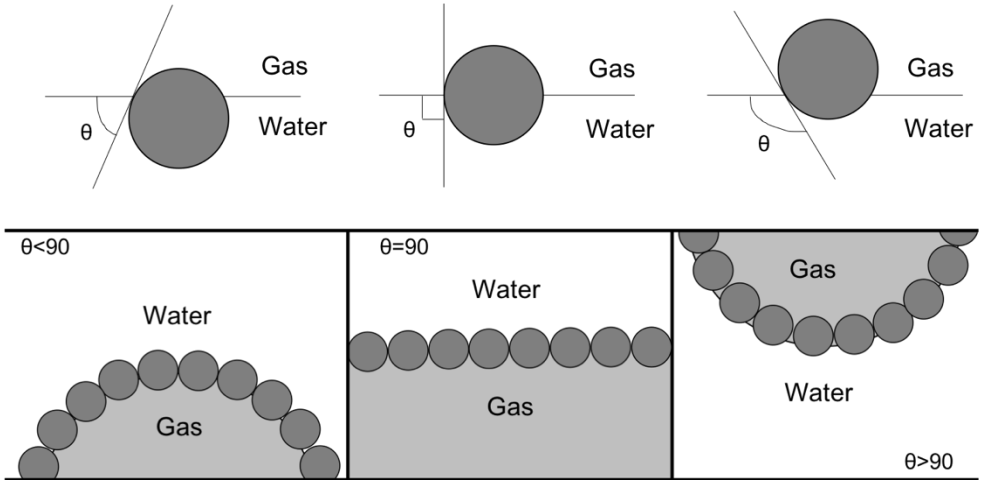


Figure 2.13: (Above) positioning of a particle at a planar gas/water interface with a contact angle of <90° (left), =90° (middle) and >90° (right). (Below) positioning of particles at the curved interface; particles with a contact angle of <90° (left) reside largely in the aqueous phase, whilst those with a contact angle of >90° (right) remain largely in the gas phase. Image adapted from Binks (2002).

To ensure foam stability, particles need to remain attached to the interface to prevent bubble coalescence. Based on a thermodynamic approach, if the free energy associated with the desorption of particles is larger than the free energy decrease caused by the decrease in surface area (upon coalescence), then coalescence will not be spontaneous. The energy required to remove a particle is therefore an important parameter to

understand and quantify. Equation 2.2 shows that the energy (E_{des}) required to remove a spherical particle from an interface is dependent on its radius (r), the surface tension of the a/w interface (γ_{aw}) and the contact angle (θ) (Lopetinsky, 2006).

$$E_{des} = \pi r^2 \gamma_{aw} (1 \pm cos\theta)^2 \qquad (2.2)$$

In the case of $0° \leq \theta \geq 90°$, the positive sign is used and when $\theta > 90°$, the negative sign is used. For relatively small particles, the adsorption energy can be several thousand times kT. For example, for a particle of 10 nm diameter, the maximum energy to detach the particle ($\theta=90°$) would be ≈1400 kT, but for a contact angle of 13°, it would only be ≈1 kT (Pugh, 2016). Research has also shown that if particles are packed closely at an interface, they have the potential to greatly reduce disproportionation (Dickinson, 2010). The condition that needs to be met in order for a bubble to be stable against disproportionation is called the Gibbs stability criterion (Equation 2.3). According to Gibbs stability criterion, when the interfacial elasticity, E, (mN/m), is greater than half the surface tension, the bubble can distort in order to lower the Laplace pressure during bubble shrinkage (Stocco et al., 2011). This reduces the dissolution of the bubble which can eventually stop if the pressure reaches zero.

$$E > \frac{\gamma}{2} \qquad (2.3)$$

There are a number of natural food products which innately stabilise air bubbles. For example, the air bubbles in whipped cream are stabilised by partially coalesced fat globules, which adsorb to the interface. This network of coalesced fat droplets also

provides the desired texture and yield stress, as well as stability (Dickinson, 2010). Natural proteins such as milk and egg also provide excellent foaming capabilities. Once adsorbed to the a/w interface, proteins provide a steric barrier to disproportionation and coalescence by increasing the interfacial elasticity (Ellis & Lazidis, 2018). These highly viscoelastic layers also deliver high surface shear viscosities, which result in rigid Plateau borders and therefore help to reduce the flow of liquid through the foam (Saint-Jalmes et al., 2005).

2.4.5.2 Biopolymers in foams

Both proteins and polysaccharides provide a range of structures and properties that can be utilised in order to stabilise foams. In their simplest form, biopolymers increase the viscosity of the aerated system providing stability during the foaming process e.g. gelatin stabilises the structure of marshmallows (Phillips & Williams, 2009). Alternatively, biopolymers can stabilise foams in the form of particulate entities of nano- or micro-scale dimensions. This occurs through two main mechanisms, shown in Figure 2.14, which are dependent on the surface activity of the biopolymer. Firstly, when present in sufficiently high concentrations, particles can aggregate together in foam channels providing a barrier to liquid drainage (Guillermic et al., 2009). Secondly, providing the particles are suitably hydrophobic, they can adsorb at the a/w interface, forming a protective layer against bubble coalescence and coarsening (this is Pickering stabilisation, as discussed in Section 2.4.5.1). In reality, protein stabilised foams will often experience a combination of these two mechanisms (Dickinson, 2017). In contrast, polysaccharides are inherently hydrophilic and therefore need modifying in order to act as Pickering stabilisers. In food systems, this can be manipulated chemically or using thermal treatment. For example, starch particles can be heat treated to increase their surface hydrophobicity (Seguchi,

2001). In addition, interaction with proteins such as soy, egg or milk to form polysaccharide-protein complexes can also increase polysaccharide surface activity (Binks et al., 2017; Ghosh & Bandyopadhyay, 2012).

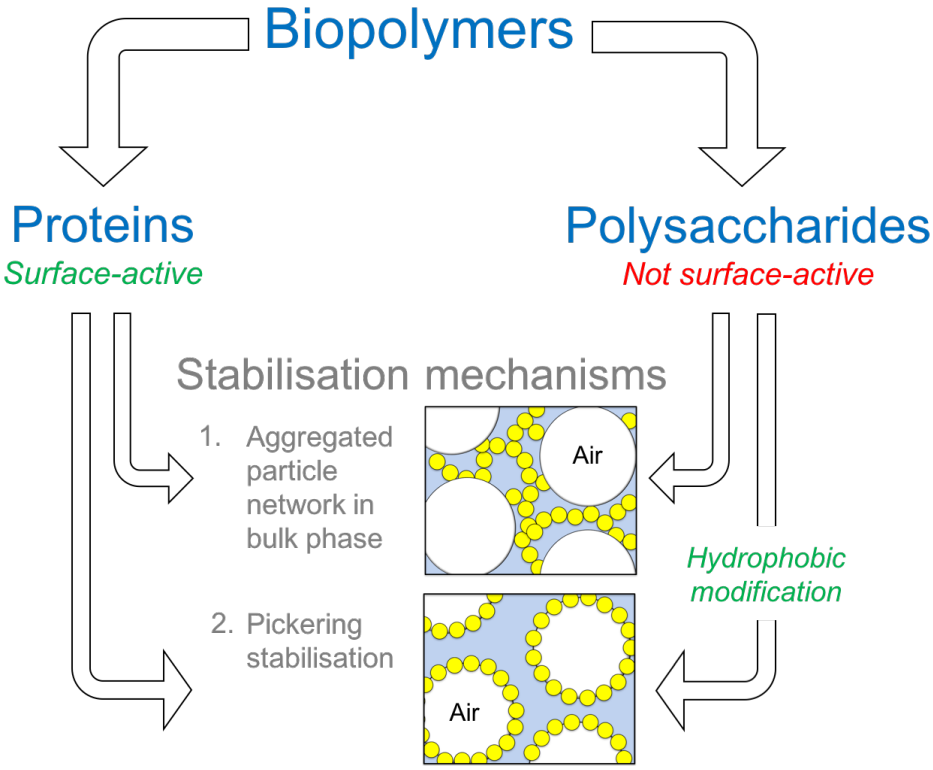


Figure 2.14: A representation of the two mechanisms of foam stabilisation available to biopolymer particles, along with the pathways for protein and polysaccharides to reach them based on their surface activity. Image from Ellis and Lazidis (2018).

2.4.5.3 Hydrophilic particles

The objective of this thesis is to understand and utilise the role of polysaccharide fluid gels in the stabilisation of foams. The role of hydrophilic particles in foam systems will therefore be explored in this Section. Foams containing hydrophilic particles can often drain like surfactant foams (Rio et al., 2014). Alternatively, particles accumulate in the Plateau borders, resulting in localised plugs, which help to reduce drainage and enhance foam stability (Carn et al., 2009; Friberg & Saito, 1976; Guignot et al., 2010; Rio et al., 2014).

Haffner, Khidas, and Pitois (2015) attempted to quantify the dependence of hydrophilic monodisperse particles on drainage velocity. They built on work conducted by Louvet, Höhler, and Pitois (2010) who studied the capture/release transition of a single spherical particle confined within the interstitial network of a foam, by investigating the collective trapping of particles. They reported that the effect of particles could be accounted for by two parameters: the volume fraction of the particles in suspension (Ψ_p) and the confinement parameter (λ), which relates the size of the particle to that of the constrictions in the foam channels. They observed that for small values of λ, drainage depends on both Ψ_p and λ (regime of flowing suspensions) for $\lambda \geq 1$, the particles are restricted and drainage is sharply decreased (capture transition). Beyond $\lambda=2$, the drainage velocity increases as the particles become too large to be included in the foam network (particle exclusion transition). Although, this study was conducted on spherical, monodisperse particles, the same principles and dependence on particle volume fraction and size can be applied to other systems.

For example, by utilising the changing confinement properties of laponite clay particles in an SDS foam, Guillermic et al. (2009) achieved complete arrest of drainage after a period of time. This can be seen in Figure 2.15, where drainage of an SDS foam doped with laponite (c_L=16 g/L) stopped at time, t_j, and eventually restarted at t_u. As the foam began to age with time (through drainage and coarsening), the laponite-SDS solutions simultaneously began to gel, this resulted in an increase in viscoelasticity and the confinement of particles. This was shown by rheological measurements (Figure 2.15), where yield stress of the solutions increased with time and also with confinement (at a

smaller gap between rheometer plates). This resulted in the jamming of interstitial fluid in the Plateau borders and nodes. The gel, however, was too weak to stop coarsening and the bubbles and foam channels begun to increase in size, until the gravitational stress became such that the laponite gel yielded and drainage re-started. Other studies have reported this non-classical arrest of drainage and also emphasise its dependence on the yield stress of the foamed suspension (Fameau & Salonen, 2014; Goyon et al., 2010; Guignot et al., 2010; Koczo, Lobo, & Wasan, 1992). For example, Lesov, Tcholakova, and Denkov (2014) looked at the role of silica particles in aqueous foams containing two different surfactants. Cationic TTAB led to particle-stabilised foams, whereas zwitterionic CAPB led to surfactant-stabilised foams. The stability of such foams to drainage and coarsening was shown to depend mostly on yield stress.

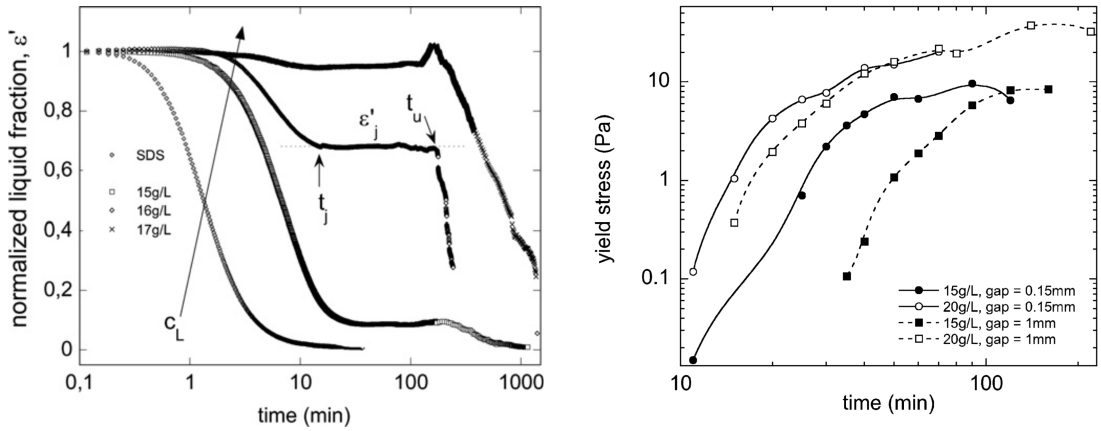


Figure 2.15: (Left) normalised liquid fraction (ε') as a function of time at a fixed position inside the foam, for SDS foams at various concentrations of laponite particles (c_L). At c_L = 16 g/L, the times t_j and t_u are indicated. (Right) yield stress as a function of time for two laponite concentrations and two values of gap height between rheometer plates (mimicking confinement). Image adapted from Guillermic et al. (2009).

2.4.5.3.1 Hydrophobic modification of hydrophilic particles

In order to increase the functionality of hydrophilic particles they can be made surface-active through modification, typically by either chemical modification or *in situ* modification with surfactants. Chemical modification is commonly used to alter

polysaccharides, such as cellulose and starch. Starch can be modified through the addition of ocentyl succinic anhydride (OSA) or by using heat treatment to change the surface character (Seguchi, 2001). In addition, polysaccharides can also be altered through *in situ* modification with surfactants. In the literature, there are many instances of foam stabilisation through particle-surfactant combinations. For example, laponite clay particles with hexylamine (Liu et al., 2009), alkylammonium bromides (Liu et al., 2010) or CTAB (Zhang et al., 2008), alumina particles with short chain carboxylic acids (Gonzenbach et al., 2006) and calcium carbonate particles with SDS (Cui et al., 2010). However, none of these combinations are suitable for food-grade systems. There are several reviews on food-grade particles for Pickering stabilisation but these mainly focus on emulsion systems (Dickinson, 2011; Rayner et al., 2014) and those that do investigate foams (Dickinson, 2017; Ellis & Lazidis, 2018) have generally not studied particle-surfactant combinations. Recently however, Binks et al. (2017) have studied the modification of calcium carbonate particles with various anionic surfactants for potential use in food systems. The modification of hydrophilic particles using surfactants *in-situ* is therefore an exciting emerging area of research for the food industry, which is only just starting to be utilised.

The majority of polysaccharides used in the food industry are anionic e.g. carrageenan, alginate, pectin and xanthan. A cationic surfactant would therefore be required for potential electrostatic interaction and subsequent surface-activation. Lauric arginate (LA) is one such surfactant, which has been approved as generally regarded as safe (GRAS) within the United States for certain food applications (Benford et al., 2009). There are a small number of studies in the literature that focus on the interaction between LA and

anionic biopolymers; Bonnaud, Weiss, and McClements (2010) describe a strong binding interaction between LA and anionic biopolymers pectin, alginate, carrageenan and xanthan, indicated by isothermal titration calorimetry. Asker, Weiss, and McClements (2011) suggest that the addition of pectin to mixed LA/Tween 20 micelles leads to the formation of electrostatic complexes that have potential applications as functional ingredients.

2.4.5.4 Microgels at the a/w interface

Fluid gels are a subset of microgel particles; soft particles with three-dimensional structure, averaging 50 nm to several μm in size (Dai & Ngai, 2013). It is therefore important to discuss the interfacial behaviour of microgel particles in general. A particularly interesting behaviour exhibited by microgel particles, is their ability to deform upon adsorption to an interface. Microgels are an increasingly interesting area of research due to their vast potential as colloidal building blocks and stabilising agents due to their deformability, surface activity, reversible swelling behaviour and responsiveness to pH and temperature (Dickinson, 2015). A number of studies have demonstrated the ability of microgels to adsorb to a fluid or a/w interface and subsequently deform (Deshmukh et al., 2014; Destribats et al., 2011; Li & Ngai, 2013; Murphy, Farkas, & Jones, 2016). For example, the stabilisation of fluid and a/w interfaces by pNIPAM microgels has been shown to consist of two distinct processes: diffusion-limited adsorption to the interface and deformation of microgels once at the interface (Deshmukh et al., 2014; Li et al., 2013). In addition, Murphy et al. (2016) observed the same dependence of protein microgels in the stabilisation of fluid interfaces, which facilitated the development of highly elastic interfaces. Once adsorbed, deformation of the particles enables increased exposure to the interface, which further decreases the surface energy

(Dickinson, 2015). Dickinson (2015) recently highlighted the significant, novel potential of biopolymer-based microgels to stabilise food emulsions and foams.

LIST OF REFERENCES

Adams, S., Frith, W., & Stokes, J. (2004). Influence of particle modulus on the rheological properties of agar microgel suspensions. Journal of Rheology, 48(6), 1195-1213.

Alba, K., & Kontogiorgos, V. (2015). Seaweed Polysaccharides (Agar, Alginate Carrageenan). Retrieved from https://www.researchgate.net/profile/Vassilis_Kontogiorgos/publication/323844190_Seaweed_Polysaccharides_Agar_Alginate_Carrageenan/links/5ab9fe4aa6fdcc46d3ba3913/Seaweed-Polysaccharides-Agar-Alginate-Carrageenan.pdf.

Allen, K. E., Murray, B. S., & Dickinson, E. (2008). Development of a model whipped cream: Effects of emulsion droplet liquid/solid character and added hydrocolloid. Food Hydrocolloids, 22(4), 690-699. doi:http://dx.doi.org/10.1016/j.foodhyd.2007.01.017

Anderson, N., Dolan, T., & Rees, D. (1965). Evidence for a common structural pattern in the polysaccharide sulphates of the Rhodophyceae. Nature, 205(4976), 1060.

Araki, C. (1956). Structure of the agarose constituent of agar-agar. Bulletin of the Chemical Society of Japan, 29(4), 543-544.

Arboleya, J.-C., García-Quiroga, M., Lasa, D., Oliva, O., & Luis-Aduriz, A. (2014). Effect of highly aerated food on expected satiety. International Journal of Gastronomy and Food Science, 2(1), 14-21. doi:https://doi.org/10.1016/j.ijgfs.2013.12.002

Armisén, R., & Gaiatas, F. (2009). 4 - Agar. In Phillips, G. O., & Williams, P. A. (Eds.), Handbook of Hydrocolloids (Second Edition) (pp. 82-107): Woodhead Publishing.

Arnott, S., Fulmer, A., Scott, W., Dea, I., Moorhouse, R., & Rees, D. (1974). The agarose double helix and its function in agarose gel structure. Journal of Molecular Biology, 90(2), 269-272.

Asker, D., Weiss, J., & McClements, D. J. (2011). Formation and Stabilization of Antimicrobial Delivery Systems Based on Electrostatic Complexes of Cationic−Non-ionic Mixed Micelles and Anionic Polysaccharides. Journal of Agricultural and Food Chemistry, 59(3), 1041-1049. doi:10.1021/jf103073w

Benford, D., Harrison, R., Larsen, J., & DiNovi, M. (2009). Safety Evaluation of Certain Food Additives: Ethyl Lauroyl Arginate. World Health Organization, Geneva.

Bergeron, V., & Walstra, P. (2005). Foams (Chapter 7). In Fundamentals of interface and colloid science, volume V Soft Colloids: Elsevier Academic Press.

Bialek, J. M., Jones, M. G., & Norton, I. T. (2000). Pourable edible aqueous-continuous emulsions. In: Google Patents.

Bickerman, J. (1973). Foam films. In: Foams. Springer

Binks, B. P. (2002). Particles as surfactants—similarities and differences. Current Opinion in Colloid & Interface Science, 7(1–2), 21-41. doi:http://dx.doi.org/10.1016/S1359-0294(02)00008-0

Binks, B. P., & Horozov, T. S. (2005). Aqueous foams stabilized solely by silica nanoparticles. Angewandte Chemie International Edition, 44(24), 3722-3725.

Binks, B. P., Muijlwijk, K., Koman, H., & Poortinga, A. T. (2017). Food-grade Pickering stabilisation of foams by in situ hydrophobisation of calcium carbonate particles. Food Hydrocolloids, 63, 585-592. doi:http://dx.doi.org/10.1016/j.foodhyd.2016.10.002

Bisperink, C., Ronteltap, A., & Prins, A. (1992). Bubble-size distributions in foams. Advances in Colloid and Interface Science, 38, 13-32.

Bixler, H. J. (2017). The carrageenan controversy. Journal of Applied Phycology, 29(5), 2201-2207.

Blakemore, W. R., & Harpell, A. R. (2010). Carrageenan. (pp. 73-94). In A. Imeson (Ed.), Food stabilisers, thickeners and gelling agents: Blackwell Publishing.

Błaszak, B., Gozdecka, G., & Shyichuk, A. (2018). Carrageenan as a functional additive in the production of cheese and cheese-like products. Acta scientiarum polonorum. Technologia alimentaria, 17(2), 107-116.

Blijdenstein, T., De Groot, P., & Stoyanov, S. (2010). On the link between foam coarsening and surface rheology: why hydrophobins are so different. Soft Matter, 6(8), 1799-1808.

Bonnaud, M., Weiss, J., & McClements, D. J. (2010). Interaction of a food-grade cationic surfactant (lauric arginate) with food-grade biopolymers (pectin,

carrageenan, xanthan, alginate, dextran, and chitosan). Journal of Agricultural and Food Chemistry, 58(17), 9770-9777.

Bos, M. A., & van Vliet, T. (2001). Interfacial rheological properties of adsorbed protein layers and surfactants: a review. Advances in Colloid and Interface Science, 91(3), 437-471.

Brown, C., Cuttler, A., & Norton, I. (1990). Liquid based composition comprising gelling polysaccharide capable of forming a reversible and a method for preparing such composition. *European Patent No. EP0355908*.

Camarasa, E., Vial, C., Poncin, S., Wild, G., Midoux, N., & Bouillard, J. (1999). Influence of coalescence behaviour of the liquid and of gas sparging on hydrodynamics and bubble characteristics in a bubble column. Chemical Engineering and Processing: Process Intensification, 38(4-6), 329-344.

Campbell, G. M., & Mougeot, E. (1999). Creation and characterisation of aerated food products. Trends in Food Science & Technology, 10(9), 283-296. doi:http://dx.doi.org/10.1016/S0924-2244(00)00008-X

Carn, F., Colin, A., Pitois, O., Vignes-Adler, M., & Backov, R. (2009). Foam drainage in the presence of nanoparticle− surfactant mixtures. Langmuir, 25(14), 7847-7856.

Cassiday, L. (2012). Hydrocolloids get personal. inform, 23(6), 349-352.

Chronakis, I. S., & Kasapis, S. (1995). Food applications of biopolymer—theory and practice. In Developments in food science (Vol. 37, pp. 75-109): Elsevier.

Clegg, S. (1995). Thickeners, gels and gelling. In Physico-chemical aspects of food processing (pp. 117-141): Springer.

Coultate, T. P. (2009). Food: the chemistry of its components: Royal Society of Chemistry.

Cui, Z. G., Cui, Y. Z., Cui, C. F., Chen, Z., & Binks, B. P. (2010). Aqueous Foams Stabilized by in Situ Surface Activation of CaCO3 Nanoparticles via Adsorption of Anionic Surfactant. Langmuir, 26(15), 12567-12574. doi:10.1021/la1016559

Dai, Z. & Ngai, T. (2013). Microgel particles: The structure-property relationships and their biomedical applications. J. Polym. Sci. Part A: Polym. Chem., 51, 2995-3003. doi:10.1002/pola.26698

Deshmukh, O. S., Maestro, A., Duits, M. H., van den Ende, D., Stuart, M. C., & Mugele, F. (2014). Equation of state and adsorption dynamics of soft microgel particles at an air–water interface. Soft Matter, 10(36), 7045-7050.

Destribats, M., Lapeyre, V., Wolfs, M., Sellier, E., Leal-Calderon, F., Ravaine, V., & Schmitt, V. (2011). Soft microgels as Pickering emulsion stabilisers: role of particle deformability. Soft Matter, 7(17), 7689-7698.

Dickinson, E. (1998). Proteins at interfaces and in emulsions stability, rheology and interactions. Journal of the Chemical Society, Faraday Transactions, 94(12), 1657-1669.

Dickinson, E. (2003). Hydrocolloids at interfaces and the influence on the properties of dispersed systems. Food Hydrocolloids, 17(1), 25-39. doi:http://dx.doi.org/10.1016/S0268-005X(01)00120-5

Dickinson, E. (2010). Food emulsions and foams: Stabilization by particles. Current Opinion in Colloid & Interface Science, 15(1–2), 40-49. doi:http://dx.doi.org/10.1016/j.cocis.2009.11.001

Dickinson, E. (2011). Double emulsions stabilized by food biopolymers. Food Biophysics, 6(1), 1-11.

Dickinson, E. (2015). Microgels — An alternative colloidal ingredient for stabilization of food emulsions. Trends in Food Science & Technology, 43(2), 178-188. doi:https://doi.org/10.1016/j.tifs.2015.02.006

Dickinson, E. (2017). Biopolymer-based particles as stabilizing agents for emulsions and foams. Food Hydrocolloids, 68, 219-231. doi:http://dx.doi.org/10.1016/j.foodhyd.2016.06.024

Dickinson, E., Ettelaie, R., Kostakis, T., & Murray, B. S. (2004). Factors controlling the formation and stability of air bubbles stabilized by partially hydrophobic silica nanoparticles. Langmuir, 20(20), 8517-8525.

Dickinson, E., Ettelaie, R., Murray, B. S., & Du, Z. (2002). Kinetics of Disproportionation of Air Bubbles beneath a Planar Air–Water Interface Stabilized by Food Proteins. Journal of Colloid and Interface Science, 252(1), 202-213.

Drewnowski, A. (1997). Taste preferences and food intake. Annual Review of Nutrition, 17(1), 237-253.

Du, Z., Bilbao-Montoya, M. P., Binks, B. P., Dickinson, E., Ettelaie, R., & Murray, B. S. (2003). Outstanding stability of particle-stabilized bubbles. *Langmuir, 19*(8), 3106-3108.

Ellis, A. L., & Lazidis, A. (2018). Foams for food applications. In Gutiérrez, T., (Ed.), Polymers for Food Applications: Springer Publishing.

Ettelaie, R., & Murray, B. S. (2015). Evolution of bubble size distribution in particle stabilised bubble dispersions: Competition between particle adsorption and dissolution kinetics. Colloids and Surfaces A: Physicochemical and Engineering Aspects, 475, 27-36.

Fameau, A.-L., & Salonen, A. (2014). Effect of particles and aggregated structures on the foam stability and aging. Comptes Rendus Physique, 15(8), 748-760. doi:https://doi.org/10.1016/j.crhy.2014.09.009

Fennema, O. R. (1996). Food Chemistry 3rd. USA: Marcel Dckkcr. Ine, 9-22.

Fernández Farrés, I. (2015). Fluid gel production and tribological behaviour of alginate and agar. Univeristy of Birmingham, eThesis.

Fernández Farrés, I., Moakes, R. J. A., & Norton, I. T. (2014). Designing biopolymer fluid gels: A microstructural approach. Food Hydrocolloids, 42, Part 3, 362-372. doi:http://dx.doi.org/10.1016/j.foodhyd.2014.03.014

Foord, S., & Atkins, E. (1989). New x-ray diffraction results from agarose: Extended single helix structures and implications for gelation mechanism. Biopolymers, 28(8), 1345-1365.

Friberg, S., & Saito, H. (1976). Foam stability and association of surfactants. Paper presented at the Foams, Proceedings of a Symposium organized by the Society of Chemical Industry, Colloid and Surface Chemistry Group, and held at Brunel University, Academic Press, London.

Frith, W., Garijo, X., Foster, T., & Norton, I. (2002). Microstructural origins of the rheology of fluid gels. Gums and Stabilsers for the Food Industry, 278, 95-103.

Gabriele, A. (2011). Fluid gels: Formation, production and lubrication Univeristy of BIrmingham eThesis.

Gabriele, A., Spyropoulos, F., & Norton, I. T. (2009). Kinetic study of fluid gel formation and viscoelastic response with kappa-carrageenan. Food Hydrocolloids, 23(8), 2054-2061.

Garrec, D. (2013). Understanding Fluid Gels and Hydrocolloid Tribology. University of Birmingham, eThesis.

Garrec, D. A., Guthrie, B., & Norton, I. T. (2013). Kappa carrageenan fluid gel material properties. Part 1: Rheology. Food Hydrocolloids, 33(1), 151-159.

Garrec, D. A., & Norton, I. T. (2012). Understanding fluid gel formation and properties. Journal of Food Engineering, 112(3), 175-182.

Garrett, P. (1993). Recent developments in the understanding of foam generation and stability. Chemical Engineering Science, 48(2), 367-392.

Gevantman, L. (2000). Solubility of selected gases in water. In CRC Handbook of Chemistry and Physics: CRC Press.

Ghosh, A. K., & Bandyopadhyay, P. (2012). Polysaccharide-protein interactions and their relevance in food colloids: INTECH Open Access Publisher.

Gonzenbach, U. T., Studart, A. R., Tervoort, E., & Gauckler, L. J. (2006). Stabilization of foams with inorganic colloidal particles. Langmuir, 22(26), 10983-10988.

Goyon, J., Bertrand, F., Pitois, O., & Ovarlez, G. (2010). Shear Induced Drainage in Foamy Yield-Stress Fluids. Physical Review Letters, 104(12), 128301. doi:10.1103/PhysRevLett.104.128301

Guignot, S., Faure, S., Vignes-Adler, M., & Pitois, O. (2010). Liquid and particles retention in foamed suspensions. Chemical Engineering Science, 65(8), 2579-2585. doi:http://dx.doi.org/10.1016/j.ces.2009.12.039

Guillermic, R.-M., Salonen, A., Emile, J., & Saint-Jalmes, A. (2009). Surfactant foams doped with laponite: unusual behaviors induced by aging and confinement. Soft Matter, 5(24), 4975-4982.

Haffner, B., Khidas, Y., & Pitois, O. (2015). The drainage of foamy granular suspensions. Journal of Colloid and Interface Science, 458, 200-208.

Harding, S. E. (1997). The intrinsic viscosity of biological macromolecules. Progress in measurement, interpretation and application to structure in dilute solution. Progress in Biophysics and Molecular Biology, 68(2), 207-262.

Hedges, N. D., & Norton, I.T. (1991). Fluid composition. EP0432835(A1).

Hermansson, A.-M., Eriksson, E., & Jordansson, E. (1991). Effects of potassium, sodium and calcium on the microstructure and rheological behaviour of kappa-carrageenan gels. Carbohydrate Polymers, 16(3), 297-320.

Hildebrand, P. C. (1981). Preparation of beverages containing a head of froth. In: Google Patents.

Hunter, T. N., Pugh, R. J., Franks, G. V., & Jameson, G. J. (2008). The role of particles in stabilising foams and emulsions. Advances in Colloid and Interface Science, 137(2), 57-81. doi:http://dx.doi.org/10.1016/j.cis.2007.07.007

Janaswamy, S., & Chandrasekaran, R. (2002). Effect of calcium ions on the organization of iota-carrageenan helices: an X-ray investigation. Carbohydrate Research, 337(6), 523-535. doi:https://doi.org/10.1016/S0008-6215(02)00017-4

Katzbauer, B. (1998). Properties and applications of xanthan gum. Polymer Degradation and Stability, 59(1-3), 81-84.

Koczo, K., Lobo, L. A., & Wasan, D. T. (1992). Effect of oil on foam stability: Aqueous foams stabilized by emulsions. Journal of Colloid and Interface Science, 150(2), 492-506. doi:https://doi.org/10.1016/0021-9797(92)90218-B

Koehler, S. A., Hilgenfeldt, S., & Stone, H. A. (2000). A generalized view of foam drainage: experiment and theory. Langmuir, 16(15), 6327-6341.

Larson, R. G. (1999). The structure and rheology of complex fluids (topics in chemical engineering). Oxford University Press, Oxford, 86, 108.

Lazidis, A., de Almeida Parizotto, L., Spyropoulos, F., & Norton, I. T. (2017). Microstructural design of aerated food systems by soft-solid materials. Food Hydrocolloids, 73, 110-119. doi:https://doi.org/10.1016/j.foodhyd.2017.06.032

Lesov, I., Tcholakova, S., & Denkov, N. (2014). Factors controlling the formation and stability of foams used as precursors of porous materials. Journal of Colloid and Interface Science, 426, 9-21. doi:https://doi.org/10.1016/j.jcis.2014.03.067

Li, Z., Geisel, K., Richtering, W., & Ngai, T. (2013). Poly(N-isopropylacrylamide) microgels at the oil-water interface: adsorption kinetics. Soft Matter, 9(41), 9939-9946. doi:10.1039/C3SM52168K

Li, Z., & Ngai, T. (2013). Microgel particles at the fluid–fluid interfaces. Nanoscale, 5(4), 1399-1410.

Liu, Q., Zhang, S., Sun, D., & Xu, J. (2009). Aqueous foams stabilized by hexylamine-modified Laponite particles. Colloids and Surfaces A: Physicochemical and Engineering Aspects, 338(1-3), 40-46.

Liu, Q., Zhang, S., Sun, D., & Xu, J. (2010). Foams stabilized by Laponite nanoparticles and alkylammonium bromides with different alkyl chain lengths. Colloids and Surfaces A: Physicochemical and Engineering Aspects, 355(1-3), 151-157.

Lopetinsky, R. (2006). Solids-stabilized emulsions: a review. In Binks, B. P., & Horozov, P. (Ed.), Colloidal Particles at Liquid Interfaces: Cambridge University Press.

Louvet, N., Höhler, R., & Pitois, O. (2010). Capture of particles in soft porous media. Physical Review E, 82(4), 041405.

Lundin, L., & Hermansson, A.-M. (1995). Supermolecular aspects of xanthan-locust bean gum gels based on rheology and electron microscopy. Carbohydrate Polymers, 26(2), 129-140.

Medin, A. S. (1995). Studies of structure and properties of agarose. Acta Universitatis, PhD Thesis.

Mitchell, J. (1976). Rheology of gels. Journal of Texture Studies, 7(3), 313-339.

Moakes, R., Sullo, A., & Norton, I. (2015a). Preparation and characterisation of whey protein fluid gels: The effects of shear and thermal history. Food Hydrocolloids, 45, 227-235.

Moakes, R. J. A., Sullo, A., & Norton, I. T. (2015b). Preparation and characterisation of whey protein fluid gels: The effects of shear and thermal history. Food Hydrocolloids, 45, 227-235. doi:http://dx.doi.org/10.1016/j.foodhyd.2014.11.024

Möbius, D., Miller, R., & Fainerman, V. B. (2001). Surfactants: chemistry, interfacial properties, applications (Vol. 13): Elsevier.

Mori, I. (2016). Vegan Society Poll. Retrieved from

Morris, E., Cutler, A., Ross-Murphy, S., Rees, D., & Price, J. (1981). Concentration and shear rate dependence of viscosity in random coil polysaccharide solutions. Carbohydrate Polymers, 1(1), 5-21.

Morris, E. R. (1994). Rheological and organoleptic properties of food hydrocolloids. In Food Hydrocolloids (pp. 201-210): Springer.

Morris, E. R., Rees, D. A., Norton, I. T., & Goodall, D. M. (1980). Calorimetric and chiroptical evidence of aggregate-driven helix formation in carrageenan systems. Carbohydrate Research, 80(2), 317-323.

Murphy, R. W., Farkas, B. E., & Jones, O. G. (2016). Dynamic and viscoelastic interfacial behavior of β-lactoglobulin microgels of varying sizes at fluid interfaces. Journal of Colloid and Interface Science, 466, 12-19.

Murray, B. S., & Ettelaie, R. (2004). Foam stability: proteins and nanoparticles. Current Opinion in Colloid & Interface Science, 9(5), 314-320.

NHS. (2017). How does sugar in our diet affect our health?

NHS. (2018, 01/05/2017). Fat: the facts.

Nishinari, K., & Doi, E. (2012). Food hydrocolloids: structures, properties, and functions: Springer Science & Business Media.

Nishinari, K., & Fang, Y. (2017). Relation between structure and rheological/thermal properties of agar. A mini-review on the effect of alkali treatment and the role of agaropectin. Food Structure, 13, 24-34. doi:https://doi.org/10.1016/j.foostr.2016.10.003

Nishinari, K., Zhang, H., & Ikeda, S. (2000). Hydrocolloid gels of polysaccharides and proteins. Current Opinion in Colloid & Interface Science, 5(3), 195-201.

Norton, A. (2016). Microstructural understanding of hydrocolloid and mixed hydrocolloid systems for biomedical applications. Univeristy of Birmingham, eThesis.

Norton, I., Jarvis, D., & Foster, T. (1999). A molecular model for the formation and properties of fluid gels. International Journal of Biological Macromolecules, 26(4), 255-261.

Norton, I. T., Foster, T., & Brown, R. (1998). The science and technology of fluid gels. In Williams, P. A., & Phillips G. O. (Eds.), Gums and Stabilisers for the Food Industry, (Vol. 9, pp. 259-268): Royal Society of Chemistry, Cambridge.

Norton, I. T., Goodall, D. M., Morris, E. R., & Rees, D. A. (1983). Role of cations in the conformation of iota and kappa carrageenan. Journal of the Chemical Society, Faraday Transactions 1: Physical Chemistry in Condensed Phases, 79(10), 2475-2488.

Norton, J. E., & Norton, I. T. (2010). Designer colloids—towards healthy everyday foods? Soft Matter, 6(16), 3735-3742.

Oakenfull, D., & Glicksman, M. (1987). Gelling agents. Critical Reviews in Food Science & Nutrition, 26(1), 1-25.

Phillips, G. O., & Williams, P. A. (2009). Handbook of Hydrocolloids: Elsevier.

Pickering, S. U. (1907). Emulsions. Journal of the Chemical Society, Transactions, 91, 2001-2021.

Pugh, R. J. (2016). Bubble and foam chemistry: Cambridge University Press.

Rayner, M., Marku, D., Eriksson, M., Sjöö, M., Dejmek, P., & Wahlgren, M. (2014). Biomass-based particles for the formulation of Pickering type emulsions in food and topical applications. Colloids and Surfaces A: Physicochemical and Engineering Aspects, 458, 48-62.

Rees, D. (1963). The carrageenan system of polysaccharides. Part I. The relation between the κ-and λ-components. Journal of the Chemical Society (Resumed), 1821-1832.

Rees, D. A. (1969). Structure, Conformation, and Mechanism in the Formation of Polysaccharide Gels and Networks. In Wolfrom, M. L., Tipson, R. S., & Horton, D. (Eds.), Advances in Carbohydrate Chemistry and Biochemistry (Vol. 24, pp. 267-332): Academic Press.

Rio, E., Drenckhan, W., Salonen, A., & Langevin, D. (2014). Unusually stable liquid foams. Advances in Colloid and Interface Science, 205, 74-86.

Rochas, C., & Rinaudo, M. (1984). Mechanism of gel formation in κ-carrageenan. Biopolymers: Original Research on Biomolecules, 23(4), 735-745.

Rousseau, D. (2000). Fat crystals and emulsion stability—a review. Food Research International, 33(1), 3-14.

Rovers, T. A., Sala, G., Van der Linden, E., & Meinders, M. B. (2016). Potential of Microbubbles as Fat Replacer: Effect on Rheological, Tribological and Sensorial Properties of Model Food Systems. Journal of Texture Studies, 47(3), 220-230.

Saha, D., & Bhattacharya, S. (2010). Hydrocolloids as thickening and gelling agents in food: a critical review. Journal of Food Science and Technology, 47(6), 587-597.

Saint-Jalmes, A. (2006). Physical chemistry in foam drainage and coarsening. Soft Matter, 2(10), 836-849.

Saint-Jalmes, A., Peugeot, M.-L., Ferraz, H., & Langevin, D. (2005). Differences between protein and surfactant foams: microscopic properties, stability and coarsening. Colloids and Surfaces A: Physicochemical and Engineering Aspects, 263(1-3), 219-225.

Seguchi, M. (2001). Oil binding ability of chlorinated and heated wheat starch granules and their use in breadmaking and pancake baking. Starch-Stärke, 53(9), 408-413.

Stanley, D., Goff, H., & Smith, A. (1996). Texture-structure relationships in foamed dairy emulsions. Food Research International, 29(1), 1-13.

Stocco, A., Rio, E., Binks, B. P., & Langevin, D. (2011). Aqueous foams stabilized solely by particles. Soft Matter, 7(4), 1260-1267.

Sworn, G., Sanderson, G. R., & Gibson, W. (1995). Gellan gum fluid gels. Food Hydrocolloids, 9(4), 265-271. doi:http://dx.doi.org/10.1016/S0268-005X(09)80257-9

Thomas, S. (2008). Hydrocolloid dressings in the management of acute wounds: a review of the literature. International Wound Journal, 5(5), 602-613.

Walstra, P. (1989). Principles of foam formation and stability. In Wilson, A. J. (Eds.), Foams: Physics, chemistry and structure (pp. 1-15): Springer.

Walstra, P. (2003). Physical chemistry of foods: CRC Press.

Weaire, D. H., S. (1999). The physics of foams. New York: Oxford University Press.

Weaire, D. L., & Hutzler, S. (2001). The physics of foams: Oxford University Press.

Wilde, P., Mackie, A., Husband, F., Gunning, P., & Morris, V. (2004). Proteins and emulsifiers at liquid interfaces. Advances in Colloid and Interface Science, 108-109, 63-71. doi:https://doi.org/10.1016/j.cis.2003.10.011

Williams, P. A., Phillips, G O., & de Vries, J. (2004). Hydrocolloid gelling agents and their applications. In Williams, P. A., Phillips, G O. (Eds.), Gums and Stabilisers for the Food Industry (Vol. 12, pp. 23-31). Cambridge: The Royal Society of Chemsitry.

Williams, P. A., & Phillips, G. O. (2000). 1 - Introduction to food hydrocolloids. In Phillips G. O., & Williams, P. A. (Eds.), Handbook of Hydrocolloids (Second Edition) (pp. 1-22): Woodhead Publishing.

Zhang, S., Lan, Q., Liu, Q., Xu, J., & Sun, D. (2008). Aqueous foams stabilized by Laponite and CTAB. Colloids and Surfaces A: Physicochemical and Engineering Aspects, 317(1-3), 406-413.

Zúñiga, R. N., & Aguilera, J. M. (2008). Aerated food gels: fabrication and potential applications. Trends in Food Science & Technology, 19(4), 176-187. doi:http://dx.doi.org/10.1016/j.tifs.2007.11.012

Chapter 3: AGAR FLUID GELS AND THE STABILISATION OF THEIR FOAMS

Based on work published as: Ellis, A. L., Norton, A.B., Mills, T.B., & Norton, I.T. (2017). Stabilisation of foams by agar gel particles. *Food Hydrocolloids, 73*, 222-228.

3.1 Background

The aim of this chapter was ultimately to relate the properties of agar fluid gels before and after aeration in order to predict foaming characteristics. Firstly, the production methods and their effect upon gel particles were studied to advance the understanding from previous literature. The effect of added surfactant on fluid gel formation and properties upon storage was explored along with changing agar concentration, using rheology and texture analysis. Agar fluid gels were then aerated; foamability and foam stability were measured allowing an overall mechanism of stability to be determined. Furthermore, the thixotropy of a fluid gel compared to a quiescently set gel was investigated in order to provide insight into the advantage of using fluid gels in aerated systems. In addition, the temperature at which fluid gels exit the pin stirrer during production (T_{exit}) was altered to investigate the effect of quiescent ordering on structural recovery and in turn, foam stability.

3.2 Materials and Methods

3.2.1 Materials

Agar and Tween 20 were obtained from Sigma Aldrich (UK). All concentrations were calculated as a weight percentage. Materials were used with no further purification or modification.

3.2.2 Preparation of agar fluid gels using a rheometer

The required mass of agar ± 0.5 wt% Tween 20 was dispersed in deionised water heated to 90 °C, whilst stirring. Tween 20 was used to allow the aeration of fluid gels. As the CMC of Tween 20 is quite low (0.0074 wt% (Mittal, 1972)), which is typical of non-ionic surfactants, it was used at this concentration in order to increase foamability. Solutions were covered to minimise loss of water due to evaporation. Fluid gels were produced in a rheometer using vane geometry (Kinexus, Malvern, UK). Aliquots of solution were transferred to the rheometer cup, pre-heated to 90 °C. The temperature was allowed to equilibrate for 5 min and was then decreased from 90 °C to 5 °C at a cooling rate of 2 °Cmin^{-1}, whist the sample was under a shear rate of 500 s^{-1}. Each sample was prepared in triplicate and stored at 5 °C.

3.2.3 Preparation of agar fluid gels using pin stirrer

Fluid gels for the application of foaming were prepared in a continuous process pin stirrer as this allows larger scale production. The required mass of agar and 0.5 wt% Tween 20 was dispersed in deionised water heated to 90 °C, whilst stirring. The solution was then fed into the jacketed pin stirrer cooled to 5 °C, through a peristaltic pump. The inlet temperature was controlled to ≈ 70 °C and the outlet to 5 °C to ensure gelation occurred under shear (gelation temperature ≈ 30 °C). The speed of the pump was set to 20 mLmin^{-}

[1] to achieve a residence time of 7.5 min in the pin stirrer resulting in a cooling rate of 8 °Cmin^{-1}. The shaft rotation speed was set to 1500 rpm as this has been previously reported by Gabriele, Spyropoulos, and Norton (2010) to give a narrow size distribution of particles. Fluid gels were stored at 5 °C.

3.2.4 Preparation of foams and determination of foam overrun

Mechanical agitation using a Hobart mixer was employed to aerate fluid gels. Air sparging was attempted, however it produced very large bubbles due to flow rate and sample viscosity limitations. Mechanical agitation was therefore used at high mixing speeds to provide high overruns, whilst also mimicking the techniques used commercially. Equal volumes of fluid gels were whipped at the highest speed setting for 5 minutes. The foaming ability of the systems was investigated by determining foam overrun (Equation 3.1), measuring the amount of air incorporated into the system by weighing equivalent volumes of the original fluid gel sample and the sample after whipping. Experiments were carried out in three replicates.

$$\text{Overrun (\%)} = \left(\frac{m_{\text{fluid gel}}}{m_{\text{foam}}}\right) \text{x } 100 \quad (3.1)$$

3.2.5 Determination of foam half-life

The stability of the foams was determined using foam half-life measurements. The reduction of the foam height by half was recorded using a CCD camera and the half-life was later calculated. Experiments were carried out in three replicates.

3.2.6 Rheological methods

Rheological measurements were performed using a Kinexus rheometer (Malvern, UK) at 25 °C and 48 hours after production, to ensure post-production particle ordering completion (de Carvalho & Djabourov, 1997; Gabriele, Spyropoulos, & Norton, 2009; Garrec, Guthrie, & Norton, 2013). Equilibrium flow curves were obtained by recording shear viscosity through a range of applied shear rates (0.001-500 s^{-1}). Amplitude sweeps were conducted at a frequency of 1 Hz as a function of applied oscillatory strain. A cone, with an angle of 4° and diameter of 40 mm, and plate geometry was used. To avoid slip a serrated parallel plate geometry was used (60 mm parallel plate and serrated bottom plate set at a 1 mm gap). Thixotropic loops were conducted by increasing the shear rate from 0.1-500 s^{-1} and then backwards with no holding time. Experiments were carried out in three replicates.

3.2.7 Surface tension measurements

Surface tension measurements of agar fluid gels produced in the pin stirrer and later aerated were performed using a Kruss GmbH K100 tensiometer (Hamburg, Germany). The Wihelmy plate method was used to measure static surface tension at an immersion depth of 2mm for an equilibration time of 2400 s at 25 °C. Experiments were carried out in three replicates.

3.2.8 Imaging fluid gel particles

The phase contrast setting of an optical microscope (Leica Microsystems, UK) was used to image fluid gel particles using objective lenses up to 20x magnification. Fluid gels were diluted with deionised water (1:4) and dropped onto a microscope slide with a coverslip.

3.2.9 Texture Analysis

Quiescently cooled agar gels were stored at 5 °C for 48 hours to ensure their exposure to the same conditions as fluid gels. Compression tests were completed using a TA XT plus Texture Analyser (Stable Micro Systems Ltd, UK). A 40 mm diameter cylindrical aluminium probe was used at a compression rate of 1 mms^{-1}. Prepared samples of 21 mm in diameter and 10 mm in height were compressed to 50% strain and tests were carried out in three replicates. The force/distance data was converted to true strain (ε) and true stress (σ). From the gradient of the linear region at 0-5% strain, the initial Young's modulus was determined (Bradbeer, Hancocks, Spyropoulos, & Norton, 2014). Experiments were carried out in three replicates.

3.2.10 Micro Computed Tomography (Micro-CT)

Foam samples were scanned using a desktop X-ray micro-CT system (Skyscan 1172, Bruker, Belgium) at a voltage of 61 kV and current of 100 μA. The radiograph images of each scan were reconstructed into 582 2D images using the Nrecon software and analysis was done using CTan software.

3.3 Results and Discussion

3.3.1 Preparation and characterisation of agar fluid gels

Agar fluid gels were produced using a rheometer, as this method allows the kinetics of fluid gel formation to be monitored (Figure 3.1). The viscosity increase was measured whilst cooling through the ordering and gelation temperature under an applied shear. The viscosity increased gradually as the temperature was decreased, until a sharp rise was observed at ≈ 30 °C, indicating the beginning of gelation. Norton, Jarvis, and Foster (1999) described the formation of small gel nuclei, which upon further cooling continue to grow to an equilibrium particle size determined by the shear rate. The effect of shear rate on final fluid gel particle size has been previously studied by Gabriele (2011) and particle size was found not to significantly change above a critical shear rate (and at the shear rates used in this study). Agar concentration, however, is a significant parameter and so its effect on fluid gel formation is evaluated here. From Figure 3.1, the temperature of ordering can be observed to increase with agar concentration. This is a result of quicker gelation due to a higher number of particles (Norton, Foster, & Brown, 1998). The final shear viscosity (at 5 °C) also increased with agar concentration. This is because firstly, a higher concentration of agar relates to a higher volume fraction and therefore particle interaction (Garrec et al., 2013; Norton et al., 1999) and secondly, the rigidity of the particles themselves increase (Frith et al., 2002).

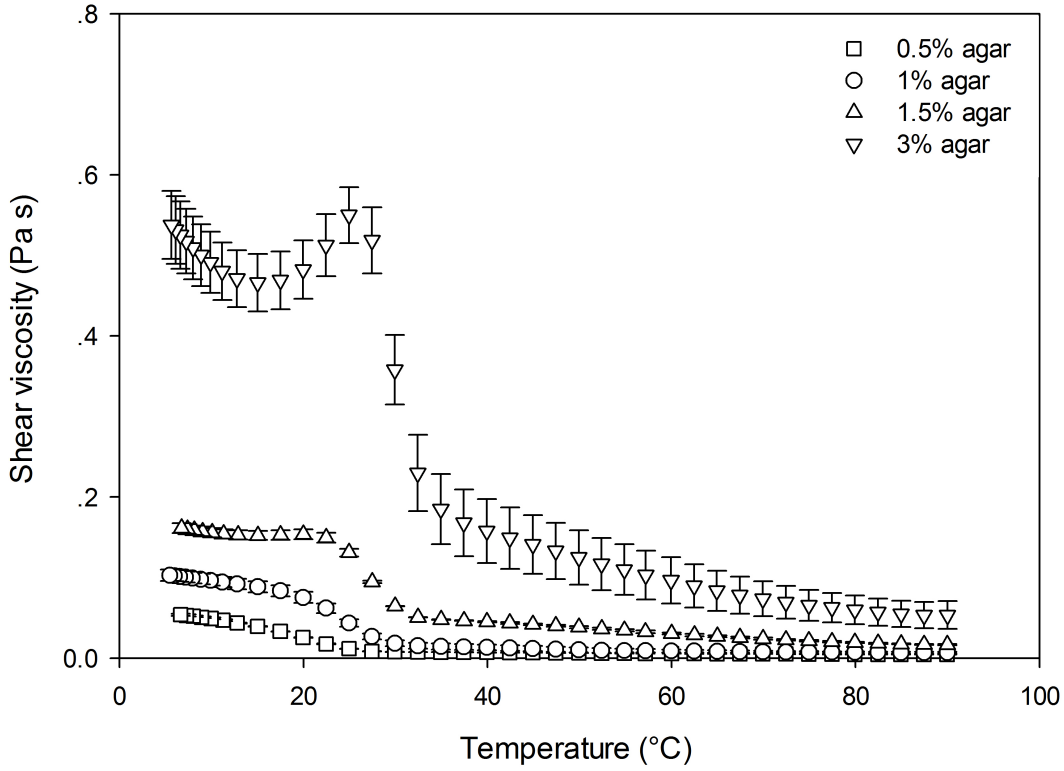


Figure 3.1: Viscosity profiles during fluid gel production at different agar concentrations.

The aim of this study was to produce fluid gels with the ability to be aerated. Therefore, a non-ionic surfactant, Tween 20, was incorporated into the fluid gels at a fixed concentration. Tween 20 has the highest water-solubility of all the Tweens and forms a mobile monomolecular layer when stabilising foams (Patino, Niño, & Gómez, 1997). The effect of incorporating this non-ionic surfactant into agar fluid gels at various agar concentrations was investigated (Table 3.1). Firstly, it is likely some Tween 20 was entrapped within the fluid gel particles, however, it has been reported that if interactions do occur between agar and non-ionic surfactants they are likely to be weak (Prasad et al., 2005). Secondly, gelation temperatures appear to decrease in the presence of Tween 20 (Table 3.1) however this is by less than 10% and is unlikely to be statistically different. A potential explanation is the effect of solvent quality, as the addition of Tween 20 leaves less water available for structuring. In addition, the viscosity of the agar fluid gels were measured after 48 hours storage (Table 3.1) and the presence of Tween 20 did not appear

to significantly affect their rheological behaviour. Furthermore, the material properties were investigated. The initial Young's moduli of quiescently cooled gels at the same agar concentration were measured. The initial Young's modulus reflects the stiffness/deformability of the gel matrix, until structure failure occurs (Bradbeer et al., 2014) and has been reported by Frith et al. (2002) to reflect the rigidity of the fluid gel particles themselves. The addition of Tween 20 did not significantly affect the Young's initial modulus of quiescently cooled agar gels (Table 3.1) and is therefore inferred not to significantly affect the rigidity of agar fluid gel particles.

Table 3.1: The effect of Tween 20 addition on the gelation temperatures and material properties upon storage of fluid gels at different agar concentrations. Initial Young's modulus was measured from quiescently set gels.

Concentration of agar (%)	Concentration of Tween 20 (%)	Gelation temperature (°C)	Viscosity at 1 s^{-1} (Pa s)	Initial Young's initial modulus (kPa)
0.5	0	27.3 (±0.3)	1.1 (±0.0)	5.3 (±0.5)
	0.5	25.2 (±0.4)	0.9 (±0.1)	5.1 (±0.4)
1	0	31.7 (±0.2)	1.7 (±0.2)	30.7 (±2.0)
	0.5	30.8 (±0.3)	1.4 (±0.0)	31.0 (±4.4)
1.5	0	33.0 (±0.2)	2.1 (±0.1)	62.3 (±5.3)
	0.5	32.3 (±0.3)	1.9 (±0.2)	66.6(±11.7)
3	0	34.09 (±0.2)	10.0 (±0.2)	246.1 (±10.4)
	0.5	N/A	N/A	253.2 (±31.9)

In order to produce larger quantities of fluid gel for aeration purposes, a continuous process pin stirrer was used to manufacture fluid gels (described in Section 3.2.3). The conformation of gel particles is an important factor when considering the rheological behaviour of fluid gels and their behaviour upon aeration, in particular when they are confined to foam channels. Fluid gels were therefore diluted and imaged using phase contrast microscopy. Agar fluid gels at 1% agar produced by different methods are shown

in Figure 3.2. These micrographs show that particle shape was significantly affected by the production method. Fluid gels produced using a vane geometry in the rheometer appeared as previously reported by Norton et al. (1999); individual slightly "hairy" anisotropic particles (Figure 3.2a). Agar fluid gels manufactured in the pin stirrer, however, consisted of particles with smaller cores and protruding tails into the continuous phase (Figure 3.2b). The difference in particle shape can be attributed to the difference in shear environment and the effect this has upon the kinetics of gelation (including cooling rate) and consequently, particle formation and shape. Fluid gel particles form through the growth of initial gel nuclei to an equilibrium particle size dictated by the shear. The shear environment experienced in the rheometer resulted in particles with larger, more spherical cores and smoother surfaces. Fluid gels produced on the pin stirrer, however, experienced a shear profile that resulted in the formation of particles with small cores and many protruding long 'tails' into the continuous phase, resulting in a larger hydrodynamic volume. It is likely that these tails usually re-form with the main particle core during further molecular ordering to produce smother particles with a more spherical shape (e.g. those produced in the rheometer) (Gabriele et al., 2009; Norton et al., 1999). However, this did not occur during pin stirrer production. This was the first time that agar fluid gel particles made using the pin stirrer have been visualised, however, recent work by Holland, Tuck, and Foster (2018) reported similar structures when producing agar fluid gels using a stirred pot. The authors gave a similar explanation where less controlled flow fields were said to be responsible. They also reported a difference in particle conformation between agar of different sources.

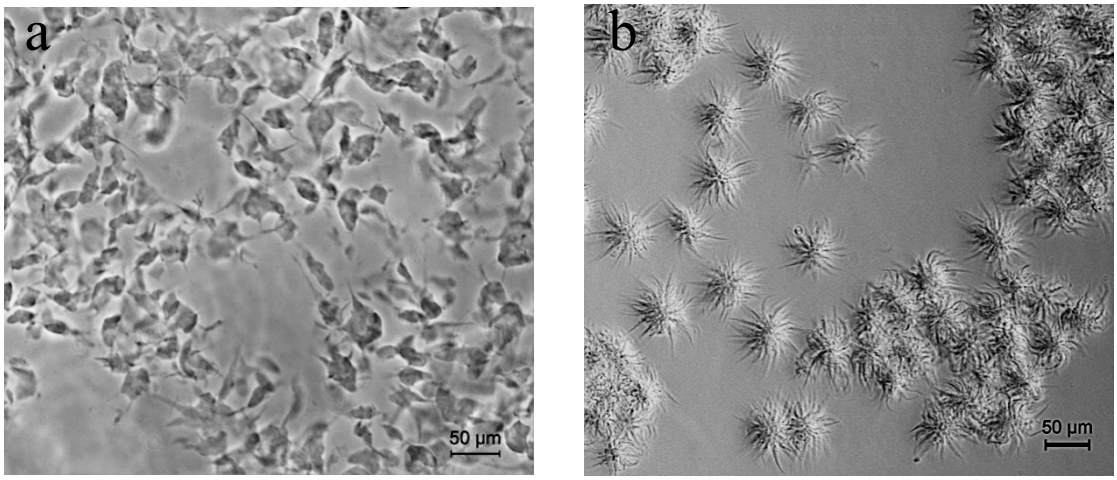


Figure 3.2: Micrographs of 1% agar with Tween 20 fluid gels produced in (a) a rheometer with vane geometry and (b) in a pin stirrer, using phase contrast microscopy.

In order to investigate how particle shape can affect the interactions between particles and therefore their rheological behaviour, yield stress values were evaluated. These were determined from amplitude sweeps on a rheometer, as seen in Figure 3.3. Yield stress was calculated as the stress required to decrease G' by 5% from the linear viscoelastic region (LVR), i.e. the critical stress required to disrupt particle interactions and cause particles to flow. The yield stress of 1% agar fluid gel prepared on the rheometer was 0.17 (±0.06) Pa whilst on the pin stirrer it was 0.63 (±0.13) Pa. Fluid gels manufactured on the pin stirrer had higher yield stress values and, therefore, more particle interaction. It is thought that the branched nature of the particles caused them to interact to a higher extent than the more spherical, less branched rheometer made particles. Manufacture using the pin stirrer provided a different shear profile that therefore resulted in kinetically trapping gelled regions into these novel-shaped particles, which resulted in enhanced particle interaction.

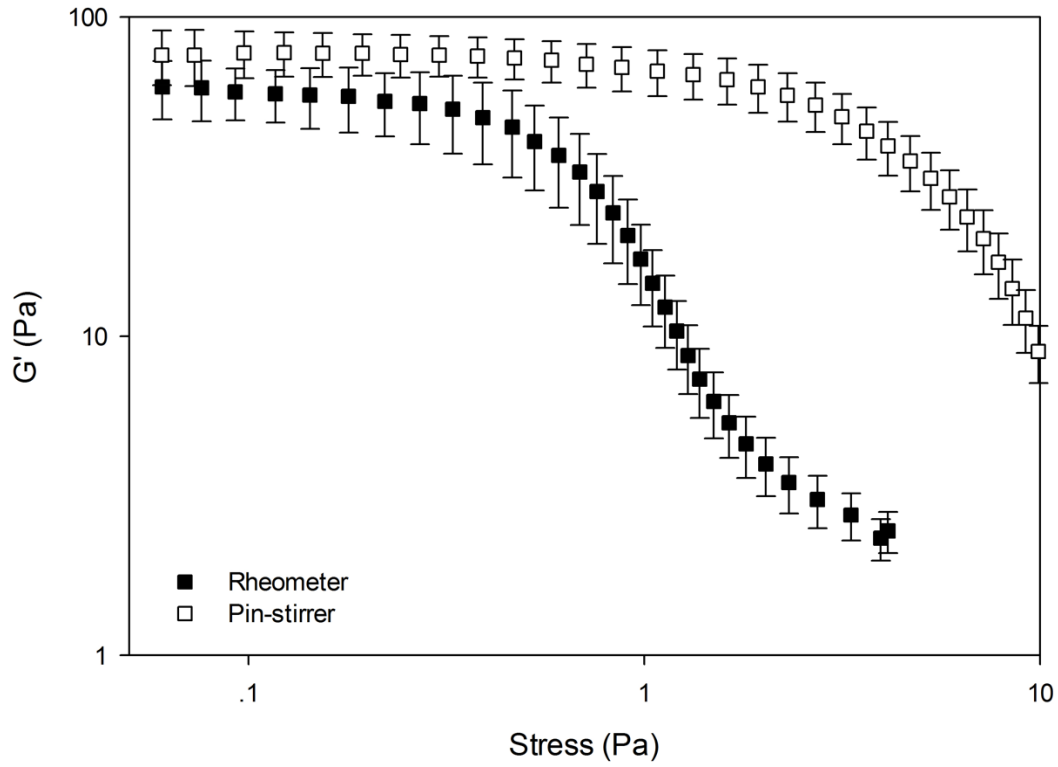


Figure 3.3: Storage modulus (G') as a function of stress during oscillatory strain sweeps of agar fluid gels produced on both the rheometer and pin stirrer, 48 hours after production. Yield stress was calculated as the stress required to decrease G' from the LVR by 5%.

3.3.2 Rheological properties

The bulk viscosity of foaming solutions affect the mobility of the continuous phase and therefore drainage velocity (Saint-Jalmes, 2006). The viscosity profiles of agar fluid gels at various concentrations were measured 48 hours after production (Figure 3.4). All systems showed shear thinning behaviour as expected for interacting particulate systems; at low shear rates, particles were aggregated together resulting in a high viscosity, however, as the shear rate was increased, interactions were disrupted and viscosity reduced (Saha & Bhattacharya, 2010). At low phase volumes, particles typically behave as highly aggregated systems dominated by colloidal forces, however at high phase volumes like those here, particle modulus influences rheology, as well as particle interactions (Moakes, Sullo, & Norton, 2015). Shear viscosity increased upon raising agar concentration (Figure 3.4) due to an increase in phase volume, as well as an increase in

particle rigidity (particles contain a higher concentration of agar). The flow curves of fluid gels at 2.5% and 3% agar (coloured in grey in Figure 3.4) overlapped. This suggests that although particle rigidity was still increasing, volume fraction was limiting the viscosity.

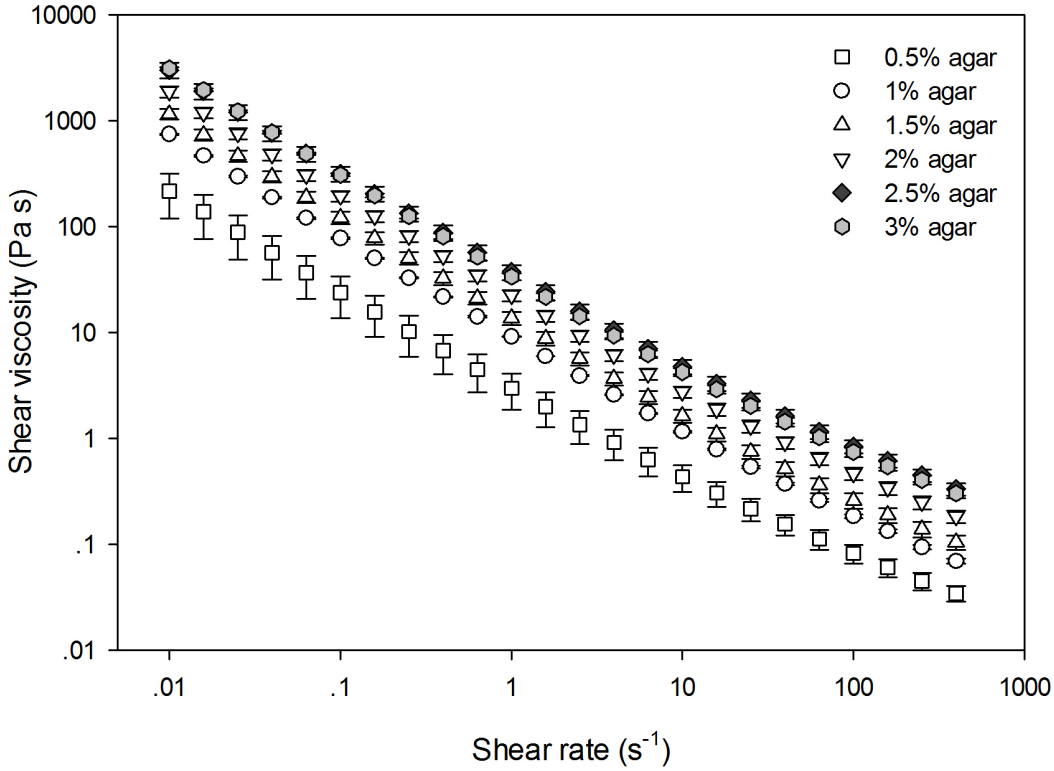


Figure 3.4: Viscosity profiles of agar fluid gels produced at different concentrations, 48 hours after production. The viscosity curves of 2.5% and 3% agar overlap and are therefore highlighted for clarity.

The viscoelastic behaviour of the fluid gel systems was assessed using oscillatory rheological data (Figure 3.5). Figure 3.5a shows that at each concentration, the storage modulus (G') dominated over the loss modulus (G'') which is indicative of interconnected structures (Ross-Murphy, 1994). G' increased with agar concentration due to an increase in volume fraction and particle rigidity (Garrec et al., 2013). The linear viscoelastic region (LVR) continued to a critical strain, where particle interactions were then disrupted. This causes the system to flow which can be seen by a decrease in G' (Figure 3.5b). The yield stress of fluid gels at different concentrations were determined from the strain sweeps as the stress required to decrease G' in the LVR by 5%. Yield

stress increased with agar concentration due to an increase in particle stiffness and enhanced particle interaction caused by higher phase volumes (Garrec et al., 2013). Fluid gels at 2.5% and 3% agar still observed differences in their G' and yield stress despite their similar viscosity profiles, which had indicated a maximum packing fraction. G' increased from 498 (±27) Pa at 2.5% agar to 695 (±32) Pa at 3% agar and the yield stress increased from 2.0 (±0.2) Pa to 3.3 (±0.2) Pa (Figure 3.5). This can therefore be attributed to the difference in particle rigidity; agar particles at 3% were less deformable and so a greater stress was required to facilitate the movement of particles past one another and, hence, initiate flow. A similar observation has been reported by Adams, Frith, and Stokes (2004), who measured an increase in storage modulus of agar microgel particles by two orders of magnitude upon increasing particle modulus in suspension with phase volumes above maximum packing.

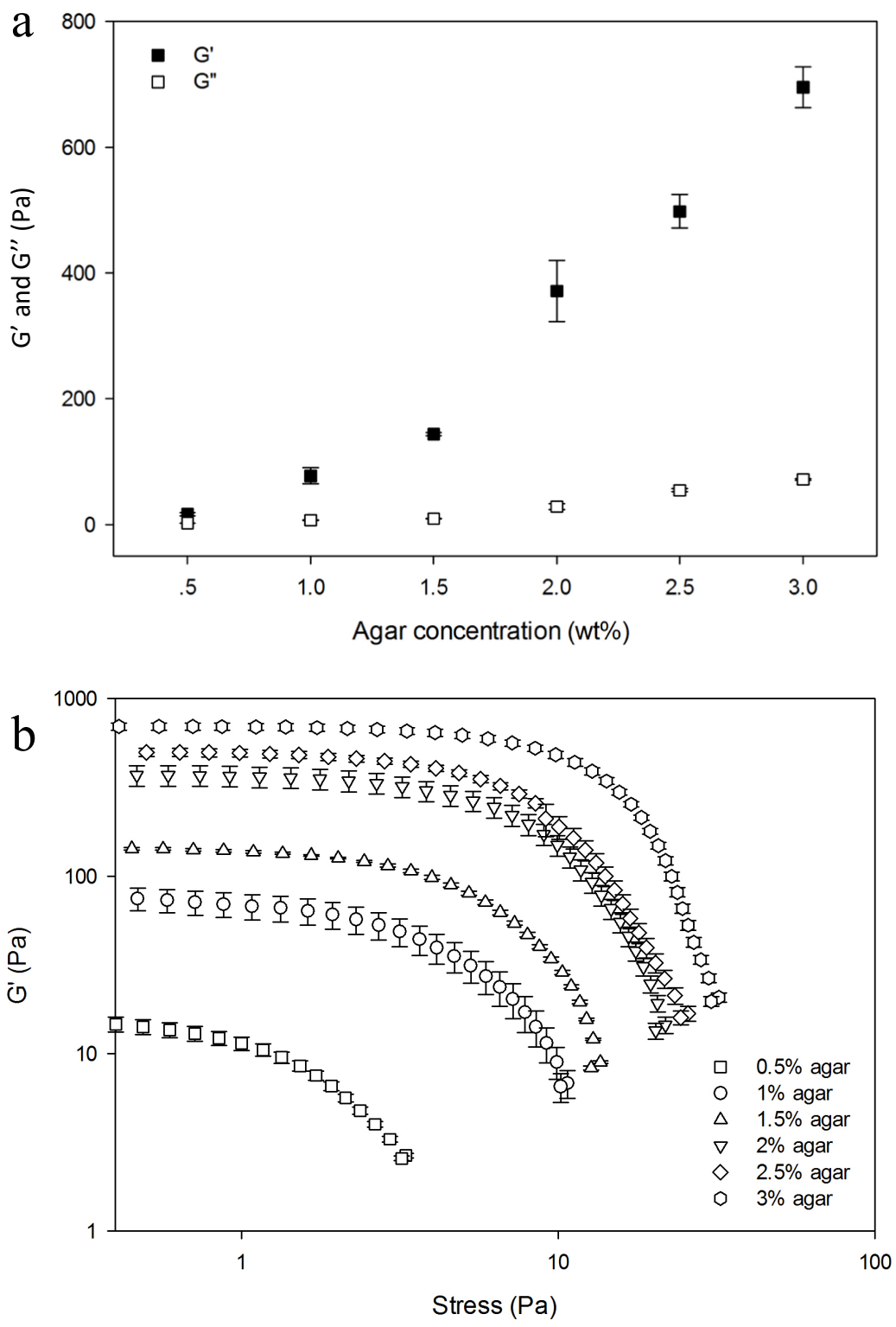


Figure 3.5: (a) Storage (G') and loss (G'') moduli as a function of applied oscillatory strain of agar fluid gels, 48 hours after production. (b) Storage modulus as a function of stress during oscillatory strain sweeps of agar fluid gels, 48 hours after production.

3.3.3 Foaming capabilities

The functionality of agar fluid gels with Tween 20 to produce stable foams was investigated. The ability of the systems to incorporate air was determined using foam overrun. Despite the reported difficulty of whipping air into particulate systems (Murray & Ettelaie, 2004), the soft elastic nature of the particles ensured foam overrun was high. The surface tension of the fluid gels was similar at all agar concentrations (Table 3.2). This suggests that when aerated, Tween 20 saturated the air-water interface in all cases and was therefore free to move within the continuous phase and not restricted by interactions with agar. However, overrun was observed to decrease upon increasing agar concentration (Table 3.2). Hence, this decrease in foam overrun was due to the viscoelastic properties of the fluid gels.

Table 3.2: Surface tension and foam overrun measurements of agar fluid gels with 0.5% Tween 20 at various agar concentrations.

Agar concentration (%)	**Surface tension after 2400 s (mN m^{-1})**	**Foam overrun (%)**
0	36.2 (±0.15)	2045 (±52)
0.5	39.3 (±1.4)	1270 (±27)
1	39.7 (±1.5)	820 (±28)
1.5	39.5 (±0.9)	671 (±13)
2.5	37.2 (±1.7)	448 (±61)
3	38.7 (±2.4)	281 (±37)

3.3.4 Foam stability mechanism

The foam stability at each concentration was assessed in terms of half-life measurements (Figure 3.6). The addition of agar into the system (from 0% to 0.5% agar) improved foam stability by a factor of eight. Foam half-life then continued to increase with agar concentration. Interestingly, foams produced at 0.5% to 2.5% agar exhibited a half-life of 24 hours or less, whereas the foam produced at 3% agar, displayed a half-life of six days. At this concentration, agar particles appeared to cease drainage for a considerable amount of time. Similar observations of particulate systems have been reported, where particles form a weak gel network, which results in a non-classical arrest of drainage. Several studies relate this to an increased yield stress of the foamed suspension (Gonzenbach et al., 2006; Guillermic et al., 2009; Lesov, Tcholakova, & Denkov, 2014).

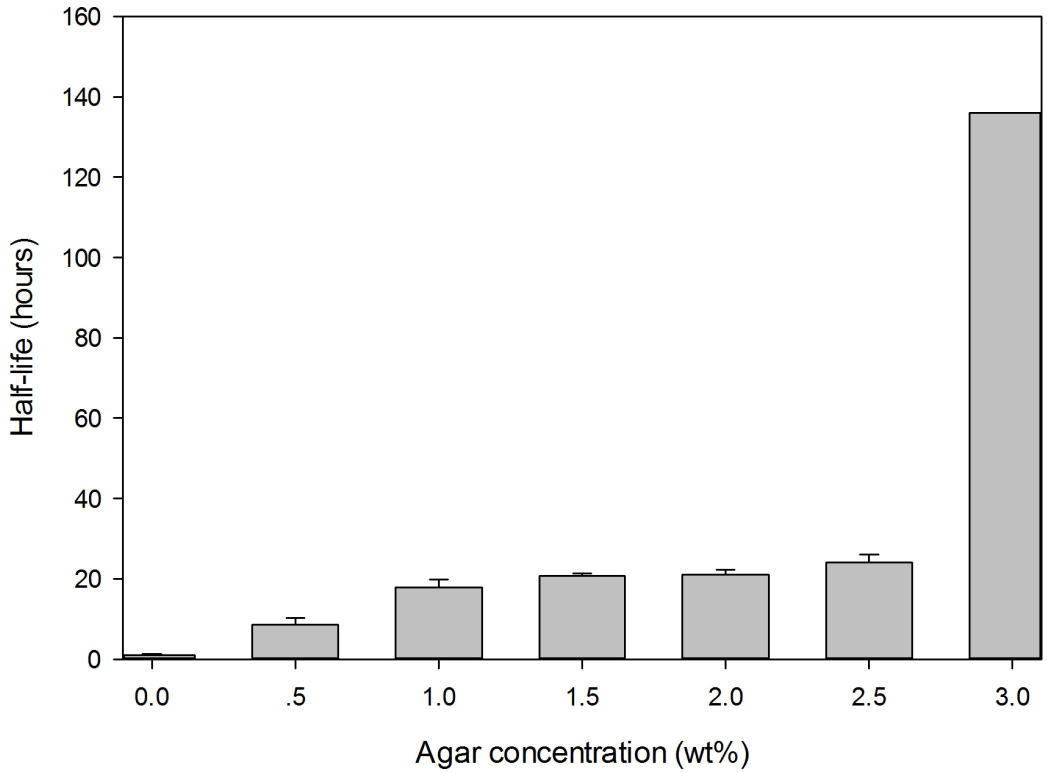


Figure 3.6: Foam half-life measurements as a function of agar concentration of aerated agar fluid gels with 0.5% Tween 20.

In order to investigate the mechanism of foam stability, the rheological properties of the suspending fluid (fluid gel) need to be considered. As discussed in Section 3.3.1, manufacturing fluid gels using the pin stirrer produced uniquely shaped particles that provided systems with high particle interaction. Increasing the concentration of agar, further increased particle interaction (through volume fraction) as well as particle rigidity, resulting in an increased yield stress (Figure 3.5b). This yield stress was plotted as a function of foam half-life in Figure 3.7. Foam half-life gradually increased with yield stress from 0.5% to 2.5% agar until stability dramatically improved at 3% agar. This behaviour appears to be a result of the yield stress of the suspending fluid reaching a critical point at 3% agar, which considerably slowed drainage. This can occur when the yield stress is larger than the gravitational stress inside the foam channels, as shown by Equation 3.2 (Guillermic et al., 2009; Sun & Gunasekaran, 2009), where p = fluid density, g = gravity and d = bubble radius. The bubble radius inside these foams ranged from 25 μm to 0.9 mm and so the gravitational stress inside the foams was typically in the order of 0.25-9 Pa. It is therefore feasible that this could have been overcome, especially when particles were confined in foam channels and nodes, which would have reduced gravitational stress whilst increasing their yield stress.

$$\sigma_y > pgd \qquad (3.2)$$

Agar fluid gels therefore provided stability through acting as a network of particles with a finite yield stress. Once confined within the foam network, the concentration of particles and therefore viscoelasticity would have been heightened. As the viscosity of fluid gels at 2.5% and 3% agar were very similar, the enhanced foam stability at 3% agar can be

attributed to a difference in viscoelasticity, in particular an increased particle modulus, as discussed in Section 3.3.2, which altered yield stress and ultimately enhanced foam stability.

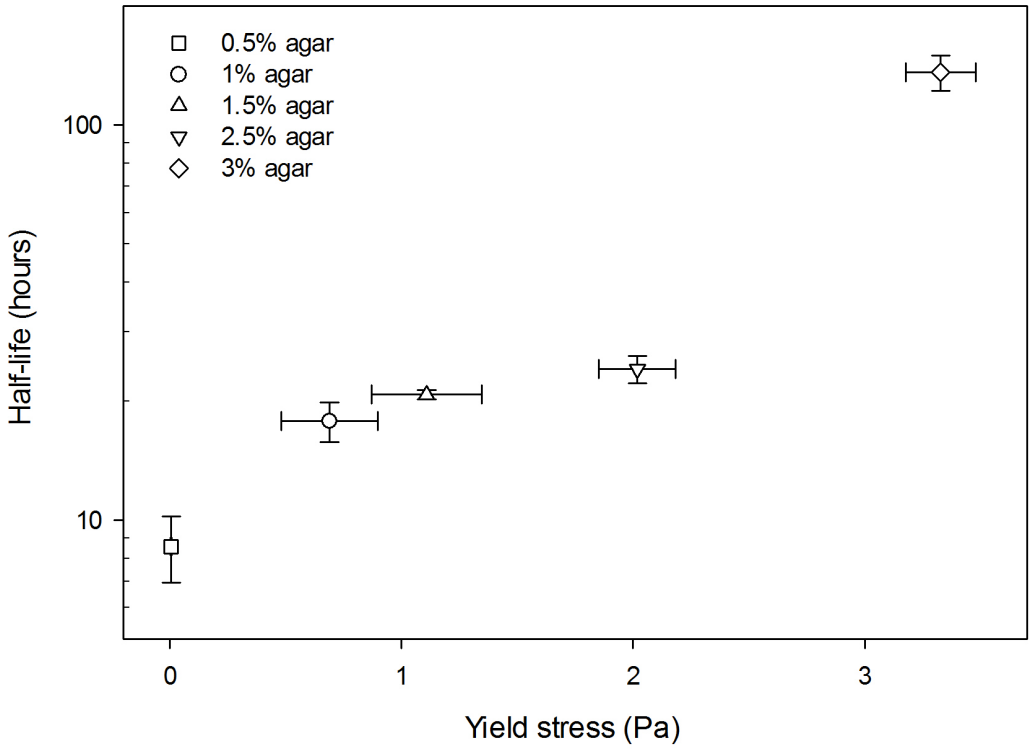


Figure 3.7: Yield stresses of agar fluid gels as a function of half-life measurements of their foams.

The microstructure of the aerated fluid gel at 3% agar was investigated using X-ray tomography. Figure 3.8 shows a 2D slice of the foam 30 minutes after aeration (a) and six days after aeration (b) at the foam half-life. Both images were taken at the same cross-section. X-ray images probe the internal microstructure of the foam; the size of foam components such as air cells and foam channels can therefore be observed. Initial air cells were polydisperse; bubbles ranged in size from ≈ 50 μm to 1.8 mm and liquid content was reasonably high resulting in wider channels within the foam network, where aggregated particles were likely "jammed". The number of air cells had decreased greatly and their size increased when the foam reached its half-life (Figure 3.8b). This highlights the importance of disproportionation and coarsening in the final collapse of the foam. In

addition, phase contrast optical microscopy of an aerated 1% agar fluid gel (Figure 3.8c) illustrated the ability of particles to be confined within the foam channels and nodes, as well as their ability to move within these channels due to their soft, elastic nature.

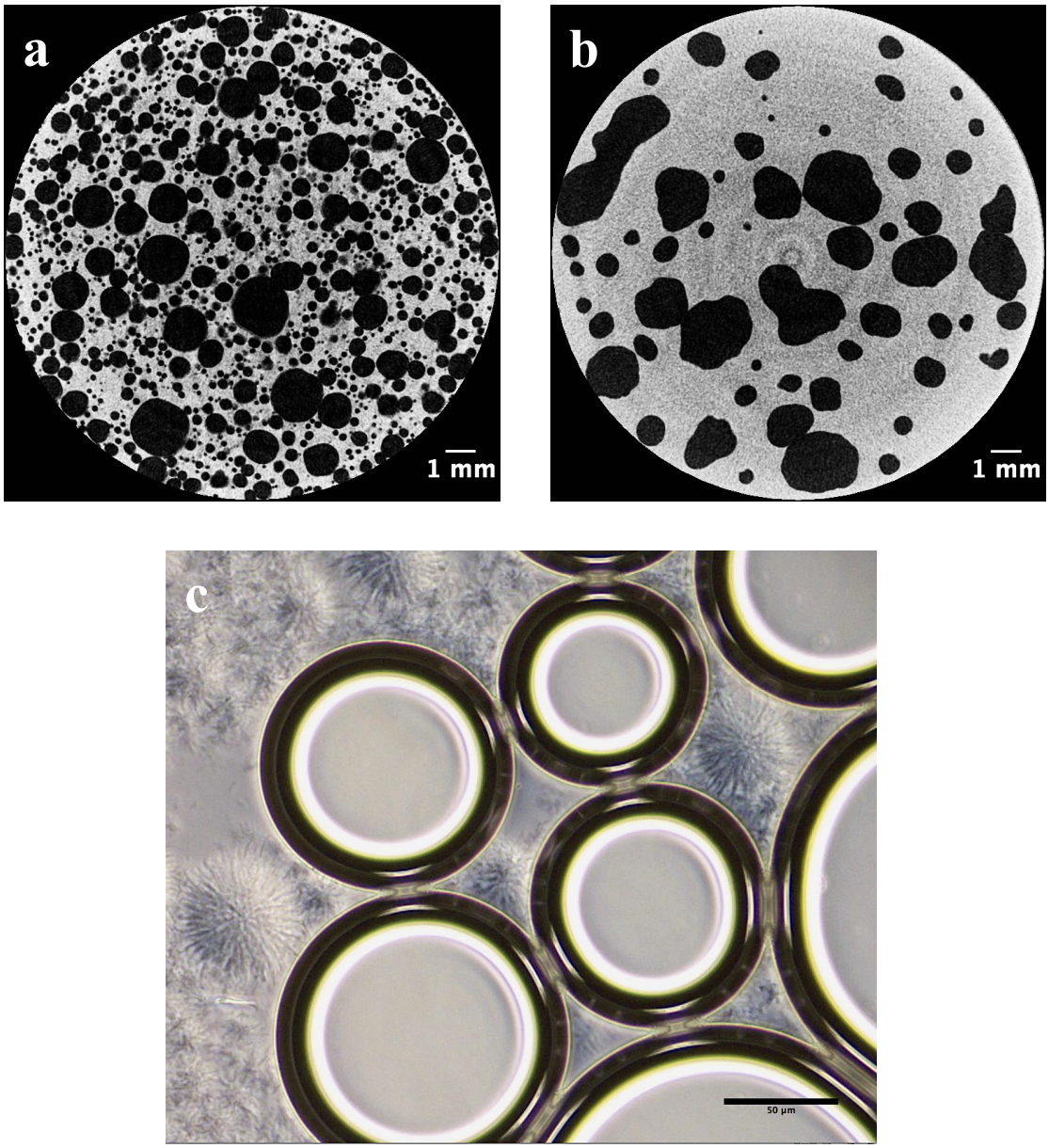


Figure 3.8: Micro-CT images of aerated 3% agar with Tween 20 fluid gels (a) 30 min after aeration and (b) 6 days after aeration. (c) Still of a video showing the microstructure of aerated 1% agar fluid gel and the plugging of particles in foam channels, observed using phase contrast microscopy.

From this evidence, the mechanism of foam stability can be thought of as follows: Tween 20 was used to establish short term stability and therefore creation of the foam through quick adsorption to the interface, which reduced the surface tension. Once the foam had

been generated, the continuous phase started to drain, allowing particles to be confined within the foam network. This accumulation of particles increased their effective concentration within the foam and therefore the viscoelasticity of the confined particle network. Once the yield stress was large enough, drainage was considerably reduced and the foam considerably more stable. The foams, however, did all eventually collapse. This was due to the ageing of the foam itself; coarsening of the gas phase would have caused an increase in bubble radius and therefore gravitational stress (Equation 3.2). Eventually, the suspension yield stress would have been overcome and drainage of the continuous phase would have increased (or re-started). Consequently, the foam channels would have narrowed considerably and few particles would have remained in the foam network. Eventually these particles would have been excluded from the foam network, resulting in the coalescence of bubbles and the ultimate collapse of the foam. The Micro-CT image of aerated 3% agar fluid gel at its half-life (Figure 3.8b) supports this hypothesis, as the foam channels are wide and few air cells remain.

3.3.5 Fluid gel thixotropy

It was hypothesised that the advantage of particulate gels over weak, flowable biopolymer gels is their ability to recover upon shear. Biopolymer gels at low concentrations can also reduce liquid drainage through possessing the required yield stress (Blom et al., 2016) however, most weak gels cannot recover upon shear. Gel particulate systems can therefore show benefits in some practical applications that require robust system performance upon shearing. In addition, using fluid gels provides further ways to manipulate yield stress (through both processing and formulation), which can be useful when designing microstructure for specific applications. For example, volume fraction, particle shape, rigidity and interactions can be altered, whereas only the volume fraction

and gel strength of quiescent gels can be manipulated. To investigate the rheological recovery of a fluid gel compared to a quiescently set gel, thixotropic loops were conducted on systems of a similar initial shear viscosity. Thixotropy tests describe a material's time-dependent rheological properties, which is particularly useful when studying suspensions which display inter-particle ordering. In these tests, the shear rate was ramped up from rest to 500 s^{-1} and then decreased backwards with no hold. The shear stress is plotted as a function of shear rate in Figure 3.9, for a fluid gel (1.5% agar) and a quiescently set gel (0.3% agar). These concentrations were chosen as the materials exhibited similar initial shear viscosities (105.5 ± 10.3 Pa s for 1.5% agar fluid gel and 123.3 ± 14.6 Pa s for 0.3% quiescent gel). Both structures revealed thixotropic behaviour since a hysteresis was displayed between the forward and backward curve (Figure 3.9). This indicates a time-dependent behaviour where the rate of structure breakdown is greater than that of re-building. To measure thixotropy and therefore structure recovery, the area of the hysteresis loop i.e. the area enclosed by the forward and backward curve was calculated. This provides an estimate of the magnitude of thixotropy, where higher values indicate higher thixotropy and less recovery of the structure after shear. As shown in Table 3.3, the hysteresis loop area was lower for the fluid gel than the quiescently set gel (879 ± 47 to 1576 ± 293). This suggests that the fluid gel exhibited less thixotropy and therefore greater structural recovery (rebuilding) than the quiescent gel. As the fluid gel was exposed to shear, the interactions between particles were disrupted causing a structural breakdown, however, upon decreasing the shear rate back to rest, particles were capable of re-organising themselves thus allowing inter-particle interactions to rebuild. Due to the soft, elastic nature of the fluid gel particles, they have the ability to deform and absorb any stress applied to the system, it was therefore only the interactions between

particles that were broken during shear and not the gel structure within the particles themselves. Conversely, once the quiescently set gel was exposed to shear, the gel network was ruptured and broken. Without melting and re-gelling, the junction zones which construct the gel cannot be rebuilt (Morris & Stephen, 1995). It is worth mentioning that although the fluid gel exhibited a lower thixotropy, its shear viscosity still did not fully recover during these experiments. This was likely due to kinetics; interactions are likely to fully recover given enough time to meet neighbouring particles.

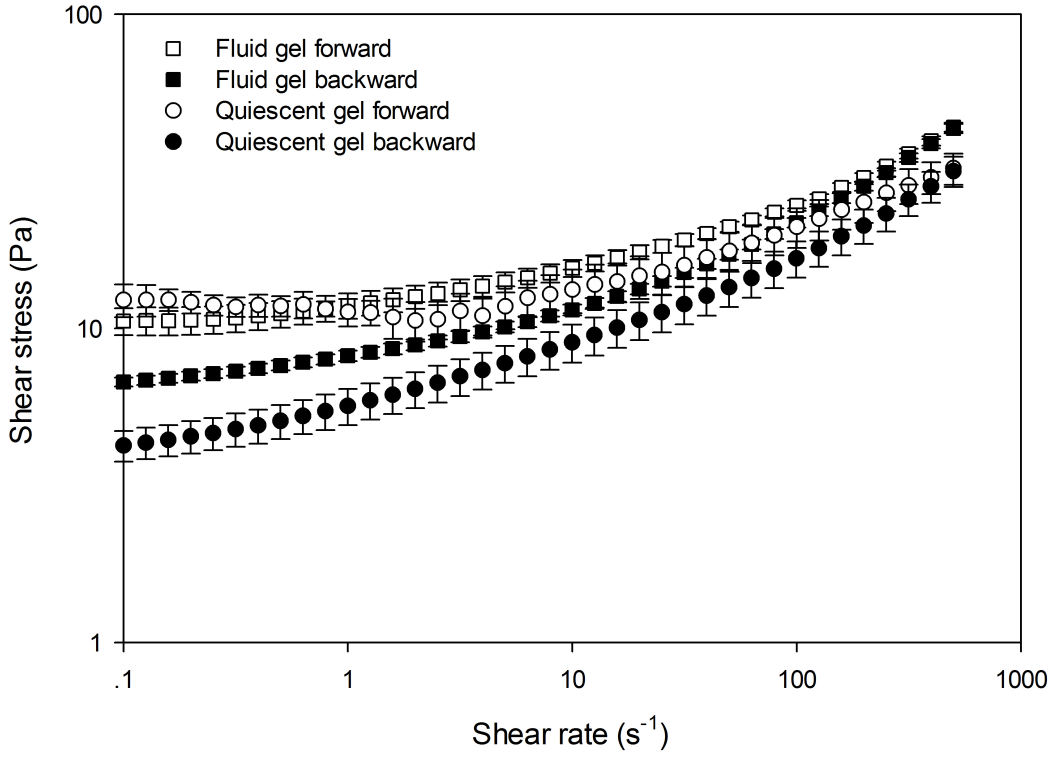


Figure 3.9: Thixotropic loop tests conducted on an agar fluid gel (1.5% agar) and a weak quiescently set gel (0.3% agar). Shear stress was plotted as a function of shear rate. Shear rate was increased from 0.1 s^{-1} to 500 s^{-1} (forward curves unfilled symbols) and decreased backwards (filled symbols) with no hold.

To explore this further, the forward and backward curves were modelled using the Herschel-Buckley equation to calculate yield stress (Table 3.3). The yield stress calculated from the forward curve for both samples was similar (10.8 ± 0.8 Pa for quiescent gel and 10.2 ± 1.2 Pa for fluid gel) indicating a similar stress was required to initiate flow and break the structure. However, the yield stress of the backward curves,

known as the dynamic yield stress i.e. the minimum stress required to maintain flow were different; it was higher for the fluid gel (6.8 ± 0.2 Pa) than that of the quiescent gel (3.9 ± 0.3 Pa). This again suggests that the fluid gel structure recovered to a higher extent than the quiescent gel.

Table 3.3: Hysteresis loop area and yield stress values determined from model-fitting thixotropic loops shown in Figure 3.9. The correlation coefficients were ≥ 0.9997.

Sample	Hysteresis loop area	Yield stress from thixotropic forward curve fitted to Herschel-Buckley model (Pa)	Yield stress from thixotropic backward curve fitted to Herschel-Buckley model (Pa)
0.3% agar quiescent gel	1576 (±293)	10.8 (±0.8)	3.9 (±0.3)
1.5% agar fluid gel	879 (±47)	10.2 (±1.2)	6.8 (±0.2)

3.3.6 Effect of pin stirrer exit temperature

As well as the recovery having an effect on the foam's performance once sheared, it is also likely to affect foam stability. As discussed in Section 3.3.4, yield stress of the suspending fluid directly affects the liquid drainage of the foam. The extent (and time) to which yield stress is built back up through the interactions between particles (i.e. structural recovery) will therefore have an impact on the lifetime of the foam. In order to investigate this, the difference in structural recovery of a fluid gel and a quiescently set gel was utilised by altering the extent of quiescent ordering during fluid gel production. The effect this had upon final rheological properties, as well as foaming properties was studied.

The extent of quiescent ordering was manipulated by changing the outlet temperature during fluid gel production on the pin stirrer (T_{exit}). Previously in this chapter, the temperature that agar fluid gels exited the pin stirrer during production was always maintained at 5 °C. This was to ensure that the molecular ordering process was completed under shear (Garrec, 2013). In addition, they were immediately stored at 5 °C, as previous research has stated that fluid gels are only stable if their transition midpoint temperature (T_m) is sufficiently greater than the storage temperature (Norton et al., 1999). T_m is the temperature where the number of moles of saccharide residues in the disordered state is equal to those in the ordered state i.e the coil-helix transition is in dynamic equilibrium (Goodall & Norton, 1987). For agar this temperature is 35 °C. The closer the gel is to its T_m, the greater the amount of disorder and order events take place. Therefore, if T_{exit} was increased from 5 °C, the number of disorder-order events that take place out of shear (quiescently) would increase. In the absence of shear, the re-ordering takes place between fluid gel particles (as well as within particles). Garrec et al. (2013) studied the effect of T_{exit} on kappa carrageenan fluid gel rheology; they observed that upon increasing T_{exit}, G' and yield stress increased. This was due to bridging of particles via quiescent ordering, which could be irreversibly broken with shear. If the same occurs for agar fluid gels, as predicted by Norton et al. (1999), it will be interesting to observe the effect this has upon foaming properties, in particular how, after aeration and structure breakdown, the interactions are rebuilt within the foam and how this affects its stability.

Firstly, the effect of pin stirrer T_{exit} on the rheological behaviour of agar fluid gels was studied. A 3% agar with 0.5% Tween 20 fluid gel was produced at three different exit temperatures (5 °C, 12.5 °C and 20 °C). Amplitude sweeps were conducted 48 h after

production (Figure 3.10) and yield stresses were determined from this data as the stress required to decrease G' by 5%. The fluid gel formed at T_{exit} = 20 °C, exhibited a higher G' and yield stress than those produced at T_{exit} = 5 °C and 12.5 °C (Table 3.4). These results agree with the data collected by Garrec (2013) who linked these observations to an increase in particle bridging via quiescent ordering in kappa carrageenan fluid gels. However, G' and yield stress of fluid gels T_{exit} = 5 °C and 12.5 °C were very similar, suggesting a similar structure and level of inter-particle interactions.

Table 3.4: Rheological data determined from Figure 3.10 and 3.11 (G' and yield stress from amplitude sweeps and hysteresis loop area from thixotropic tests) of agar fluid gels produced at different pin stirrer exit temperatures, together with their foam half-life measurements.

T_{exit} (°C)	**G' from amplitude sweep (Pa)**	**Yield stress from amplitude sweep (Pa)**	**Hysteresis loop area**	**Foam half-life (h)**
5	670 (±31)	3.0 (±0.4)	2352 (±192)	136 (±14)
12.5	672 (±83)	2.4 (±0.4)	2506 (±158)	119 (±16)
20	1210 (±268)	6.9 (±2.1)	4016 (±128)	36 (±2)

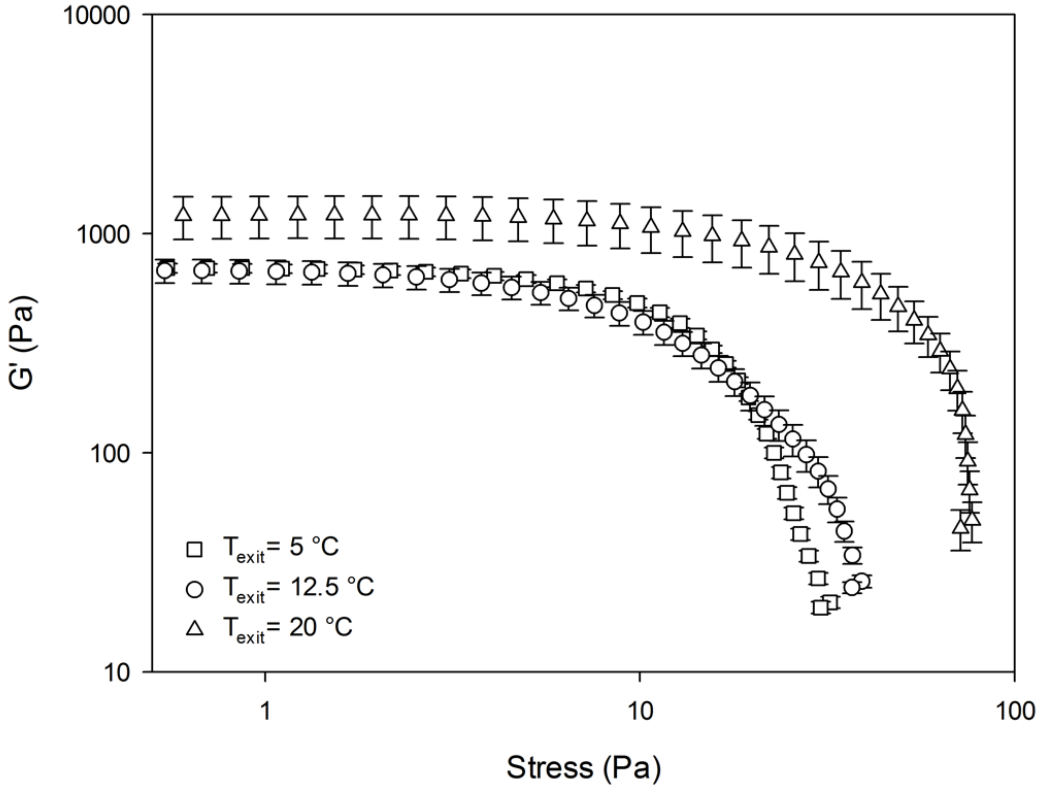


Figure 3.10: Storage modulus as a function of stress during oscillatory strain sweeps of 3% agar with 0.5% Tween 20 fluid gels produced at different pin stirrer exit temperatures, 48 hours after production.

To understand the effect this has upon the thixotropic behaviour of these fluid gels, thixotropic loops were conducted where shear was increased from rest to 500 s^{-1} and back with no holding time (Figure 3.11). All fluid gels exhibited hysteresis between the forward and backward curve indicating time-dependent behaviour where the rate of structure breakdown is greater than that of re-building. The area of the hysteresis loop was calculated and shown in Table 3.4. The fluid gel formed at T_{exit} = 20 °C exhibited the largest hysteresis loop area (4016 ±128) compared to those at T_{exit} = 5 °C and 12.5 °C whose were similar (2352 ±192 and 2506 ±158, respectively). This indicates that the structure of T_{exit} = 20 °C did not rebuild to as high an extent as that of T_{exit} = 5 °C and 12.5 °C, supporting the conclusion that a greater number of disorder-order events occurred out of shear resulting in the bridging of particles by quiescent ordering events.

In addition, the forward curve data for T_{exit} = 20 °C appears to show some slip at low shear rates (Figure 3.11), this would have likely been caused by larger gelled areas (particles bridged together) resulting in inhomogeneity of the sample. However, as there is no real difference in the hysteresis area of T_{exit} = 5 °C and 12.5 °C, nor G' or yield stress values from the amplitude data, it can be inferred that perhaps at 12.5 °C, the exit temperature is sufficiently lower than T_m to overcome these quiescent ordering events.

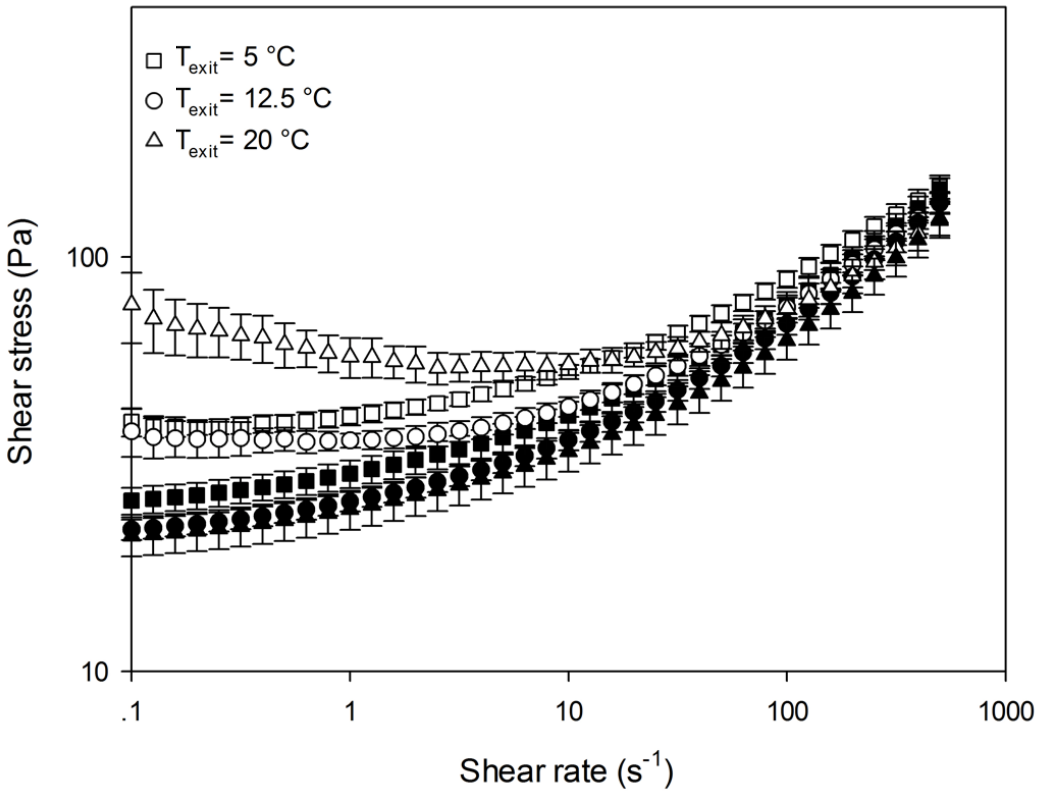


Figure 3.11: Thixotropic loop tests conducted on 3% agar with 0.5% Tween 20 fluid gels produced at different pin stirrer exit temperatures. Shear stress was plotted as a function of shear rate. Shear rate was increased from 0.1 s^{-1} to 500 s^{-1} (forward curves unfilled symbols) and decreased backwards (filled symbols) with no hold.

Optical microscopy was used to investigate the microstructure of these fluid gels produced at different T_{exit} (Figure 3.12). Agar particles produced at exit temperatures of 5 °C and 12.5 °C appeared similar; individual particles around 50 μm in size that interacted through their protruding 'tails' (Figure 3.12a and 3.12b). However, particles produced at T_{exit} = 20 °C appeared notably different (Figure 3.12c); particles were much

smaller and aggregated together. There were also larger gelled portions, which resulted in an inhomogeneous structure. This further supports the hypothesis that at this exit temperature, a greater number of disorder-order events occurred out of shear resulting in the bridging of particles by quiescent ordering events.

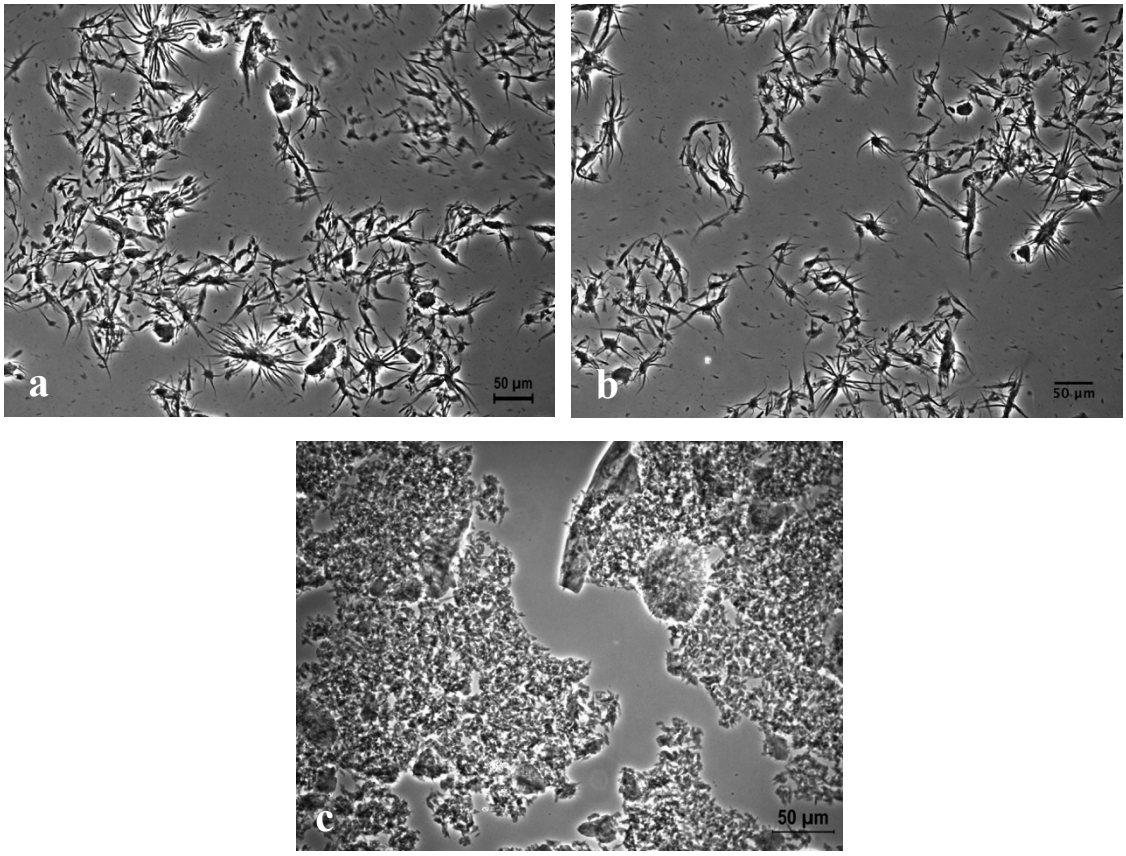


Figure 3.12: Micrographs of 3% agar with 0.5% Tween 20 fluid gels produced at different pin stirrer exit temperatures (a) 5 ℃, (b) 12.5 ℃ and (c) 20 ℃, using phase contrast microscopy.

To explore how structural recovery can affect foam structure and stability, fluid gels were aerated and their foam half-life was recorded and shown in Table 3.4. Foam half-life was largest for fluid gels produced at T_{exit} = 5 °C and 12.5 °C (136 ± 14 h and 119 ± 16 h respectively), whereas the foam produced from fluid gel with T_{exit} of 20 °C, displayed a half-life of only 36 ± 2 h. During aeration, inter-particle interactions were disrupted as air was incorporated into the fluid. Particles were subsequently confined to foam channels and with time, the interactions between particles began to rebuild. Fluid gels produced at

T_{exit} = 5 °C and 12.5 °C were able to recover to a higher extent in the foam channels due to their more particulate and ordered nature (less quiescent ordering between particles) resulting in their greater flexibility to move within the foam channels and rebuild interactions. Whereas, shear would have broken up large quiescent-ordered regions of the structure produced at T_{exit} = 20 °C resulting in more disorder and less structural recovery. It is also possible that some larger aggregates remained after aeration causing bridging between air cells and therefore film rupture.

3.4 Conclusions

With the potential use of fluid gels in reduced-fat food foams, this chapter explored the production and characterisation of agar fluid gels along with their ability to be aerated. Agar fluid gel particles were visualised for the first time in recent years, which allowed the effect of production method on gelation to be explored. Agar fluid gels were produced at various concentrations and aerated, allowing conclusions to be drawn on the relationships between the foam and the fluid gel's properties, particularly the dependence of foam stability. Finally, the advantage of using fluid gels over weak biopolymer gels was demonstrated using thixotropic rheology and further explored by altering the pin stirrer exit temperature to increase quiescent ordering.

The surfactant Tween 20, was incorporated into agar fluid gels without affecting their rheological and material properties but allowing foam production. Producing these gels using a pin stirrer produced novel particle shapes which increased particle interactions, indicated by yield stress. All systems showed good foaming properties where foam stability was affected by the yield stress of the fluid gels, which was influenced by particle interaction and rigidity, manipulated by agar concentration. A substantial increase in stability was observed for systems from 2.5% to 3% agar. Both formulations had very similar viscosities; the increase in foam stability was therefore caused by an increase in particle rigidity, which made the network of particles less deformable in the foam channels, providing a strong barrier to drainage.

The advantage of fluid gels over weak biopolymer gels is that they are able to recover upon shear; a fluid gel with similar viscosity to a weak quiescent gel exhibited lower

thixotropy and a greater dynamic yield stress when modelling the backward curve, indicating higher structural recovery. Manipulating the exit temperature of agar fluid gels during production allowed a relationship between quiescent ordering and foam stability to be established, where greater quiescent ordering in the fluid gel (at a T_{exit} approaching T_m) reduced its stability upon aeration, due to less structural recovery in the system.

LIST OF REFERENCES

Adams, S., Frith, W., & Stokes, J. (2004). Influence of particle modulus on the rheological properties of agar microgel suspensions. Journal of Rheology, 48(6), 1195-1213.

Blom, W. A. M., Koppenol, W. P., Schuring, E. A. H., Abrahamse, S. L., Arnaudov, L. N., Mela, D. J., & Stoyanov, S. D. (2016). Sustained satiety induced by food foams is independent of energy content, in healthy adults. Appetite, 97, 64-71. doi:https://doi.org/10.1016/j.appet.2015.11.023

Bradbeer, J. F., Hancocks, R., Spyropoulos, F., & Norton, I. T. (2014). Self-structuring foods based on acid-sensitive low and high acyl mixed gellan systems to impact on satiety. Food Hydrocolloids, 35, 522-530.

de Carvalho, W., & Djabourov, M. (1997). Physical gelation under shear for gelatin gels. Rheologica Acta, 36(6), 591-609.

Frith, W., Garijo, X., Foster, T., & Norton, I. (2002). Microstructural origins of the rheology of fluid gels. In Williams, P. A., Phillips, G O. (Eds.), Gums and Stabilisers for the Food Industry (Vol. 11, pp. 95-103). Cambridge: The Royal Society of Chemsitry.

Gabriele, A. (2011). Fluid gels: Formation, production and lubrication. University of Birmingham, eThesis.

Gabriele, A., Spyropoulos, F., & Norton, I. T. (2009). Kinetic study of fluid gel formation and viscoelastic response with kappa-carrageenan. Food Hydrocolloids, 23(8), 2054-2061.

Gabriele, A., Spyropoulos, F., & Norton, I. T. (2010). A conceptual model for fluid gel lubrication. Soft Matter, 6(17), 4205-4213.

Garrec, D. A. (2013). Understanding Fluid Gels and Hydrocolloid Tribology. University of Birmingham, eThesis.

Garrec, D. A., Guthrie, B., & Norton, I. T. (2013). Kappa carrageenan fluid gel material properties. Part 1: Rheology. Food Hydrocolloids, 33(1), 151-159.

Gonzenbach, U. T., Studart, A. R., Tervoort, E., & Gauckler, L. J. (2006). Stabilization of foams with inorganic colloidal particles. Langmuir, 22(26), 10983-10988.

Goodall, D. M., & Norton, I. T. (1987). Polysaccharide conformations and kinetics. Accounts of Chemical Research, 20(2), 59-65.

Guillermic, R.-M., Salonen, A., Emile, J., & Saint-Jalmes, A. (2009). Surfactant foams doped with laponite: unusual behaviors induced by aging and confinement. Soft Matter, 5(24), 4975-4982.

Holland, S., Tuck, C., & Foster, T. (2018). Fluid gels: a new feedstock for high viscosity jetting. Food Biophysics, 13(2), 175-185.

Lesov, I., Tcholakova, S., & Denkov, N. (2014). Factors controlling the formation and stability of foams used as precursors of porous materials. Journal of Colloid and Interface Science, 426, 9-21. doi:https://doi.org/10.1016/j.jcis.2014.03.067

Mittal, K. (1972). Determination of CMC of polysorbate 20 in aqueous solution by surface tension method. Journal of pharmaceutical sciences, 61(8), 1334-1335.

Moakes, R. J. A., Sullo, A., & Norton, I. T. (2015). Preparation and characterisation of whey protein fluid gels: The effects of shear and thermal history. Food Hydrocolloids, 45, 227-235. doi:http://dx.doi.org/10.1016/j.foodhyd.2014.11.024

Morris, V. (1995). Bacterial Polysaccharides. In Stephens, A. M. (Ed), Food polysaccharides and their applications (pp. 341-375): CRC Press.

Murray, B. S., & Ettelaie, R. (2004). Foam stability: proteins and nanoparticles. Current Opinion in Colloid & Interface Science, 9(5), 314-320.

Norton, I., Jarvis, D., & Foster, T. (1999). A molecular model for the formation and properties of fluid gels. International Journal of Biological Macromolecules, 26(4), 255-261.

Norton, I. T., Foster, T., & Brown, R. (1998). The science and technology of fluid gels. In Williams, P. A., & Phillips G. O. (Eds.), Gums and Stabilisers for the Food Industry, (Vol. 9, pp. 259-268): Royal Society of Chemistry, Cambridge.

Patino, J. M. R., Niño, R. R., & Gómez, J. M. Á. (1997). Interfacial and foaming characteristics of protein—lipid systems. Food Hydrocolloids, 11(1), 49-58.

Prasad, K., Siddhanta, A. K., Rakshit, A. K., Bhattacharya, A., & Ghosh, P. K. (2005). On the properties of agar gel containing ionic and non-ionic surfactants. International Journal of Biological Macromolecules, 35(3–4), 135-144. doi:http://dx.doi.org/10.1016/j.ijbiomac.2005.01.004

Ross-Murphy, S. B. (1994). Rheological characterization of polymer gels and networks. Polymer Gels and Networks, 2(3-4), 229-237.

Saha, D., & Bhattacharya, S. (2010). Hydrocolloids as thickening and gelling agents in food: a critical review. Journal of Food Science and Technology, 47(6), 587-597.

Saint-Jalmes, A. (2006). Physical chemistry in foam drainage and coarsening. Soft Matter, 2(10), 836-849.

Sun, A., & Gunasekaran, S. (2009). Yield stress in foods: measurements and applications. International Journal of Food Properties, 12(1), 70-101.

Chapter 4: THE EFFECT OF SUGARS ON AGAR FLUID GELS AND THE STABILISATION OF THEIR FOAMS

Based on work published as: Ellis, A., Mills, T., Norton, I., & Norton-Welch, A. (2019). The effect of sugars on agar fluid gels and the stabilisation of their foams. *Food Hydrocolloids, 87*, 371-381.

4.1 Background

The aim of this work was to investigate the effect of sugars on the microstructure of agar fluid gels and their foaming properties. The knowledge gained in Chapter 3, including the production and characterisation of agar fluid gels and their foams, provides the basis to further understand this system with the inclusion of an additional ingredient. Sugar is an important ingredient in many whipped products as it provides taste, texture and structure (Coultate, 2009). However, there are strong demands to reduce its content in food. The UK Government introduced The Sugar Reduction Program in 2017, which outlines guidelines for the food industry to achieve a 20% reduction in sugar across products aimed at children (*Sugar Reducion: Achieving the 20%*, 2017). These include desserts, sweet confectionary and ice cream. In order to achieve this reduction, it is essential to understand the role of sugar and how it contributes to the overall microstructure of products.

This work will focus on the effect of sugar (type and concentration) on agar fluid gel microstructure, which is now understood from Chapter 3, and how this relates to their foam properties. The simplest monosaccharides and disaccharide (glucose, fructose and sucrose) were chosen to allow size effects to be investigated. Firstly, the influence of sugar on the gelation of agar fluid gels was studied to provide a foundation for exploring subsequent material properties, such as particle size. In addition, the gel strength of quiescent agar gels was measured to provide information on the intrinsic polymeric network of fluid gel particles, before examination of their bulk rheology and trends in foamability and stability. Finally, the manipulation of particle size through altering processing parameters was used to modify foam drainage.

4.2 Experimental

4.2.1 Materials

Agar (A7002), D-glucose (G7021), D-fructose (F0127), sucrose (S0389) and Tween 20 were purchased from Sigma Aldrich (UK) and used without further purification. All concentrations were calculated as weight percentage.

4.2.2 Preparation of agar fluid gels using pin stirrer

Agar (1 wt%) was dispersed in deionised water at room temperature, then heated to 90 °C. After complete dissolution, the solution temperature was lowered to 70 °C and Tween 20 (0.5 wt%) and the required concentration of sugar were added. The solution was transferred into the cooled jacketed pin stirrer through a peristaltic pump at 70 °C. The outlet temperature was controlled to 5 °C to ensure gelation occurred under shear (gelation temperature ≈ 30 °C). A retention time of 7.5 min was achieved through using a pump speed of 20 mL min^{-1}, resulting in a cooling rate of 8 °C min^{-1}. The shaft rotation speed was set to 1500 rpm to give a narrow distribution of particle size (Gabriele, Spyropoulos, & Norton, 2010). Fluid gels were stored at 5 °C.

4.2.3 Preparation of agar fluid gels using a rheometer

Solutions of agar (1 wt%) with Tween 20 (0.5 wt%) and sugar were prepared as described in Section 2.2. Fluid gels were produced using the vane geometry in a rheometer (Kinexus, Malvern, UK). Solutions at 70 °C were transferred into the pre-heated rheometer cup and the temperature allowed to equilibrate for 5 min. The temperature was then decreased from 70 °C to 5 °C at a cooling rate of 2 °C min^{-1}, under an applied shear of 500 s^{-1}. A slower cooling rate was used compared to preparation in the pin stirrer to increase the accuracy of gelation temperature determination through viscosity

measurements. Experiments were carried out in three replicates and fluid gels were then stored at 5 °C.

4.2.4 Optical microscopy

Fluid gels were imaged using phase contrast microscopy (Leica Microsystems, UK). They were diluted with deionised water (1:4), placed onto a microscope slide with a coverslip and observed using objective lenses up to 20x magnification. ImageJ software was used to measure 300 fluid gel particles (longest dimension was measured) from 10 different micrographs in order to achieve a good representation of the particles.

4.2.5 Texture analysis of quiescent agar gels

Agar gels of 1 wt% agar + 0.5 wt% Tween 20 and various concentrations (10-60 wt%) of fructose, glucose and sucrose were quiescently set and stored at 5 °C for 48 h. Tween 20 was added to keep the formulation the same as fluid gel production (Tween 20 was required for aeration). Compression tests were then carried out using a TA XT plus texture analyser (Stable Micro Systems Ltd, UK) with a 40 mm diameter cylindrical probe. Samples of 21 mm diameter and 10 mm height were compressed at a rate of 1 mms^{-1}. The force/distance data was converted to true strain (ε) and true stress (σ). From the gradient of the linear region at 0-5% strain, the initial Young's modulus was determined (Bradbeer et al., 2014). Experiments were carried out in three replicates.

4.2.6 Bulk rheology

A Kinexus rheometer (Malvern, UK) was used to perform rheological measurements at 25 °C. Fluid gels were tested after 48 h to ensure post-production particle ordering completion (de Carvalho & Djabourov, 1997; Gabriele, Spyropoulos, & Norton, 2009). All measurements were conducted using a serrated parallel plate of 60 mm diameter set

to a 1 mm gap. Shear viscosity at 1 s^{-1} was determined from viscosity profiles at shear rates of 0.1-500 s^{-1}. Amplitude sweeps were conducted at a frequency of 1 Hz as a function of applied oscillatory strain. All experiments were carried out in three replicates.

4.2.7 Aeration

Fluid gels of equal volumes were aerated using a Hobart mixing unit. The highest speed setting was used for 7 min as this ensured all systems were in the wet foam boundary (air fraction within 0.65-0.95). Air fraction was determined to assess foamability using Equation 4.1, by weighting equivalent volumes of fluid gel and foam, using three replicates.

$$\text{Air fraction} = 1 - \left(\frac{m_{foam}}{m_{fluid\ gel}}\right) \qquad (4.1)$$

The stability of foams was measured using foam half-life of three replicates. The reduction of the foam height was recorded using a CCD camera and the half-life was later calculated as the time taken to reduce the foam height by half.

4.2.8 Foam liquid drainage measurements

Liquid drainage measurements were conducted using a Krüss DFA100LCM foam analyser (Krüss, Germany). The corresponding fluid gel was poured into the foam cell to cover the reference electrode followed by the externally produced foam. The decrease in liquid fraction was then recorded using electrical conductivity measurements at 7 pairs of electrodes along the cell height. Drainage profiles were recorded for the first four hours from initial aeration. Experiments were carried out in three replicates.

4.3 Results and Discussion

4.3.1 Effect of sugar on gelation

In order to explore the influence a variety of sugars have on the material properties of agar fluid gels, it is necessary to first understand their effect upon gelation. Agar is a mixture of agarose and agaropectin fractions, where agarose is responsible for gelation. The role of agaropectin is not as well understood, although recent work by Nishinari and Fang (2017) reported that it may enhance gelation rather than inhibit it. The gelation mechanism as described by the Domain model (Arnott et al., 1974) states that agarose molecules exist as random coils in solution, which undergo a coil-helix transition as the temperature is lowered. The helices, which are stabilised by hydrogen bonds with water (Foord & Atkins, 1989), then aggregate together. The formation of a wider 3D network occurs when these helical domains are linked through junction zones. During fluid gel preparation, this process occurs under shear resulting in the production of gel particles dispersed in a continuous phase, typically water.

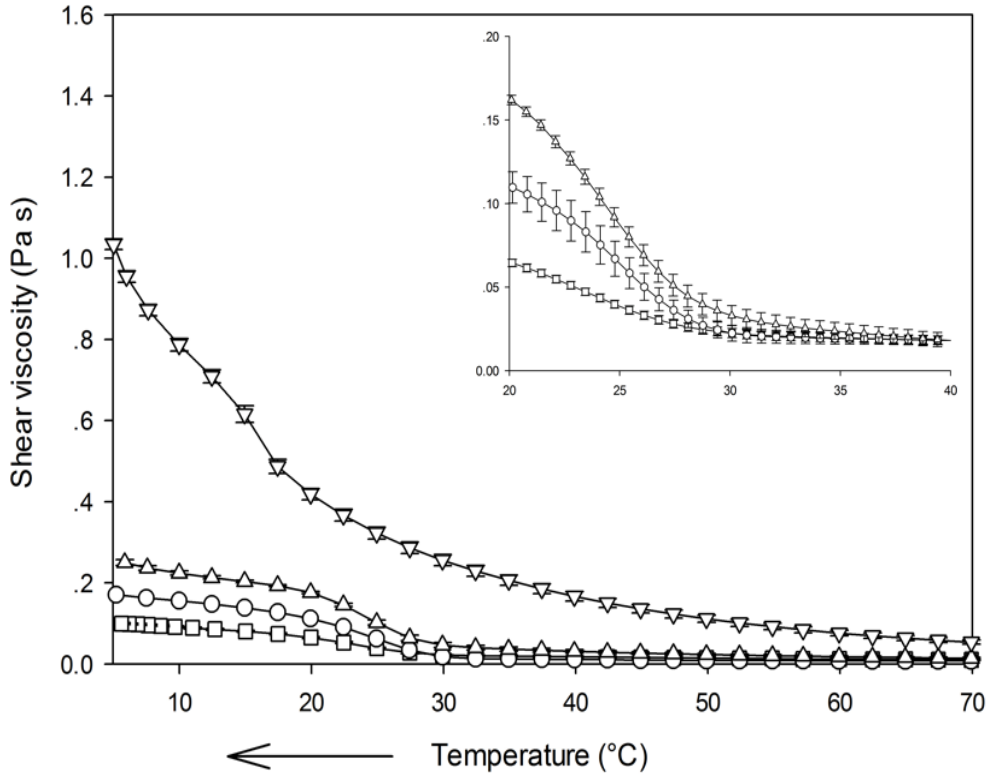
Gelation during fluid gel preparation was studied by preparing 1% agar fluid gels with varying concentrations of glucose, fructose and sucrose using a rheometer. It is important to note that solutions were prepared by first dissolving agar in water, followed by the addition of sugar. Yang et al. (2015) highlights the importance in the order of sugar addition by reporting a weaker and more inhomogeneous gel structure when sucrose (above 50%) was dissolved before agar. The solutions of agar were cooled from 70 °C to 5 °C whilst under a fixed shear rate (500 s^{-1}) and the viscosity was measured. The viscosity profiles of agar fluid gels with 0%, 20% and 40% glucose (Figure 4.1a), fructose (Figure 4.1b) and sucrose (Figure 4.1c) all exhibited a sharp increase in viscosity just

below 30 °C indicating the occurrence of considerable ordering and structuring. This occurred close to the gelation temperature of agar and so can be attributed to the formation of gel particles during the coil-to-helix transition (Norton, Jarvis, & Foster, 1999). This can be more clearly seen in the inset graphs in Figure 4.1, which focus on the region between 20 °C and 40 °C. The inset graph in Figure 4.1c highlights a difference between the onset temperature of ordering at different concentrations of sucrose, where ordering occurred at a higher temperature upon raising sucrose concentration. Similar results were observed for quiescent agarose gels; Watase et al., (1990) revealed that the presence of sucrose decreased the size and increased the number of cross-links during gelation, due to hydrogen bonds formed between sugar and agarose. This was enhanced by the high number of equatorial hydroxyl groups, *n*(e-OH) and therefore increased viscosity of sucrose (Nishinari et al., 1990). This theory can be translated to agar fluid gels and explains the increase in ordering temperature upon increased sucrose concentration. However, the onset temperature of ordering for glucose and fructose fluid gels (Figure 4.1a and 4.1b) was similar regardless of sugar concentration. The difference in trend between these two sugars and sucrose is likely a product of the different sugar size; *n*(e-OH) increases in the order of fructose < glucose < sucrose, where the rotational freedom of parallel links in the gels decreases with increasing *n*(e-OH) (Watase, Kohyama, & Nishinari, 1992).

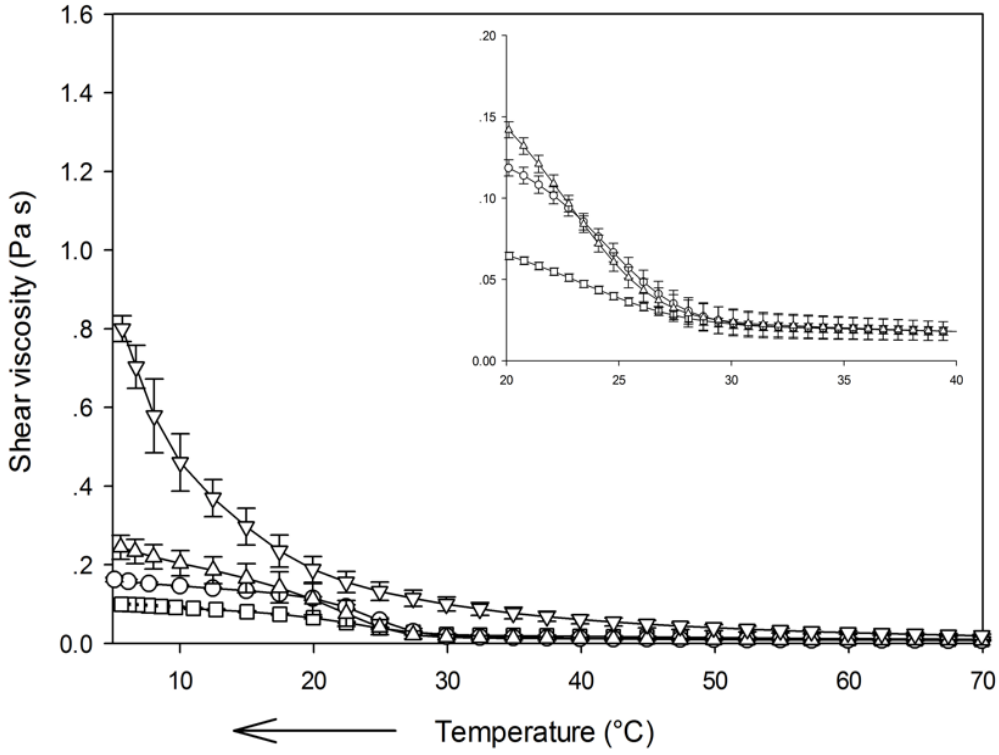
The shear viscosity curves for 1% agar fluid gels with 60% glucose (Figure 4.1a), fructose (Figure 4.1b) and sucrose (Figure 4.1c), did not display a sharp increase in viscosity. This slower, more gradual transition from sol-gel suggests that 60% sugar was somewhat inhibiting gel formation. It is likely that at this concentration, the glass transition

temperature, T_g, was close to the gelation temperature and therefore the sol-gel transition was hindered. A similar observation was observed by Deszczynski, Kasapis, and Mitchell (2003); upon gelation of agarose in the presence of high levels of co-solute (50:50 sucrose/glucose syrup), a broader temperature band of gelation was observed indicating a less co-operative process of coil-to-helix formation. This will be further investigated in Section 4.3.4, when the rheological properties of fluid gels at higher sugar concentrations are explored.

a


Shear viscosity (Pa s)
1.6
1.4
1.2
1.0
.8
.6
.4
.2
0.0
10
20
30
40
50
60
70
Temperature (°C)
.20
.15
.10
.05
0.00
20
25
30
35
40

b


Shear viscosity (Pa s)
1.6
1.4
1.2
1.0
.8
.6
.4
.2
0.0
10
20
30
40
50
60
70
Temperature (°C)
.20
.15
.10
.05
0.00
20
25
30
35
40

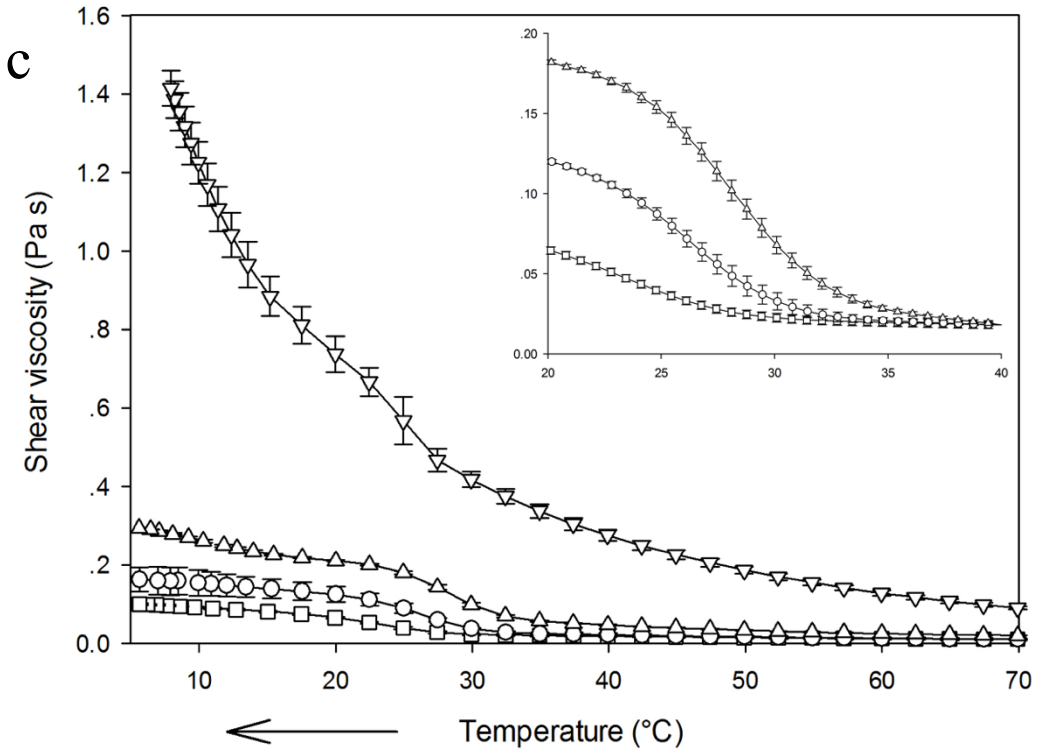


Figure 4.1: Viscosity profiles during fluid gel preparation of 1% agar fluid gels + 0.5% Tween 20 with 0% (square), 20% (circle), 40% (triangle up) and 60% (triangle down) of (a) glucose, (b) fructose and (c) sucrose. The temperature was decreased from 70 °C to 5 °C at a cooling rate of 2 °C min^{-1}, under a fixed applied shear of 500 s^{-1}. The inset graphs focus on the region between 20 °C and 40 °C for the three lower concentrations of sugar, where viscosity was normalised at 40 °C. This allows the ordering transition and its onset temperature to be observed more clearly.

4.3.2 Effect of sugar on microstructure

The investigation into the influence of sugar during gelation of agar fluid gels in Section 4.3.1 provides a good foundation to explore such effects on their microstructure. Fluid gels henceforth in the paper were prepared using a continuous pin stirrer, as described in Section 4.2.2. The rheometer was used in Section 4.3.1 only to study gelation kinetics, therefore the difference between it and the pin stirrer's shear environment on the properties of fluid gels produced is not relevant. Firstly, fluid gel particle size and shape were studied as it is important to consider their impact on foam stability. 1% agar fluid gels with increasing levels of added sugar were produced and subsequently diluted and

imaged using phase contrast microscopy. ImageJ software was used to measure particle size.

Figure 4.2 shows particle size distributions for 1% agar fluid gels with 0%, 20%, 40% and 60% of glucose (a), fructose (b) and sucrose (c) added. With no added sugar, the most abundant particle size was 40-45 μm in diameter. Upon addition of each sugar at 20%, a shift towards smaller particles was observed. At 40% and 60% addition, particle size distributions again shifted to smaller sizes and also narrowed (Figure 4.2). To investigate this trend, it is important to consider the viscosity of the solutions entering the pin stirrer at 70 °C. Viscosity measurements for glucose, fructose and sucrose solutions from work by Telis et al., (2007) are therefore shown in Table 4.1. At higher concentrations of sugar the viscosity increased, for example from 10% to 60% sucrose, viscosity rose by a factor of 18 (Table 4.1).

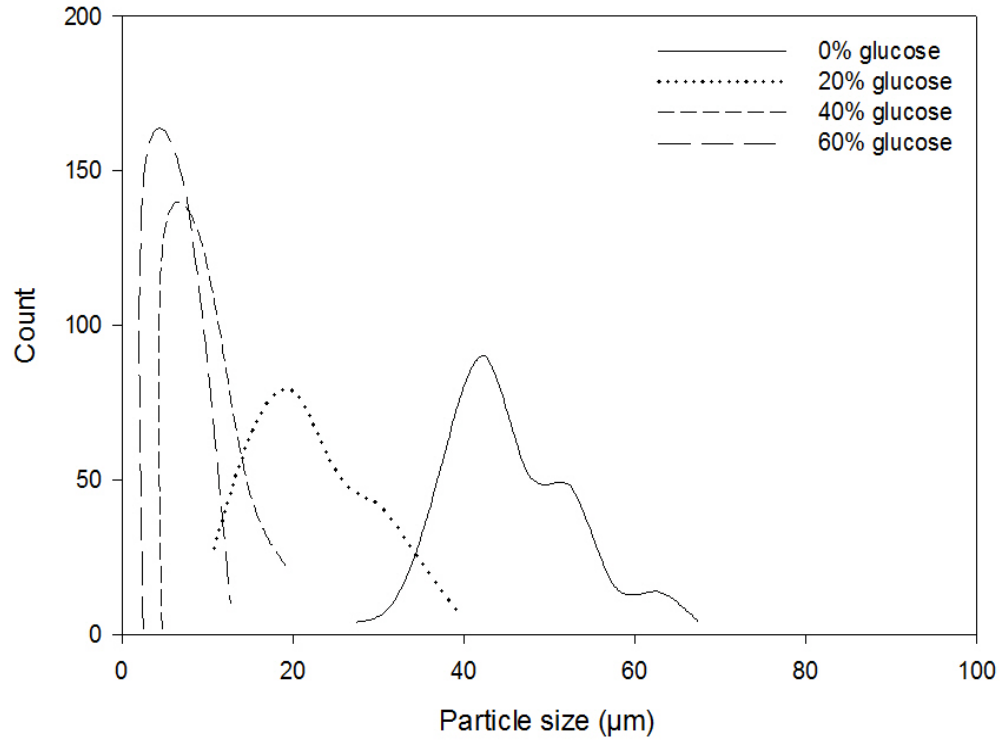
Table 4.1: Viscosity of glucose, fructose and sucrose solutions at 70 °C of concentrations 10-60 wt%. Figure adapted from Telis et al. (2007).

Concentration (%)	**10**	**20**	**30**	**40**	**50**	**60**
Sugar	Viscosity at 70 °C (mPa s)					
Glucose	0.44	0.65	0.81	1.32	1.70	4.00
Fructose	0.46	0.69	0.81	1.41	1.82	4.42
Sucrose	0.42	0.69	0.85	1.62	2.34	7.20

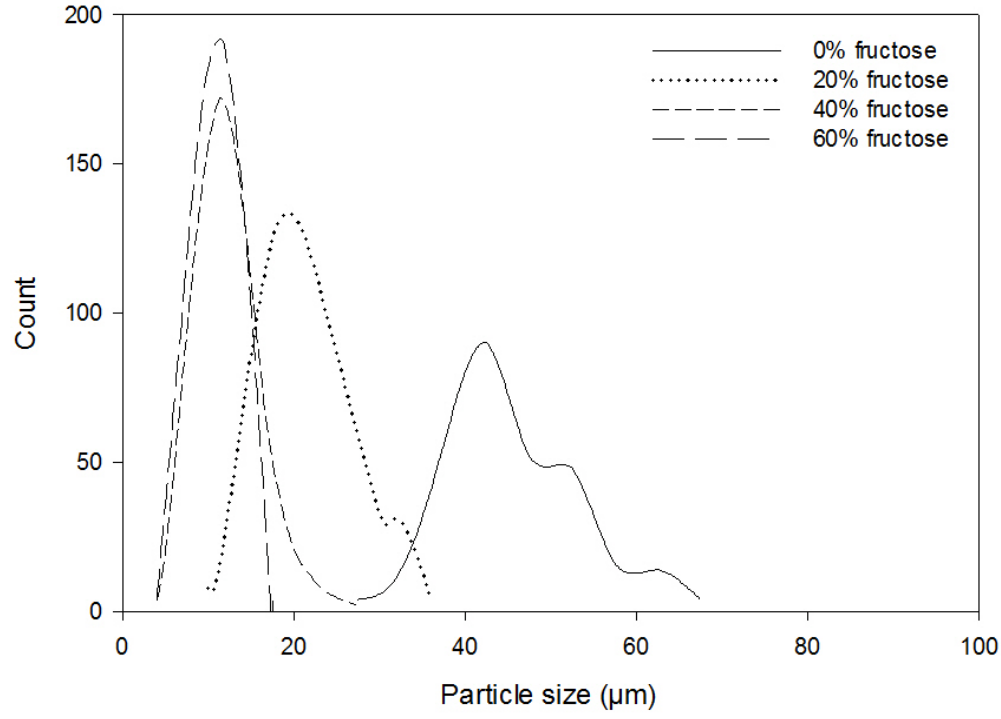
In terms of fluid dynamics, the viscosity of the solution entering the pin stirrer will affect the resistance of the fluid to deformation. A solution of higher viscosity offers more resistance and consequently feels a lower shear rate (Gabriele, 2011), which would result in the formation of larger particles (Moakes, Sullo, & Norton, 2015). However, the opposite occurred here; increasing the viscosity of the solutions through sugar addition

resulted in a decrease in particle size. The most influential factor in determining particle size was therefore likely to have been gelation kinetics. Normand et al. (2003) reported that increasing sucrose content (up to 60%) led to a reduction in the degree of aggregation during agarose gelation (observed by a smaller correlation length). This supports previous observations by Nishinari et al. (1992) and Watase et al., (1990), who reported a reduction in the quantity of helical aggregates, an increase in the number of cross links and a decrease in the length of helices with increased sucrose content. Therefore, as the concentration of sucrose in agar solutions entering the pin stirrer increased, it is likely that a reduction in helical aggregation caused a greater abundancy of initial gel nuclei, which were unable to grow to as large an equilibrium particle size, explaining the trends observed in Figure 4.2. At 60% sugar addition, gelation was observed to be somewhat inhibited (Section 4.3.1), therefore during fluid gel production on the pin stirrer, it becomes difficult to interpret particle size as a number of factors were involved. In addition, it is not known whether there is a minimum possible particle size and if there is, whether it is dependent on gelation kinetics or pin stirrer parameters.

a


0% glucose
20% glucose
40% glucose
60% glucose
Count
Particle size (µm)
0
50
100
150
200
0
20
40
60
80
100

b


0% fructose
20% fructose
40% fructose
60% fructose
Count
Particle size (µm)
0
50
100
150
200
0
20
40
60
80
100

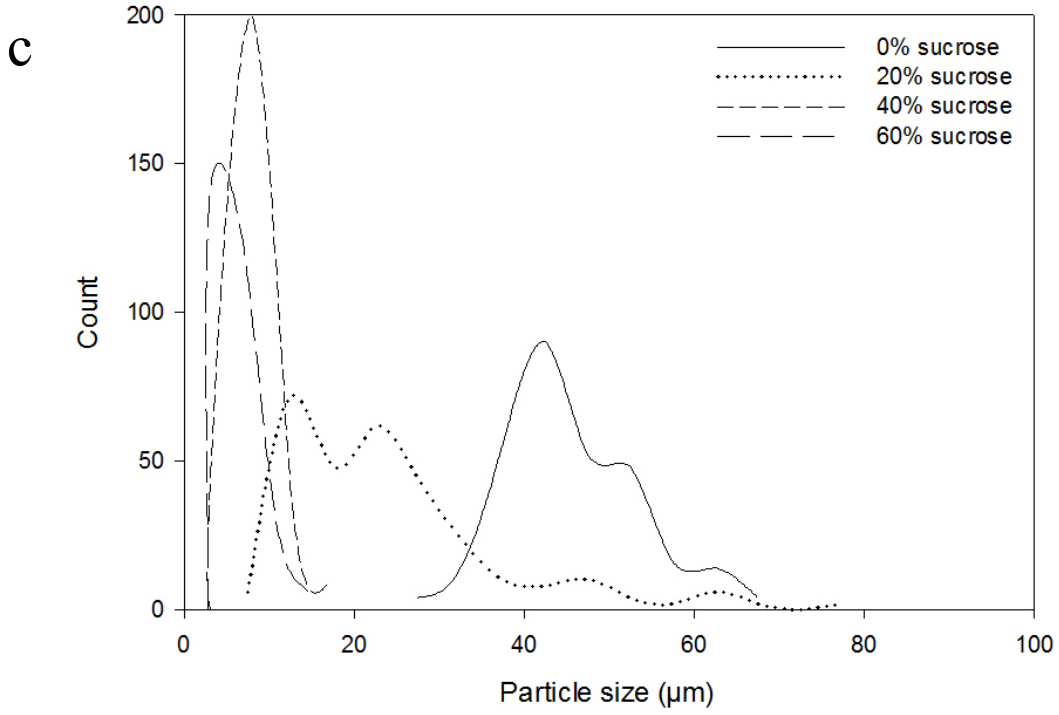


Figure 4.2: Overlapping histograms showing particle size distributions for 1% agar fluid gels + 0.5% Tween 20 with 0%, 20%, 40% and 60% of (a) glucose, (b) fructose and (c) sucrose. Measured from micrographs using ImageJ software.

The shape of particles was also explored; micrographs of 1% agar with varying concentrations of sucrose are presented in Figure 4.3. In the presence of no sugar, agar fluid gel particles produced on the pin stirrer have previously been described as particles with nearly spherical cores and long protruding tails (Ellis et al., 2017). It is thought that the 'tails' usually order within the main particle core resulting in smoother particles, but because of the shear environment experienced in the pin stirrer, this does not occur. This structure was confirmed by the micrograph in Figure 4.3a. Upon addition of 20% sucrose, similar particles were observed but there were also smaller, more spherical particles (Figure 4.3b). At 40% and 60% sucrose addition (Figure 4.3c and 4.3d), these star-like structures had disappeared and smaller particles with no tails were observed. These observations support the theory that at higher concentrations of sucrose, agar fluid gel particles were unable to grow to as large a size; at 60% sucrose, only small particles

existed but by decreasing sugar concentration and therefore increasing helical aggregation, these core particles were able to grow and form larger structures (observed at 20% and 0% sucrose). Together with the shape and size of the fluid gel particles, exploring their rheology will allow a greater understanding of the overall material properties.

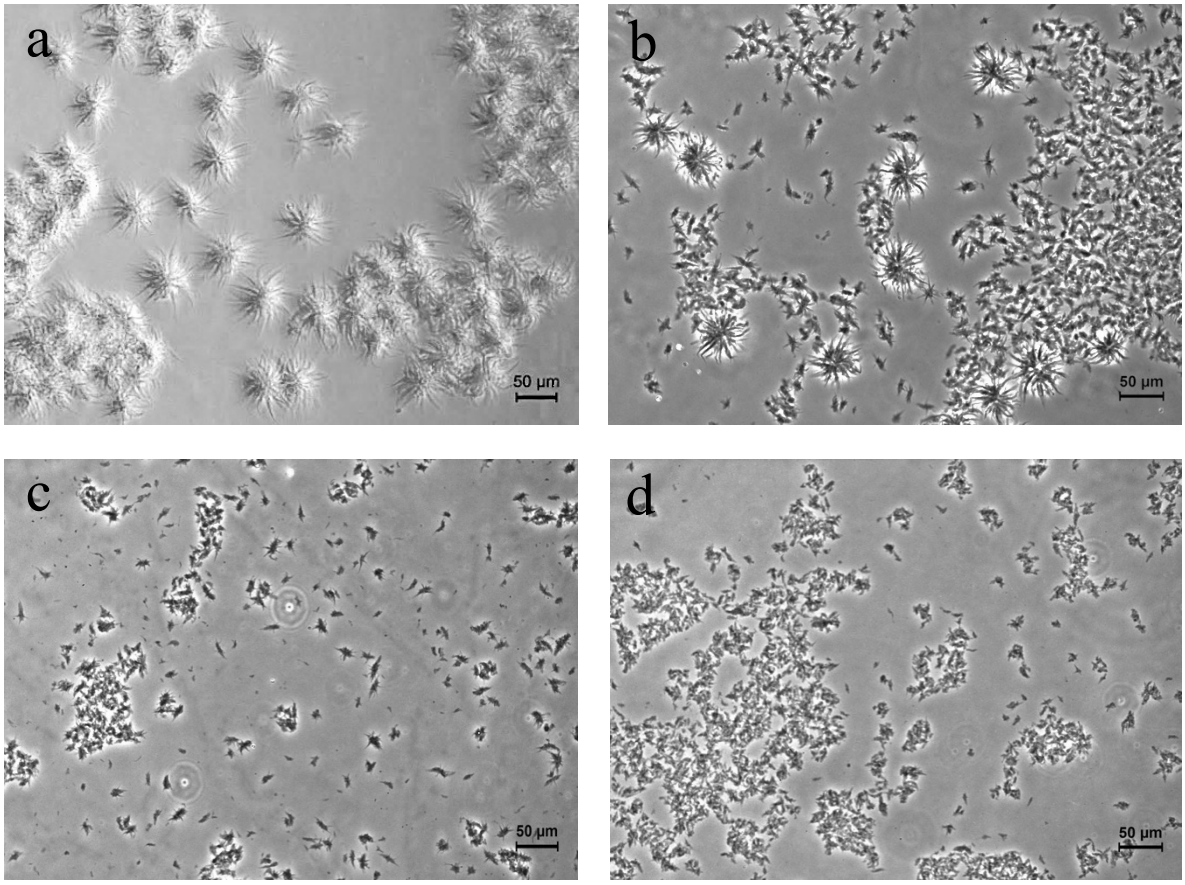


Figure 4.3: Optical micrographs of diluted 1% agar fluid gels + 0.5% Tween 20 with 0% (a), 20% (b), 40% (c) and 60% (d) sucrose, using phase contrast microscopy.

4.3.3 Effect of sugar on quiescent agar gels

In order to understand fluid gel rheological properties, it is necessary to first understand the effect of sugar on quiescently set agar gels and in particular, gel strength. To measure this, texture analysis was conducted on 1% agar quiescent gels with varying concentrations of glucose, fructose and sucrose (Figure 4.4). The intrinsic polymeric

network of agar fluid gel particles and therefore their textural properties can be inferred by their quiescently set counterparts (Frith et al., 2002). The gels were cold-set for 48 hours and subsequently compressed to 50% strain. Initial Young's modulus was determined using the gradient of the linear region at 0-5% strain on a true strain (ε) true stress (σ) graph. It is a measure of the stiffness/deformability of the gel network, until structure failure occurs (Bradbeer et al., 2014). It is worth noting here that material properties of 1% agar quiescent and fluid gels with glucose and sucrose were explored first at 10% concentration intervals from 0–60%. Once the trends had been revealed, it was considered unnecessary to test gels at 10% and 30% fructose.

The initial Young's modulus increased with concentration of each sugar until 50% addition (Figure 4.4) and therefore resulted in stiffer agar gels. However, the addition of sugar at 55% and 60% resulted in a lack of available water for the formation of stable junction zones and consequently a fall in the initial Young's modulus was observed (Figure 4.4). The enhanced elastic modulus of agar gels on addition of sugar can be explained by the increased number of junction zones and decrease in both the number of parallel links and their rotational freedom (Nishinari et al., 1992), which appears to accelerate the gelation process (Normand et al., 2003). In addition, the initial Young's modulus observed for agar gels with up to 30% sucrose was higher than those of fructose and glucose (Figure 4.4). This again is likely to be a function of *n*(e-OH), which increases in the order of fructose < glucose < sucrose (Nishinari et al., 1992). The trends in gel strength reported here will be comparable to particle stiffness in corresponding fluid gels.

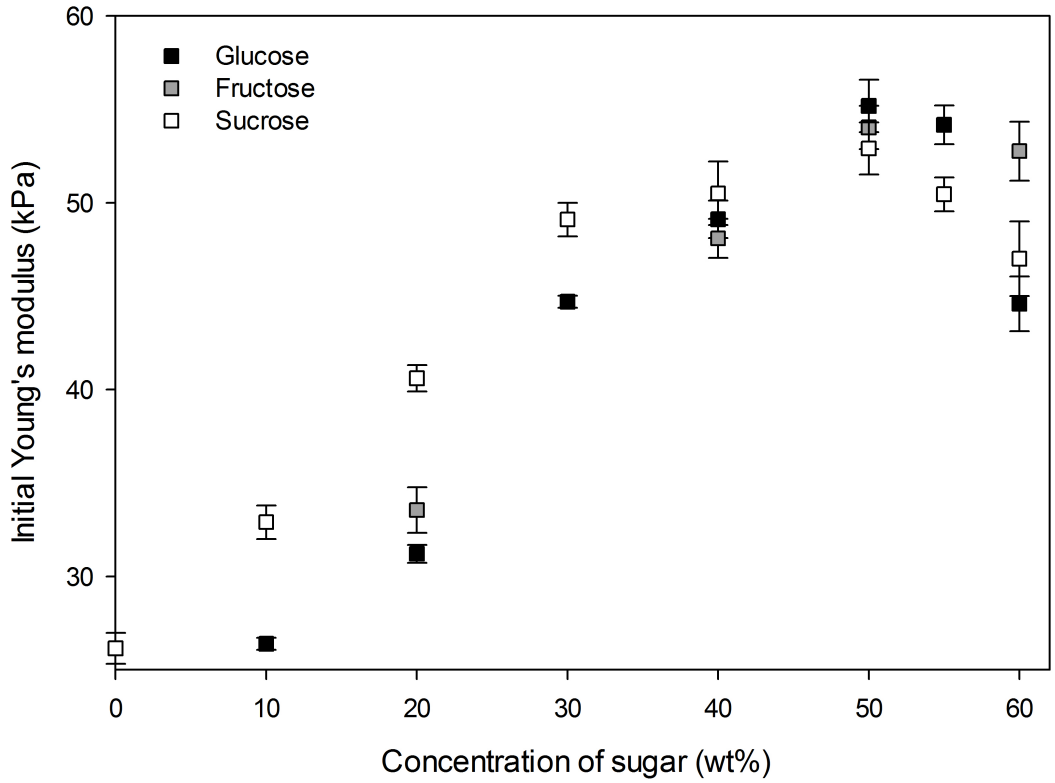


Figure 4.4: Initial Young's modulus of quiescently set 1% agar gels + 0.5% Tween 20 when compressed to 50% strain at a rate of 1 mms^{-1} as a function of sugar concentration. This reflects fluid gel particle stiffness. Measurements were conducted at 25 ℃.

4.3.4 Bulk rheological properties

The bulk rheology of the fluid gels was studied 48 hours after production. At 55% glucose, and 60% fructose and sucrose, crystallisation of the samples began, thus these measurements were not taken as the sample was not homogenous and therefore not representative. This supports the explanation given in Section 4.3.1, where the inhibition of gelation at 60% sugar (Figure 4.1) was said to be a result of the proximity to its glass transition. Figure 4.5a and 4.5b show viscosity and oscillatory data as a function of sugar concentration. Shear viscosity rose gradually upon increased concentration of sugar until 50% addition (Figure 4.5a). At 50% glucose and fructose, shear viscosity appeared to be noticeably higher and the error bars were larger (Figure 4.5a). The same observation can be made at 55% sucrose. The viscoelastic behaviour of the fluid gel systems was assessed

using oscillatory rheological data and storage modulus (G') has been plotted as a function of sugar concentration (Figure 4.5b). A similar trend to viscosity can be observed for G'.

To explain these results, it is helpful to consider the data from Figure 4.4. The addition of each sugar to quiescently set agar gels (up to 50%) resulted in an increased modulus. This trend is reflected in the modulus of the corresponding fluid gel particles and can therefore be attributed to the observed increase in viscosity and G' with sugar concentration (Figure 4.5a and 4.5b). Beyond 50% sugar, the lack of available water resulted in a decrease in quiescent agar gel strength (Figure 4.4). However, viscosity and G' of the corresponding fluid gels increased (Figure 4.5a and 4.5b). At these high levels of sugar, upon cooling of the agar/sugar solution during the fluid gel formation process, the sugar will have approached its glass transition. The fluid gels produced were therefore rubbery, exhibiting a high G' and shear viscosity. Tsoga, Kasapis, and Richardson (1999) described how agarose prevents sugar crystallisation in high levels of co-solute through encouraging intermolecular interactions, leading to high viscosity glass mixtures. The larger error bars at higher concentrations are also likely to be a function of this behaviour.

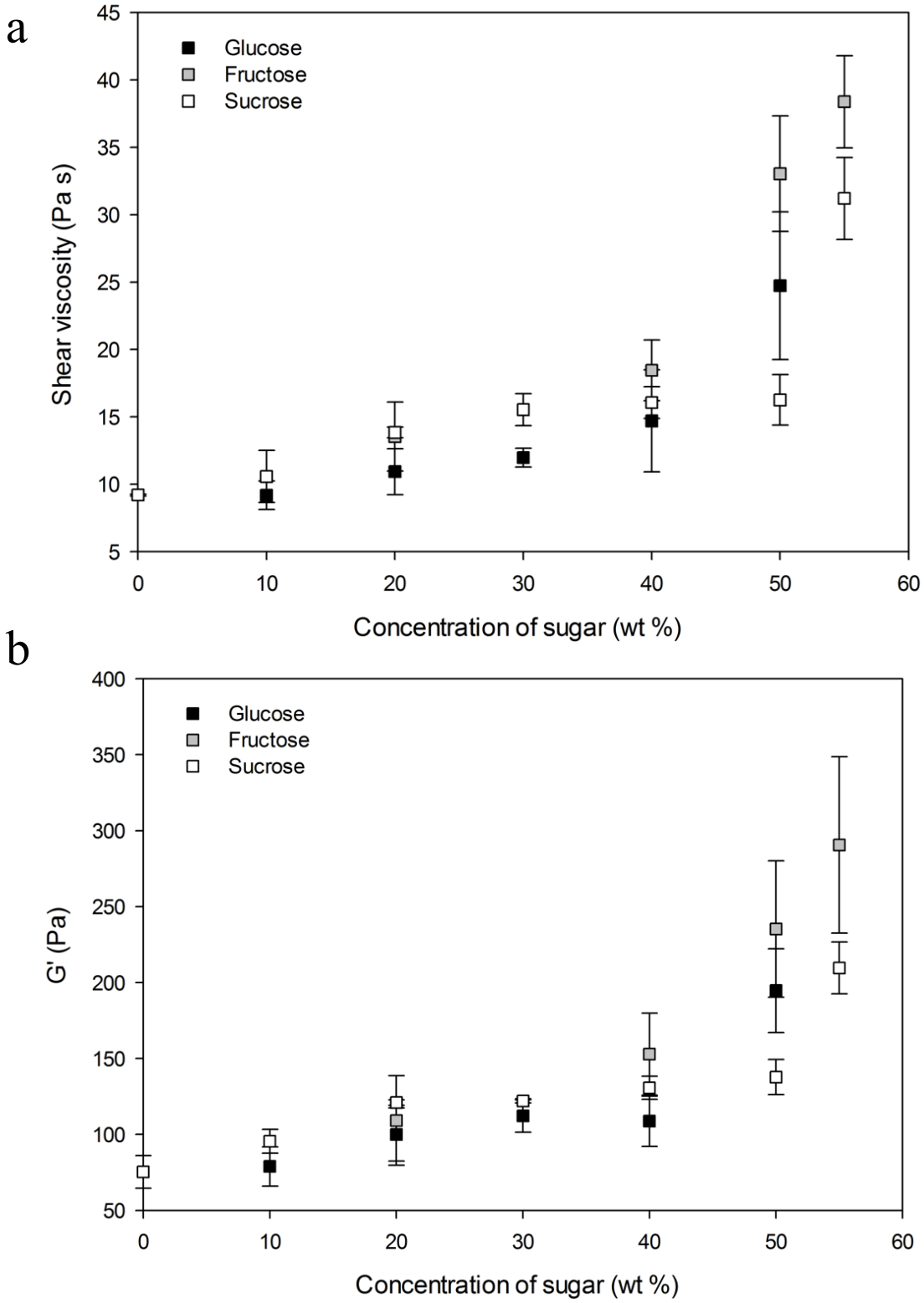


Figure 4.5: Rheological measurements of 1% agar + 0.5% Tween 20 fluid gels as a function of sugar concentration (glucose, fructose and sucrose). (a) shear viscosity at a shear rate of 1 s^{-1} measured from a flow curve (0.1 s^{-1} to 500 s^{-1}) and (b) storage modulus (G') from the LVR region of a strain controlled amplitude sweep. Measurements were carried out using a serrated parallel plate 48 h after production at 25 °C.

A similar trend can also be identified when looking at the yield stress of the agar fluid gels. Yield stress was determined from an amplitude sweep with controlled strain as the stress required to decrease G' in the LVR by 5%. From Figure 4.6, it can be observed to increase gradually from 0-50% sugar. The yield stress corresponds to the disruption of particle-particle interactions within the system and the initiation of flow by particles "squeezing" past each other, therefore, both particle interaction and particle modulus influence it. As discussed in Section 4.3.2, particle shape changes with sugar concentration. Star-like structures are observed at 0% and 20% sugar, where particles consist of smaller cores with long protruding 'tails'. Upon increasing sugar concentration, smaller particles are observed with less 'tails'. The branched nature of the star-like structures facilitates higher particle interaction and more efficient packing (Ellis et al., 2017) than the smaller, less branched particles (at higher sugar concentrations). In contrast, the particle modulus increased with sugar concentration (Figure 4.4). As fluid gel yield stress also increased (Figure 4.6), particle modulus appears to be the controlling factor and therefore dictated yield stress. In addition, the large yield stress measured at 55% sucrose in Figure 4.6, further confirms the conversion of the brittle agar gel network to a more rubbery-like structure.

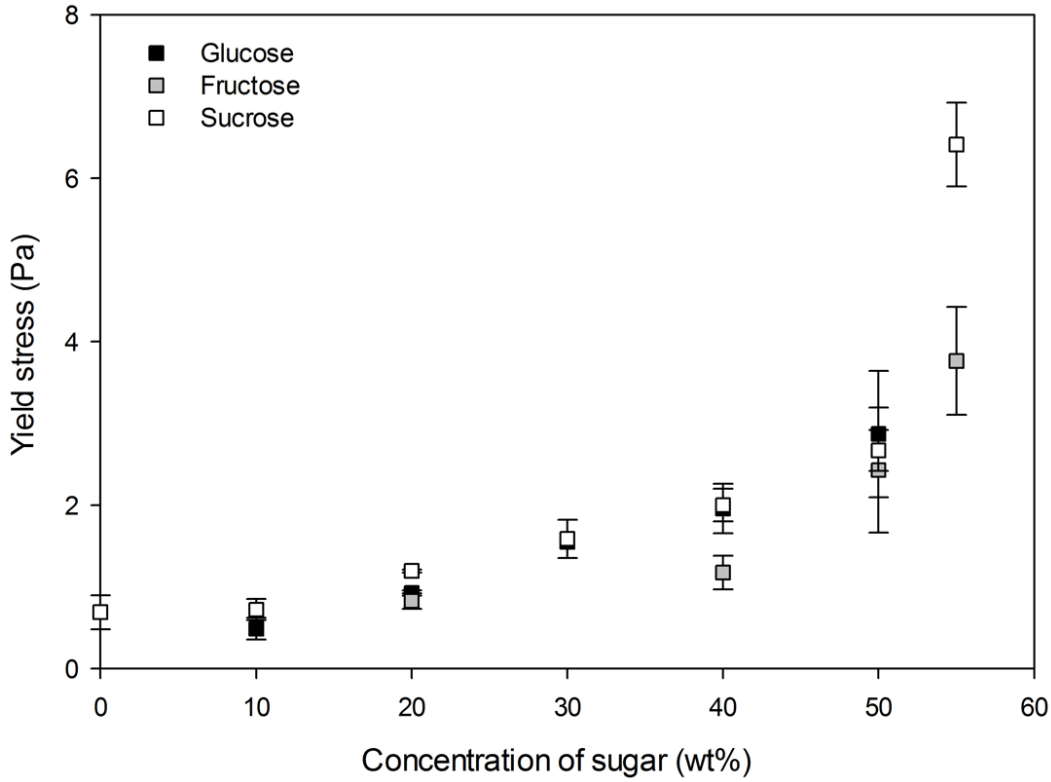


Figure 4.6: Yield stress of 1% agar + 0.5% Tween 20 fluid gels as a function of sugar concentration. Yield stress was measured as a 5% decrease in G' during an amplitude sweep conducted 48 h after production at 25 °C.

4.3.5 Foam capabilities and stability

The functionality of agar fluid gels to produce stable foams was investigated and related to their material properties. The ability of the systems to incorporate air was characterised using air fraction measurements. The soft, elastic nature of the fluid gels allowed the incorporation of air despite the opposite being true for many particulate systems (Murray & Ettelaie, 2004). Agar fluid gels were aerated in a Hobart mixer for 7 minutes, which ensured that all foams were in the wet foam boundary (air fraction within 0.65-0.95). Foam stability is another important parameter to understand when producing food foams, as they age over time leading to reduced sensory characteristics. The stabilisation of aerated agar fluid gels discussed in the previous Chapter (3) can be applied here (Ellis et al., 2017). Tween 20 was used to establish short term stability and therefore creation of the foam through quick adsorption to the interface. The half-life of the foams was directly

related to fluid gel yield stress, which increased with agar concentration. It was thought that once the foam had been generated, the continuous phase started to drain and a large number of agar particles remained in the foam channels and their nodes. This confinement caused an increase in the local viscoelasticity, which had a large impact on overall foam stability. However, eventually foam coarsening led to an increase in drainage velocity as confinement was lost, resulting in foam collapse.

Foam half-life for the systems here was measured and plotted as a function of fluid gel yield stress in Figure 4.7. Yield stress at different concentrations of each sugar were plotted, where data points correspond to concentrations in Figure 4.6. The data points closely follow the same curve, independent of sugar type. Increasing fluid gel yield stress, resulted in the foam half-life rising until it plateaued at 3-4 Pa (Figure 4.7). A similar trend was observed in previous work, where this was attributed to the yield stress reaching a value larger than the gravitational stress inside the foam. Therefore, at a fluid gel yield stress of 3-4 Pa, liquid drainage was considerably delayed. However, even without the effect of liquid drainage, the foam was limited to a certain life time. This was due to coarsening of the gas phase, which resulted in the loss of confinement. The gravitational stress would then become larger than the yield stress and the liquid quickly drained through the foam causing its collapse. This data supports the trend seen for agar fluid gels with no sugar in previous work (Ellis et al., 2017). Yield stress was enhanced through increased particle modulus and particle interaction. Previously, this was manipulated through altering agar concentration whereas in this work, it was influenced by changing solvent availability by adding sugar at various concentrations.

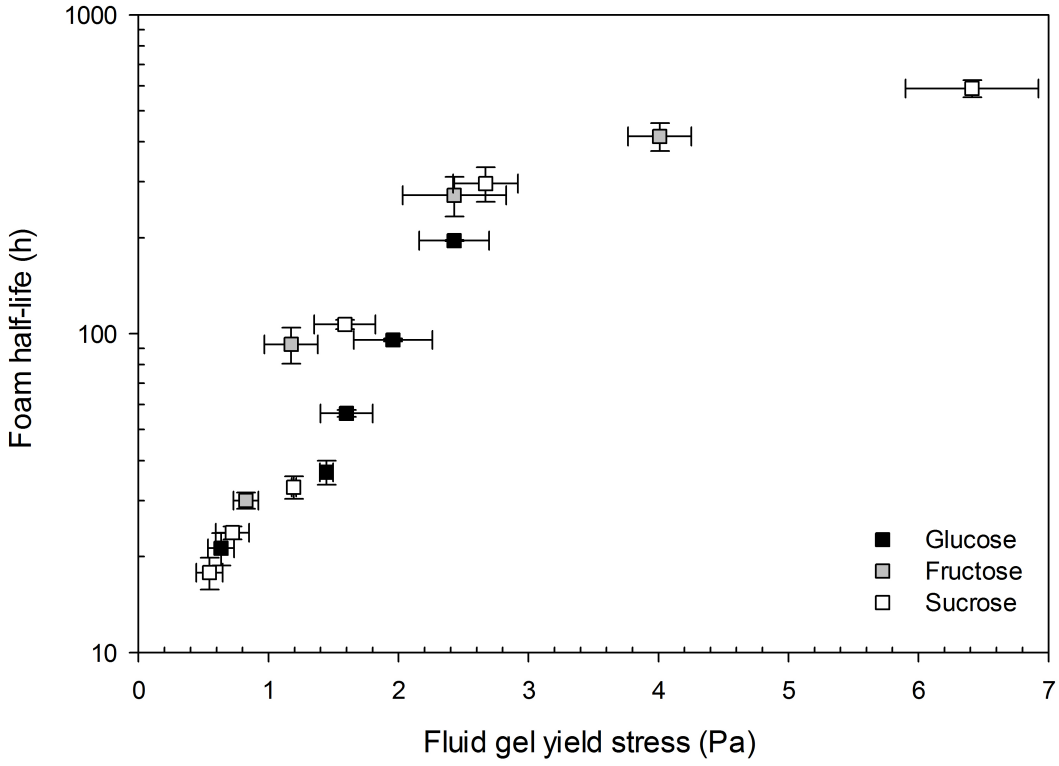


Figure 4.7: Foam half-life as a function of agar fluid gel yield stress for 1% agar + 0.5% Tween 20 with glucose, fructose and sucrose at various concentrations. The concentration of sugar to which each data point corresponds to can be determined from Figure 4.6.

4.3.6 Effect of particle size on foam drainage

In order to clarify the role of the particles in the foam stability mechanism, particle size was altered and its effect on liquid drainage was explored. Haffner, Khidas, and Pitois (2014) report a strong dependence of particle size when studying the jamming transitions in aqueous foams of granular hydrophilic particle suspensions. Here, the manipulation of production parameters provided the opportunity to investigate size effects. It was reported earlier in Section 4.3.2, that particle size was a function of solution viscosity entering the pin stirrer. The addition of an equivalent amount of sugar pre- and post-production would therefore alter solution viscosity and therefore final particle size, whilst keeping the formulation the same. Pre-production refers to the addition of sugar to the dissolved agar solution before it undergoes gelation in the pin stirrer (pre-fluid gel production) whereas post-production refers to the addition of sucrose to the fluid gel once it has been produced.

Sucrose at 20% was added pre- and post-production and particle size was measured after 48 hours (Figure 4.8). The particles were observed for two weeks after production to investigate the possibility of changes due to osmosis but none were observed. Particle sizes, as expected, were considerably different (Figure 4.8); the addition of sucrose pre-production resulted in fluid gels with a distribution of smaller particles (most abundant size approx. 10-15 μm in diameter) whereas addition post-production, yielded a distribution of larger particle sizes (most abundant approx. 40-45 μm). A difference in particle shape was also observed, where the larger particles (sugar added post-production) consisted of a small core with many tails protruding into the continuous phase, whilst the smaller particles (sugar added pre-production) had a smoother, more spherical surface. The reasons for this have been discussed in Section 4.3.2. The fluid gels were diluted by half in order to lower the volume fraction and therefore emphasise any effect observed from altering particle size. A similar yield stress (0.058 ±0.019 Pa and 0.052 ±0.005 Pa for pre- and post-production, respectively) and elastic modulus (G') was measured for the two fluid gels (Table 4.2).

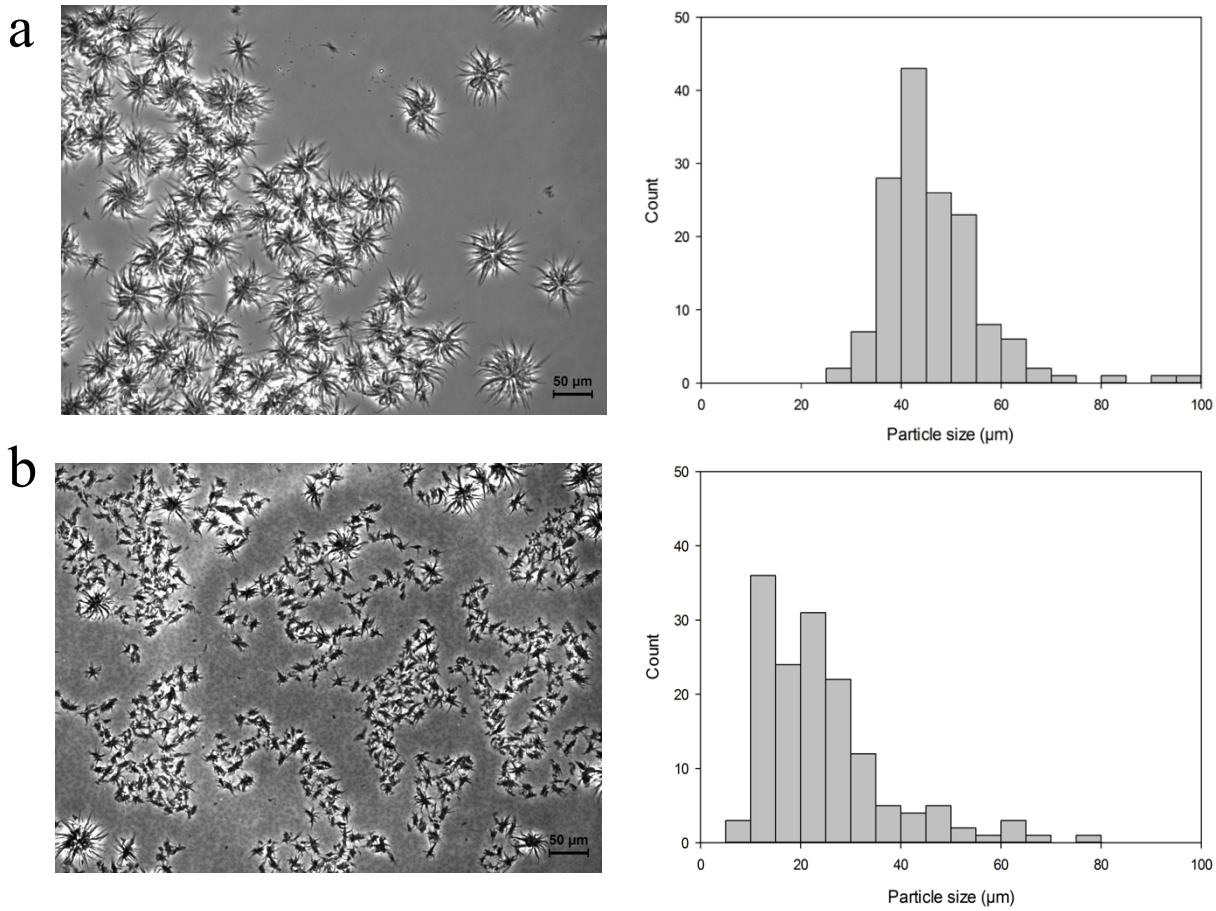


Figure 4.8: Optical micrographs and corresponding particle size distributions for 1% agar fluid gels with 0.5% Tween 20 and 20% sucrose added post-production (a) and pre-production (b).

The two samples were aerated in a Hobart mixer to a similar air fraction, 0.87 ±0.02 and 0.86 ±0.02, as seen in Table 4.2. In order to evaluate particle size effects, liquid drainage measurements were recorded using a foam analyser (DFA100). The initial liquid fraction was determined by comparison to the reference liquid and its decrease was recorded by measuring the electrical conductivity at 7 pairs of electrodes along the cell height. Drainage profiles for the first 12 hours after aeration at sensor 3 (half way down the foam) are plotted in Figure 4.9. Both samples had a very similar liquid content initially but less liquid drained through the foam when the continuous phase contained larger particles (post-production sucrose addition) than smaller particles (pre-production sucrose addition). For example, in the first four hours, liquid content decreased by only 1.9% ±1.0

compared to 6.4% ±0.8 (Figure 4.9). After initial aeration, the bulk phase would have begun to flow through the foam channels causing them to narrow. It appears that the larger particles were more effective at accumulating in the foam channels and therefore reducing the flow of liquid. It was likely that the smaller particles were not so easily confined to the channels, resulting in a higher extent of drainage of the continuous phase before confinement occurred. It is also important to note that as the larger particles consisted of many protruding 'tails', there is the possibility that they were able to interact together with greater ease than the less branched, smaller particles when confined in the foam channels and nodes, allowing them to accumulate together in these spaces more quickly.

Table 4.2: Properties of 1% agar + 0.5% Tween 20 fluid gels with sucrose added pre- and post-production, as well as their properties once aerated.

	Sucrose addition	
	Pre-production	**Post-production**
G' (Pa)	12.8 ±4.7	15.1 ±0.8
Yield stress (Pa)	0.058 ±0.019	0.052 ±0.005
Air fraction	0.87 ±0.02	0.86 ±0.02
Decrease in liquid content over first 4 h (%)	6.4 ±0.8	1.9 ±1.0
Foam half-life (h)	9.4 ±2.1	9.2 ±1.1

However, despite differences in drainage rates, the half-life of the foams (Table 4.2) was very similar (9.4 ±2.1 h for pre-production and 9.2 ±1.1 h for post-production). To explain this result, it is helpful to consider work by Haffner, Khidas, and Pitois (2015); they defined the confinement parameter, λ, which related the size of the particles to the size of

passage through constrictions in the foam network. For $\lambda>1$, particles are captured by constrictions, resulting in a sharp decrease in drainage velocity. However, as λ increases (as foam channels narrow with disproportionation and drainage), particles become too large to be included in the foam network. They become progressively excluded and drainage velocity increases. This *particle exclusion transition* therefore sees the drainage velocity evolve from its minimal value (fully included particles) to its maximum (fully excluded particles). This explanation can be used to describe what is happening in these foams; larger particles were included in the foam network quicker than smaller particles, therefore when the smaller particles were included, more liquid had drained and the foam channels were narrower. As a consequence, λ would have been similar and the particle exclusion transition occurred at a similar time, resulting in a similar time of foam collapse. This work reveals that at low volume fractions, fluid gels do not behave as a network of particles with a finite yield stress able to suspend bubbles. Instead, liquid drainage quickly occurs and is influenced by the size and shape of individual. However, when fluid gels are concentrated, they behave as a network of particles capable of suspending air bubbles and foam half-life is dependent upon yield stress.

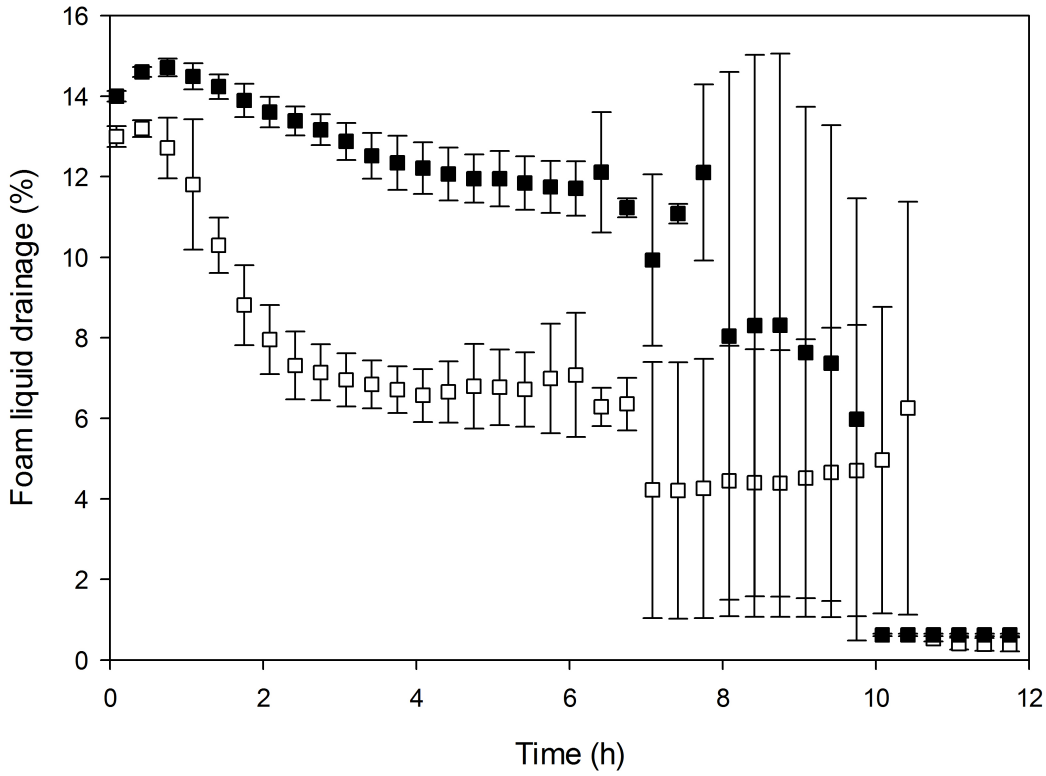


Figure 4.9: Liquid drainage profiles of aerated 1% agar + 0.5% Tween 20 fluid gels with 20% sucrose added pre-production (unfilled symbols) and post-production (filled symbols). Liquid content is shown over 12 h from initial foaming at sensor 3 in the column (positioned half way down the foam). Every 4th data point is sampled for clarity.

4.4 Conclusions

The influence of glucose, fructose and sucrose on the gelation, material and foaming properties of 1% agar fluid gel have been investigated. The temperature of ordering during gelation was only affected by the addition of sucrose, where it increased with sucrose concentration due to an increase in number of junction zones provided through hydrogen bonding. All sugars at 60% somewhat inhibited gelation as the glass transition of sugar was approached. The size of fluid gel particles decreased with increasing sugar concentration due to a higher solution viscosity entering the pin stirrer favouring helix nucleation and inhibiting the growth process. Particle size was not dependent on the type of sugar, only the viscosity change of the solution manipulated by sugar concentration. In order to infer particle strength, the strength of quiescent 1% agar gel counterparts were measured. The addition of glucose, fructose and sucrose up to 50% resulted in increased initial Young's modulus of the gel. Above 50% sugar however, the lack of available water for gelation resulted in a lower gel strength. Again the type of sugar was not so important. Furthermore, the influence of sugar on bulk rheology was explored. At high concentrations of all sugars (above 50%), shear viscosity and G' were considerably higher. This was due to a change in network formation (shorter helices and fewer aggregates). Below 50% sugar, shear viscosity, G' and yield stress increased with increasing concentration of all sugars, this was supported by the affect this had upon foam half-life measurements.

All systems showed good foaming properties, controlled by sugar concentration. Foam half-life was dependent on fluid gel yield stress and increased until the necessary stress to suspend air bubbles of this size was reached (3-4 Pa) and the half-life begun to plateau.

These results support the trend seen for agar fluid gels with no added sugar in previous work (Ellis et al., 2017). In both studies, yield stress was enhanced through increased particle elasticity and particle interaction. However, here we report the first example of influencing such parameters by changing solvent availability through the addition of sugar. Particle size was shown to affect the rate of liquid drainage when the continuous phase was dilute and yield stress was low. Larger particles were more effective at reducing liquid drainage through confinement.

This research has provided fundamental understanding of the effect of sugars on the microstructure of agar fluid gels and their foams. Increasing the understanding of the role of sugar in such systems will allow products to be engineered with alternative ingredients, which will help in the current drive for sugar reduction.

LIST OF REFERENCES

Arnott, S., Fulmer, A., Scott, W., Dea, I., Moorhouse, R., & Rees, D. (1974). The agarose double helix and its function in agarose gel structure. Journal of Molecular Biology, 90(2), 269-272.

Bradbeer, J. F., Hancocks, R., Spyropoulos, F., & Norton, I. T. (2014). Self-structuring foods based on acid-sensitive low and high acyl mixed gellan systems to impact on satiety. Food Hydrocolloids, 35, 522-530.

Coultate, T. P. (2009). Food: the chemistry of its components: Royal Society of Chemistry.

de Carvalho, W., & Djabourov, M. (1997). Physical gelation under shear for gelatin gels. Rheologica Acta, 36(6), 591-609.

Deszczynski, M., Kasapis, S., & Mitchell, J. R. (2003). Rheological investigation of the structural properties and aging effects in the agarose/co-solute mixture. Carbohydrate Polymers, 53(1), 85-93. doi:http://dx.doi.org/10.1016/S0144-8617(02)00327-2

Ellis, A. L., Norton, A. B., Mills, T. B., & Norton, I. T. (2017). Stabilisation of foams by agar gel particles. Food Hydrocolloids, 73, 222-228.

Foord, S., & Atkins, E. (1989). New x-ray diffraction results from agarose: Extended single helix structures and implications for gelation mechanism. Biopolymers, 28(8), 1345-1365.

Frith, W., Garijo, X., Foster, T., & Norton, I. (2002). Microstructural origins of the rheology of fluid gels. In Williams, P. A., Phillips, G O. (Eds.), Gums and Stabilisers for the Food Industry (Vol. 11, pp. 95-103). Cambridge: The Royal Society of Chemsitry.

Gabriele, A. (2011). Fluid gels: Formation, production and lubrication. Univeristy of Birmingham, eThesis.

Gabriele, A., Spyropoulos, F., & Norton, I. T. (2009). Kinetic study of fluid gel formation and viscoelastic response with kappa-carrageenan. Food Hydrocolloids, 23(8), 2054-2061.

Gabriele, A., Spyropoulos, F., & Norton, I. T. (2010). A conceptual model for fluid gel lubrication. Soft Matter, 6(17), 4205-4213.

Haffner, B., Khidas, Y., & Pitois, O. (2014). Flow and jamming of granular suspensions in foams. Soft Matter, 10(18), 3277-3283.

Haffner, B., Khidas, Y., & Pitois, O. (2015). The drainage of foamy granular suspensions. Journal of Colloid and Interface Science, 458, 200-208.

Moakes, R. J. A., Sullo, A., & Norton, I. T. (2015). Preparation and characterisation of whey protein fluid gels: The effects of shear and thermal history. Food Hydrocolloids, 45, 227-235. doi:http://dx.doi.org/10.1016/j.foodhyd.2014.11.024

Murray, B. S., & Ettelaie, R. (2004). Foam stability: proteins and nanoparticles. Current Opinion in Colloid & Interface Science, 9(5), 314-320.

Nishinari, K., & Fang, Y. (2017). Relation between structure and rheological/thermal properties of agar. A mini-review on the effect of alkali treatment and the role of agaropectin. Food Structure, 13, 24-34. doi:https://doi.org/10.1016/j.foostr.2016.10.003

Nishinari, K., Watase, M., Kohyama, K., Nishinari, N., Oakenfull, D., Koide, S., Phillips, G. O. (1992). The effect of sucrose on the thermo-reversible gel-sol transition in agarose and gelatin. Polymer Journal, 24(9), 871-877.

Nishinari, K., Watase, M., Williams, P. A., & Phillips, G. O. (1990). Kappa carrageenan gels: effect of sucrose, glucose, urea, and guanidine hydrochloride on the rheological and thermal properties. Journal of Agricultural and Food Chemistry, 38(5), 1188-1193.

Normand, V., Aymard, P., Lootens, D. L., Amici, E., Plucknett, K. P., & Frith, W. J. (2003). Effect of sucrose on agarose gels mechanical behaviour. Carbohydrate Polymers, 54(1), 83-95.

Norton, I., Jarvis, D., & Foster, T. (1999). A molecular model for the formation and properties of fluid gels. International Journal of Biological Macromolecules, 26(4), 255-261.

Sugar Reducion: Achieving the 20%. (PHE publications gateway number: 2016677). (2017).

Telis, V., Telis-Romero, J., Mazzotti, H., & Gabas, A. (2007). Viscosity of aqueous carbohydrate solutions at different temperatures and concentrations. International Journal of Food Properties, 10(1), 185-195.

Tsoga, A., Kasapis, S., & Richardson, R. K. (1999). The rubber-to-glass transition in high sugar agarose systems. Biopolymers: Original Research on Biomolecules, 49(4), 267-275.

Watase, M., Kohyama, K., & Nishinari, K. (1992). Effects of sugars and polyols on the gel-sol transition of agarose by differential scanning calorimetry. Thermochimica Acta, 206, 163-173.

Watase, M., Nishinari, K., Williams, P. A., & Phillips, G. O. (1990). Agarose gels: effect of sucrose, glucose, urea, and guanidine hydrochloride on the rheological and thermal properties. Journal of Agricultural and Food Chemistry, 38(5), 1181-1187.

Yang, K., Wang, Z., Brenner, T., Kikuzaki, H., Fang, Y., & Nishinari, K. (2015). Sucrose release from agar gels: Effects of dissolution order and the network inhomogeneity. Food Hydrocolloids, 43, 100-106. doi:https://doi.org/10.1016/j.foodhyd.2014.05.005

Chapter 5: THE HYDROPHOBIC MODIFICATION OF KAPPA CARRAGEENAN MICROGEL PARTICLES FOR THE STABILISATION OF FOAMS

Based on work published as: Ellis, A. L., Mills, T. B., Norton, I. T., & Norton-Welch, A. B. (2019). The hydrophobic modification of kappa carrageenan microgel particles for the stabilisation of foams. *Journal of Colloid and Interface Science, 538*, 165-173.

5.1 Background

The aim of this chapter was to hydrophobically modify fluid gel particles in order facilitate their adsorption to the air/water interface, thus increasing long-term foam stability. Particles can be modified *in-situ* through interaction with a surfactant. Hence, it should be possible to bind negatively charged fluid gel particles with a cationic surfactant through electrostatic interaction. Kappa carrageenan (κC) was chosen because it is strongly negatively charged and so has a high potential for electrostatic interaction with cationic surfactant, lauric arginate, which has been approved as generally regarded as safe (GRAS) within the United States for certain food applications (Benford et al., 2009). Lauric arginate was mixed with kappa carrageenan microgel particles at various concentrations and the potential electrostatic interaction was studied using zeta potential, turbidity and rheological measurements. Mixtures were then aerated and foaming properties were explored, in particular the location of the particles within the foam was investigated using optical and confocal microscopy. Finally, a non-ionic surfactant (Tween 20) was mixed with kappa carrageenan particles in order to confirm the change in surface activity due to electrostatic binding with lauric arginate.

5.2 Materials and methods

5.2.1 Materials

Kappa carrageenan (22048) and Tween 20 (≤3.0% impurities) were purchased from Sigma Aldrich (UK). Lauric arginate was obtained in the form of Cytoguard LA 2X (A&B Ingredients, USA) in a liquid form with propylene glycol carrier and a 20% content of lauric arginate. All were used without further purification and concentrations were calculated as weight percentage.

5.2.2 Preparation of fluid gel

Kappa carrageenan (1 wt%) was dispersed in deionised water at room temperature, then heated to 70 °C. The solution was transferred into a cooled jacketed pin stirrer through a peristaltic pump at 70 °C. The outlet temperature was controlled to 5 °C to ensure gelation occurred under shear (gelation temperature ≈ 25 °C). A retention time of 7.5 min was achieved through using a pump speed of 20 $mLmin^{-1}$, resulting in a cooling rate of 8 $°Cmin^{-1}$. The shaft rotation speed was set to 1500 rpm to give a narrow distribution of particle size (Gabriele, Spyropoulos, & Norton, 2010). Fluid gels were stored at 5 °C.

5.2.3 Preparation of κC fluid gel-LA complexes

1% κC fluid gel was diluted 1:1 with deionised water. LA at various concentrations was then added to the solution whilst stirring for 5 days at room temperature.

5.2.4 Zeta potential measurements

Zeta potential was determined using a Zetasizer (Malvern Instruments, UK) at 25 °C. κC fluid gel was diluted and its pH was altered from 1.5 to 10 using either NaOH or HCl of

1M concentrations. Complexes were measured at their natural pH. All data points were carried out in three replicates.

5.2.5 Turbidity measurements

The turbidity of κC fluid gel-LA complexes was inferred from the absorbance at 600 nm using a UV-Vis spectrophotometer (Orion AquaMate, Thermoscientific, UK) in 1 cm cuvettes against deionised water. Measurements were carried out at 25 °C in three replicates.

5.2.6 Rheology

A Kinexus rheometer (Malvern Instruments, UK) was used to perform rheological measurements at 25 °C. κC fluid gel-LA complexes were tested after 24 h to ensure post-production particle ordering completion (de Carvalho & Djabourov, 1997; Gabriele, Spyropoulos, & Norton, 2009). All measurements were conducted using a serrated parallel plate of 60 mm diameter set to a 1 mm gap. Amplitude sweeps were conducted at a frequency of 1 Hz as a function of applied oscillatory strain. All experiments were carried out in three replicates.

5.2.7 Surface tension

Surface tension measurements of κC fluid gel-LA complexes and LA solutions were performed using a Kruss GmbH K100 tensiometer (Hamburg, Germany). The Wilhelmy plate method was used to measure static surface tension at an immersion depth of 2mm at 25 °C. Experiments were carried out in three replicates. The critical micelle concentration (CMC) was calculated as the concentration at which surface tension stopped decreasing (Figure 5.8), which was 0.15 wt% for LA solutions. This was similar to values reported in the literature: 0.18-0.21 wt% (Asker, Weiss, & McClements, 2009;

Bonnaud, Weiss, & McClements, 2010). The slight difference may have been a result of a difference in the source of Lauric Arginate or in the method of obtaining CMC as isothermal titration calorimetry was used in the referenced literature.

5.2.8 Aeration

κC fluid gel-LA complexes of equal volumes were aerated using a Hobart mixing unit. The highest speed setting was used for 7 min as this ensured air fraction was high for all systems (between 0.65-0.95: the wet foam boundary). Air fraction was determined to assess foam ability using Equation 1, by weighting equivalent volumes of fluid gel and foam, using three replicates.

$$\text{Air fraction} = 1 - \left(\frac{m_{foam}}{m_{fluid\ gel}}\right) \qquad (5.1)$$

Overall foam stability was measured using half-life measurements, that is the time taken to reduce the height of the foam by half. The reduction of the foam height was recorded using a CCD camera and the half-life was later calculated for three replicates (three separate batches).

5.2.9 Liquid drainage and foam structure measurements

Liquid drainage and bubble size measurements were conducted using a Krüss DFA100LCM foam analyser (Krüss, Germany). The κC fluid gel-LA mixture was poured into the foam cell to cover the reference electrode followed by the externally produced foam. The decrease in liquid fraction was then recorded using electrical conductivity measurements at 7 pairs of electrodes along the cell height (see Figure 5.1). Drainage profiles were recorded at sensor 3 (positioned at half the foam height) for the first four

hours from initial aeration. Bubble sizes were recorded using a high resolution camera at a similar foam height. Experiments were carried out in three replicates (three separate batches).

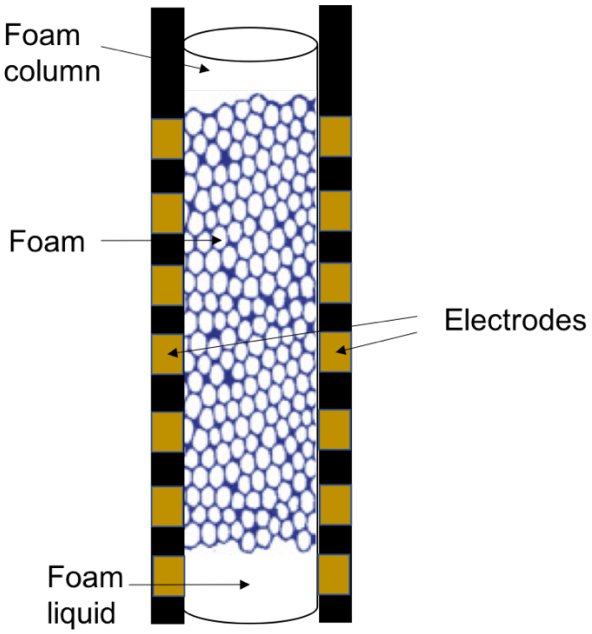


Figure 5.1: Schematic of foam column and electrodes of the Krüss DFA100LCM.

5.2.10 Optical microscopy

Aerated κC fluid gel-LA complexes were imaged using phase contrast microscopy (Leica Microsystems, UK). The sample was placed onto a microscope slide with a coverslip and observed using objective lenses up to 40x magnification.

5.2.11 Confocal microscopy

The microstructure of aerated κC fluid gel-LA complexes as well as κC fluid gel particles before complexation (1 wt% κC) were visualised using a confocal scanning laser microscope (Leica TCS SPE, Heidelberg, Germany). The κC fluid gel-LA complexes were aerated, placed onto a microscope slide and stained with 0.01 wt% rhodamine B (Sigma Aldrich, Dorset UK). A coverslip was then placed over the sample and a laser operating at a wavelength of 532 nm was used for imaging.

5.3 Results and Discussion

5.3.1 Production and characterisation of kappa carrageenan fluid gels

The gelling mechanism of kappa carrageenan (κC) is widely accepted as a thermally-reversible coil-to-helix transition followed by helix aggregation in the presence of K^+ ions (Morris, Rees, & Robinson, 1980). During fluid gel preparation, this process occurs under shear resulting in the production of gel particles dispersed in a continuous phase, typically water (Norton, Foster, & Brown, 1998). In order to attempt to bind lauric arginate (LA) to κC particles, it was first investigated whether LA could be added to a hot κC solution before it undergoes gelation under shear. Figure 5.2 displays viscosity profiles of 1% κC solutions with various concentrations of LA, upon cooling under shear. At 0% LA, as the temperature was lowered, the viscosity gradually increased until a sharp rise was observed ≈ 20 °C. This indicates the formation of gel particles, which grow to an equilibrium particle size dictated by the shear rate. Upon increasing the concentration of LA, the initial viscosity was slightly lower but a similar steep increase was observed at ≈ 20 °C, indicating that gelation had occurred. At 0.1% LA and 0.15% LA, however, this ordering transition was not so prominent, suggesting that gelation was somewhat inhibited. An important feature of the gelling mechanism of κC is the ability of monovalent cations, such as K^+, to suppress the electrostatic repulsion between κC sulphate groups allowing helix aggregation. The presence of larger LA molecules that are also positively charged would have interfered with this ordered structure by interacting with some of the sulphate groups. It was therefore not appropriate to add LA to the solution pre-fluid gel production.

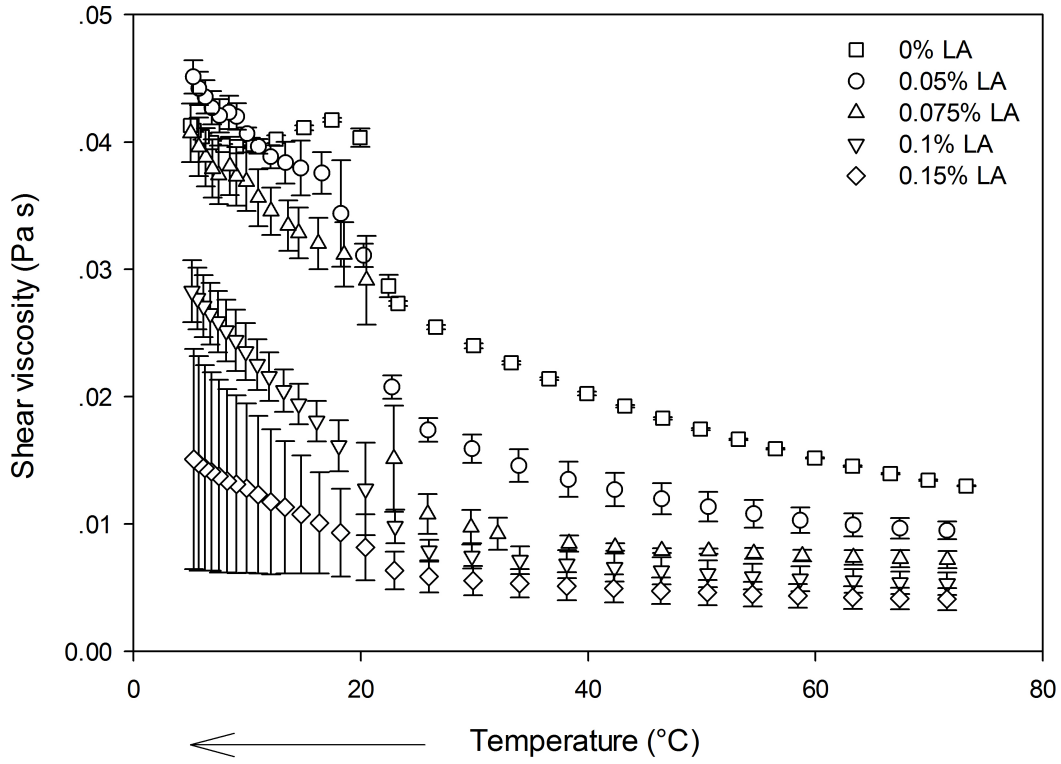


Figure 5.2: Viscosity profiles during the production of a 1% kappa carrageenan fluid gel with different concentrations of LA. The temperature was lowered from 70 °C to 5 °C at a cooling rate of 2 °Cmin^{-1}, under an applied shear rate of 500 s^{-1}.

Consequently, LA was added post fluid gel production; 1 wt% κC fluid gel was prepared by shearing a hot solution of κC whilst it underwent gelation in a cooled jacketed pin stirrer at a shaft rotation speed of 1500 rpm. The κC particles behave as soft microgel particles with penetrable "hairy" chains allowing for particle overlap and interaction (Garrec, Guthrie, & Norton, 2013). Garrec et al. (2013) previously estimated the κC fluid gel particle volume fraction at 1 wt% as 0.65, here the fluid gel was diluted by half in order to study a less concentrated suspension. Unfortunately, the particles cannot be visualised using optical microscopy as the refractive index of κC is too close to that of the water continuous phase (1.334). However, particles could be imaged using confocal microscopy (Figure 5.4a), particle diameter appeared to be in the 10-50 μm range.

It is important to note that no additional K^+ ions were added during fluid gel production. This was because previous work in the research group showed there was sufficient K^+ ions present in the kappa carrageenan starting material to facilitate helix aggregation; the final stage of gelation. However, as the extent of gelation was not measured in this study, it's worth noting that more K^+ ions may have been required to enable complete gelation under shear and therefore the formation of ideal fluid gel particles. If gelation was not complete, it is hypothesised that additional κC sulphate groups would have been available for interaction with LA upon mixing, not just those exposed at the surface of particles. This would have resulted in further aggregation of κC:LA (and less LA at the surface) and is represented in Figure 5.3.

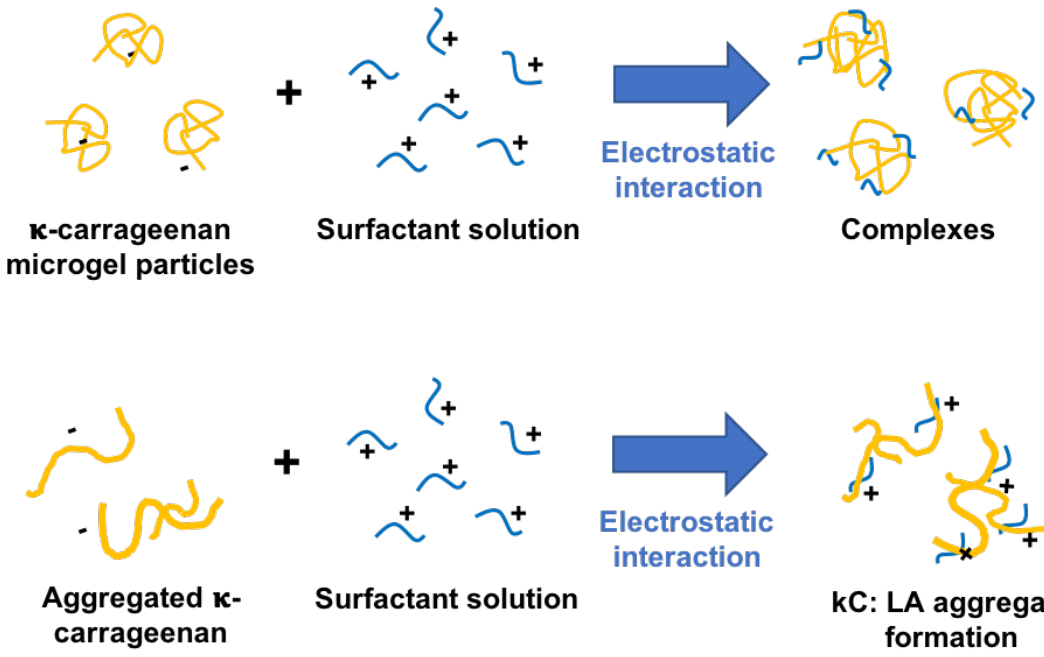


Figure 5.3: (Above) the interaction between lauric arginate and ideal κC fluid gel particles (formed in the presence of sufficient K^+ ions for complete gelation). (Below) the formation of a κC:LA aggregated system due to insufficient K^+ ions available during gelation.

The zeta (ζ) potential of diluted 1% kappa carrageenan (κC) fluid gel was measured over a pH range. At natural pH (6.8), ζ-potential was -53.1 ± 2.9 mV (Figure 5.4b), indicating κC particles were strongly negatively charged. This can be attributed to their ester sulphate groups. ζ-potential remained constant over a wide pH range, only changing considerably at pH 1.5 where particles became less negatively charged due to protonation of κC under strong acidic conditions (Figure 5.4b). The ζ-potential of lauric arginate (LA) at natural pH (2.3) was +23.8 ± 3.9 mV, which confirmed its positive charge (Figure 5.4b). The potential electrostatic interaction between κC and LA was therefore investigated at their natural pH and as a function of LA concentration.

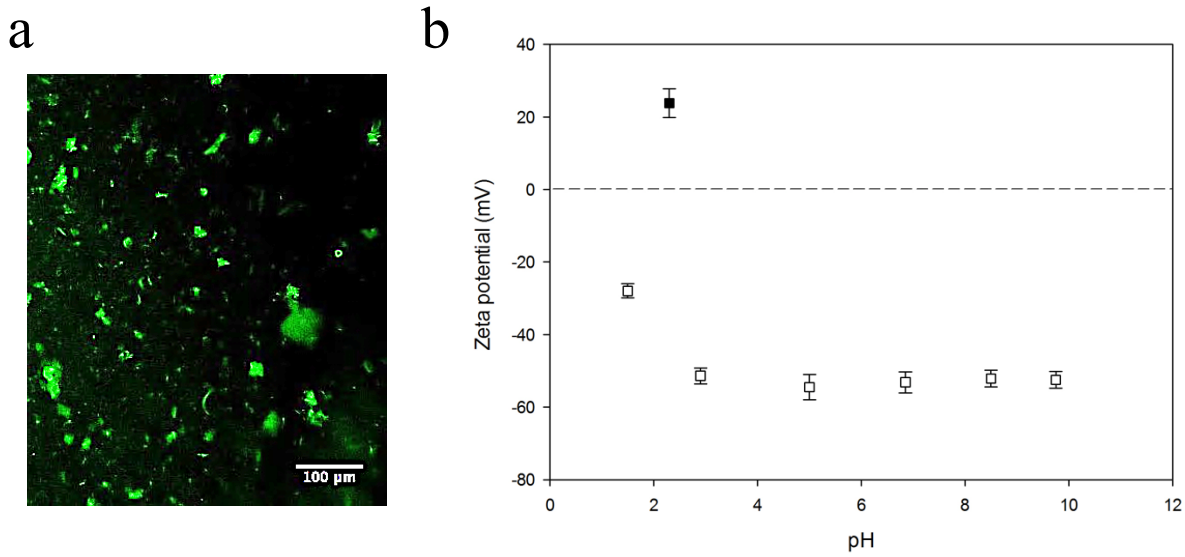


Figure 5.4: (a) Confocal micrograph of diluted 1 wt% κC fluid gel particles at natural pH (6.8) dyed with rhodamine B. (b) Zeta potential measurements of diluted 1 wt% κC fluid gel (□) over a pH range and of LA at natural pH (■).

5.3.2 Complex formation through surfactant binding

LA was added at various concentrations to a diluted 1% κC fluid gel solution. Zeta potential, turbidity and rheological measurements were used to analyse the interaction. The ζ-potential of κC particles were measured 24 h after production. At 0% LA, ζ-potential was -53.1 ± 2.9 mV, reflecting its negatively charged ester sulphate groups.

Upon increasing LA concentration, ζ-potential became increasing less negative until it reached zero at 0.15% LA (Figure 5.5). This suggests that monomers of LA were binding to κC particles reducing their negative charge and at 0.15% LA, sufficient surfactant had been added to neutralise the charge. It was hypothesised that the electrostatic interaction was facilitated by the cationic head group (L-arginine) of LA and the negatively charged sulphate groups of κC particles. It has often been reported in the literature that the ζ-potential of negatively charged particles mixed with cationic surfactants continued to increase with surfactant concentration after this charge neutralisation had occurred (Cui et al., 2010; Deleurence, Parneix, & Monteux, 2014; Liu et al., 2010). This was a result of a second layer of surfactant adsorbing onto the initial monolayer through hydrophobic interactions. However, increasing the concentration of LA beyond 0.15% (to 0.2%) revealed a decrease in ζ-potential to -3.8 ± 1.8 mV. A return to a less negative ζ-potential suggests that a bilayer of surfactant cannot form and instead added surfactant is most likely residing in the continuous phase.

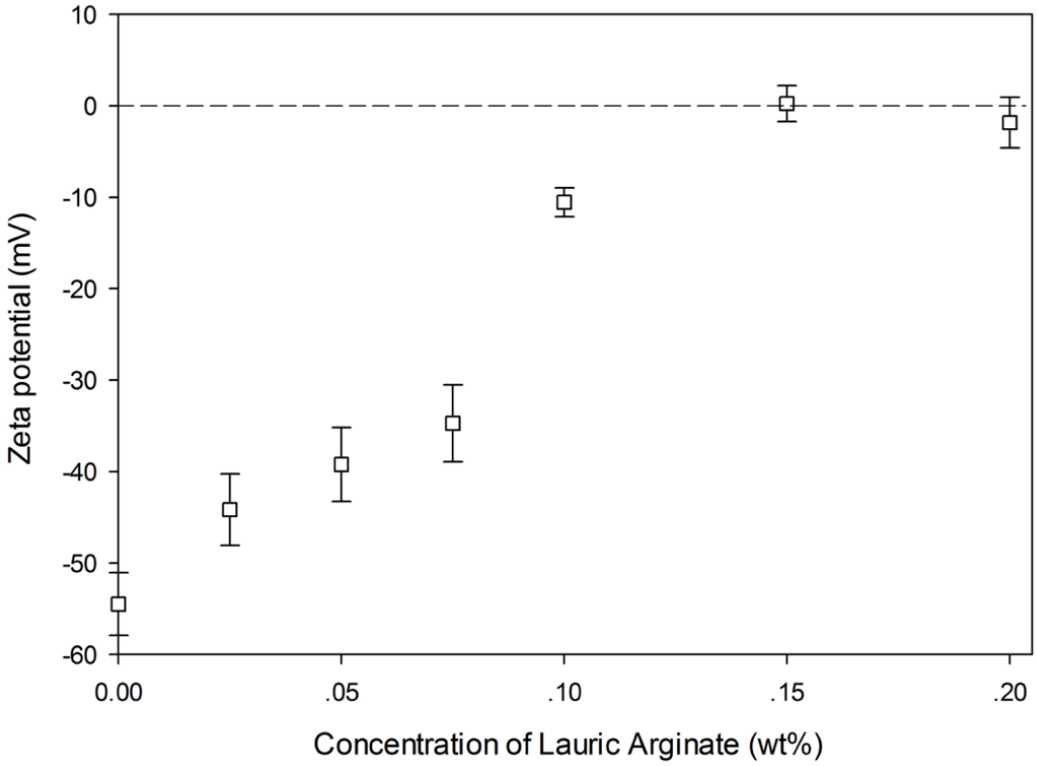


Figure 5.5: Zeta potential measurements of κC fluid gel particles as a function of increasing LA concentration. Concentration is calculated as wt% of the total solution.

Visible observations of κC + LA fluid gels confirmed a change in their structure with increasing LA concentration (Figure 5.6a). Fluid gels increased in turbidity but remained homogenous in appearance until 0.1% LA. From 0.1% LA increasingly large aggregates were observed using optical microscopy, ranging from 100 μm to 300 μm in size. Turbidity was measured using a UV-Vis spectrophotometer to quantify these observations. Absorbance can be seen to increase linearly with LA concentration (Figure 5.6b). At 0.15% and 0.2% LA, the error bars in absorbance data were considerably larger, due to substantial aggregates observed in the solutions. This turbidity data provides further evidence of complex formation, where an increase in turbidity (scattering of light by particles) corresponds to an increase in particle density, due to electrostatically bound surfactant. It is also clear that aggregation of the complexes occurred, especially at higher LA concentrations. This was caused by a reduction in particle charge, which led to less

repulsion and therefore more intermolecular interactions between particles. This effect was heightened at 0.15% LA and 0.2% LA as charge neutralisation of the complexes considerably limited their solubility. A similar trend was first observed by Bonnaud et al. (2010) where turbidity initially increased at low concentrations of LA when mixed with iota carrageenan, indicating the formation of complexes. Larger aggregates were then observed at concentrations of 0.03-0.23 wt% LA.

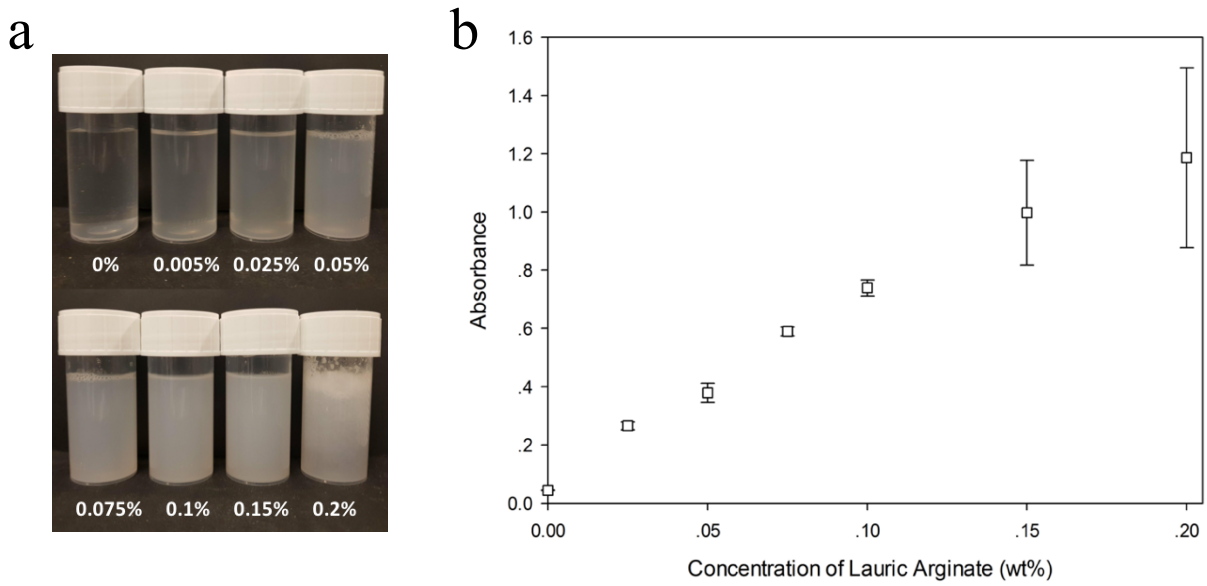


Figure 5.6: (a) Photographs of κC + LA fluid gels at various LA concentrations. (b) Absorbance of the same solutions, measured using a UV-Vis spectrophotometer.

The bulk viscosity of foams affect the mobility of the continuous phase and therefore drainage velocity (Saint-Jalmes, 2006). It is therefore essential to understand the rheological responses of these fluid gels to understand how they behave when aerated. The viscosity profiles of κC fluid gel complexes at various LA concentrations were measured (Figure 5.7a). The flow curves at all LA concentrations exhibited strongly shear thinning behaviour. This is typical of fluid gels at low volume fractions, where they behave as highly aggregated suspensions dominated mainly by colloidal forces (Moakes, Sullo, & Norton, 2015). At higher volume fractions, particles behave as soft microgels

where rheology is dependent on particle elastic modulus as well as particle-particle interactions (Fernández Farrés, Moakes, & Norton, 2014; Gabriele et al., 2009). From Figure 5.7a, at low shear rates a difference in fluid gel viscosity can be observed, where it increased with LA concentration. However at high shear rates, most fluid gels displayed a similar viscosity. This further confirms the difference in particle aggregation. Initially, particles were aggerated together to various extents, but upon shearing, the interactions between particles were broken and structures were similar. The flow curve of 0.2% LA was different at higher shear rates, where it appears to shear thicken at ~50 s^{-1}, this was likely due to the larger aggregates jamming in the geometry. The viscoelastic behaviour of the fluid gels was measured using oscillatory rheological data (Figure 5.7b). At LA concentrations up to 0.075%, the loss modulus (G'') dominated over the storage modulus (G') indicating a more viscous response from the system. However, at 0.15% and 0.2% LA, G' was dominant, which reflects a more elastic response. These structures also exhibited a yield stress. Therefore, as aggregation of the particles increased due to increased surfactant binding, a network with gel-like properties began to form, leading to an eventual dominance in G'.

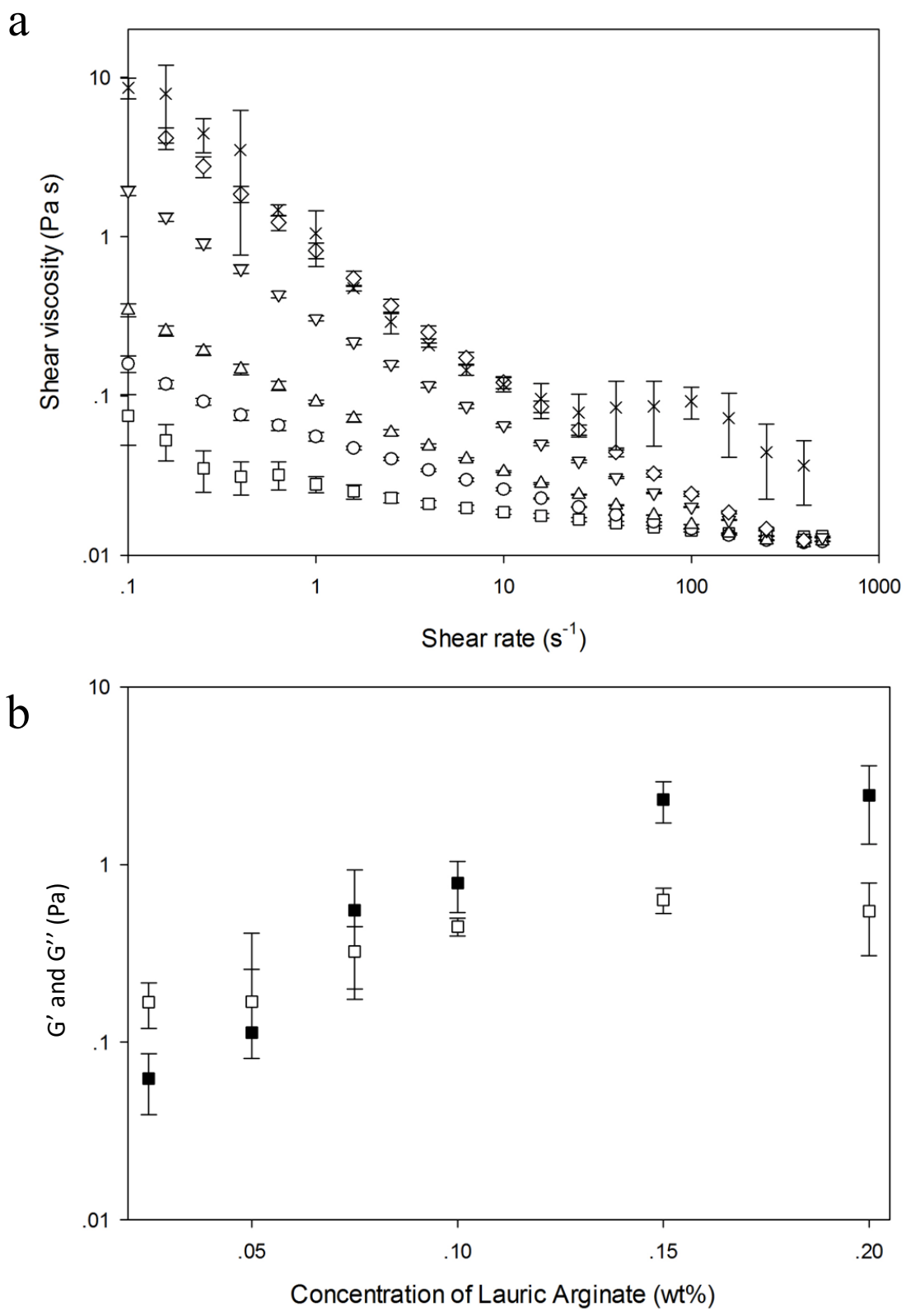


Figure 5.7: (a) Shear viscosity of 1 wt% κC fluid gel mixed with LA at 0.025% (□), 0.05% (○), 0.075% (△), 0.1% (▽), 0.15% (◇) and 0.2% (×). (b) Storage modulus (□) and loss modulus (■) of 1 wt% κC fluid gel mixed with LA as a function of LA concentration.

5.3.3 Surface activity

The functionality of LA as a surfactant depends on its ability to adsorb at the a/w interface, lowering the surface tension and stabilising the newly formed interface. In order to investigate the surface-activity of κC-LA complexes, equilibrium surface tension was measured and compared to that of pure surfactant solutions (Figure 5.8). The surface tension of pure LA solution decreased with concentration reaching a plateau at 0.15% LA with a value of 34.6 ± 0.07 mNm^{-1}. This is therefore its critical micelle concentration (CMC); above this concentration, all additional surfactant monomers added to the system form micelles. The surface tension of the complexes were then measured as a function of LA concentration and compared to the pure surfactant solutions. The surface tension of pure kappa carrageenan was 43.4 ± 0.3 mNm^{-1} (Figure 5.8). Upon addition of LA, the surface tension quickly began to decrease until it plateaued at 35.0 ± 0.6 mNm^{-1} at 0.025% LA. It then appeared to increase slightly at 0.1% LA. This is thought to be a result of the formation of aggregates affecting the measurements. Above 0.1% LA, the aggregates increased in size resulting in unreliable measurements. In surfactant-particle systems, the surface tension is often lower than that of corresponding surfactant solutions (Hunter et al., 2008). It has been suggested that particles act as surfactant carriers, thus increasing the concentration of surfactant at the a/w interface (Gonzenbach et al., 2006) and that the size of the particles (dependent on individual systems) determines the extent to which the surface tension is lowered (Binks, 2002). Particle-surfactant systems here exhibited similar surface tension values to the surfactant solutions (Figure 5.8). The aqueous conditions, as well as size and shape of the particles may have therefore not been optimal to cause a lowering of surface tension.

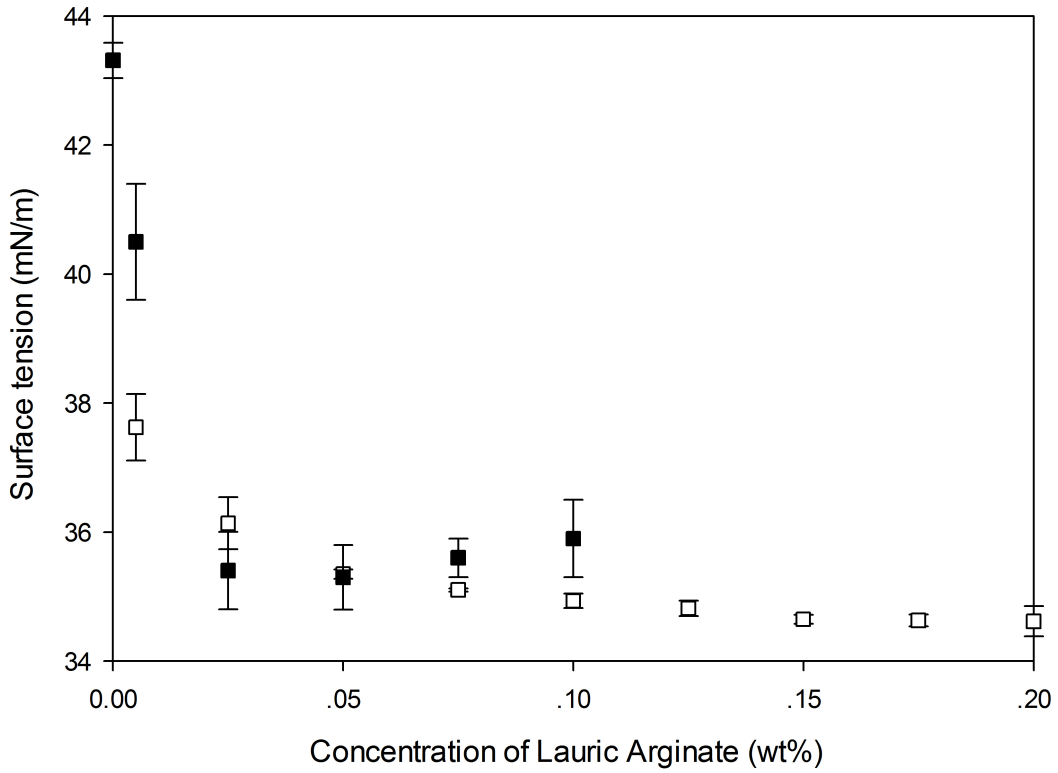


Figure 5.8: Surface tension measurements as a function of LA for pure LA solutions (□) and κC-LA complexes (■).

5.3.4 Aeration of surface-activated κC fluid gels

The ability of κC-LA complexes to incorporate air was determined using foam air fraction measurements and compared to those of pure surfactant solutions. Systems were aerated in a Hobart mixer for 7 minutes, which ensured that the air fraction was high. The air fraction of pure surfactant solutions quickly reached a constant of around 0.97 upon increasing LA concentration (Figure 5.9a). Foam capacity was high above and below the CMC suggesting the method of foaming allowed equilibrium surface tension to be reached. The air fraction of aerated κC-LA complexes followed a similar trend but values were slightly lower than those of the pure surfactant solutions (~ 0.86). This was likely a result of increased viscosity preventing the incorporation of as much air into the system. In addition, Lesov, Tcholakova, and Denkov (2014) have reported that foam air volume is also dependent on the mechanism of stabilisation as well as solution viscosity,

specifically the Pickering stabilised foams they studied had a lower air fraction when compared to surfactant-stabilised foams of similar suspension viscosities. At 0.15% and more substantially, 0.2% LA, the air fraction decreased. This was likely an effect of high particle aggregation and increased particle density, as observed by turbidity and rheology measurements, which sterically hindered the action of the surfactant. In addition, it was likely dense particles bridged and consequently ruptured bubble interfaces as they were generated, preventing the growth of the foam structure.

In order to investigate the potential Pickering stabilisation action of newly-formed κC-LA complexes, foam stability was explored. Firstly, foam half-life was measured and compared to those of pure surfactant solutions (Figure 5.9b). Foams produced at 0.005% and 0.2% LA were not measured as the air fraction was too low. Foam half-life initially increased from 35 ± 3 h at 0.025% LA up to 61 ± 8 h at 0.075% LA, where it peaked before decreasing to only 12 ± 2 h at 0.15% LA. All systems were stable for considerably longer than foams composed of pure surfactant solutions, which were only stable for 1.5 – 4 h (Figure 5.9b). A similar trend in foam stability is often seen for particle-surfactant systems where the most stable foam corresponds to the optimum ratio of particle to surfactant concentration (Cui et al., 2010; Guillermic et al., 2009; Liu et al., 2010). This is where particles are coated with a surfactant monolayer resulting in their lowest charge and maximum hydrophobicity. Foam stability then decreases due to the formation of a surfactant bilayer on the particle surface rendering them hydrophilic and resulting in the mechanism of stabilisation changing from particle-stabilised to surfactant-stabilised. This explanation does not justify the peak in foam stability observed here, as the ζ-potential data (Figure 5.5) revealed that a bilayer did not form on the surface of particles at high

LA concentrations as particles remained negatively charged. To investigate the trend observed here, the position of the particles in the foams was explored, as well as the rate of coarsening and liquid drainage.

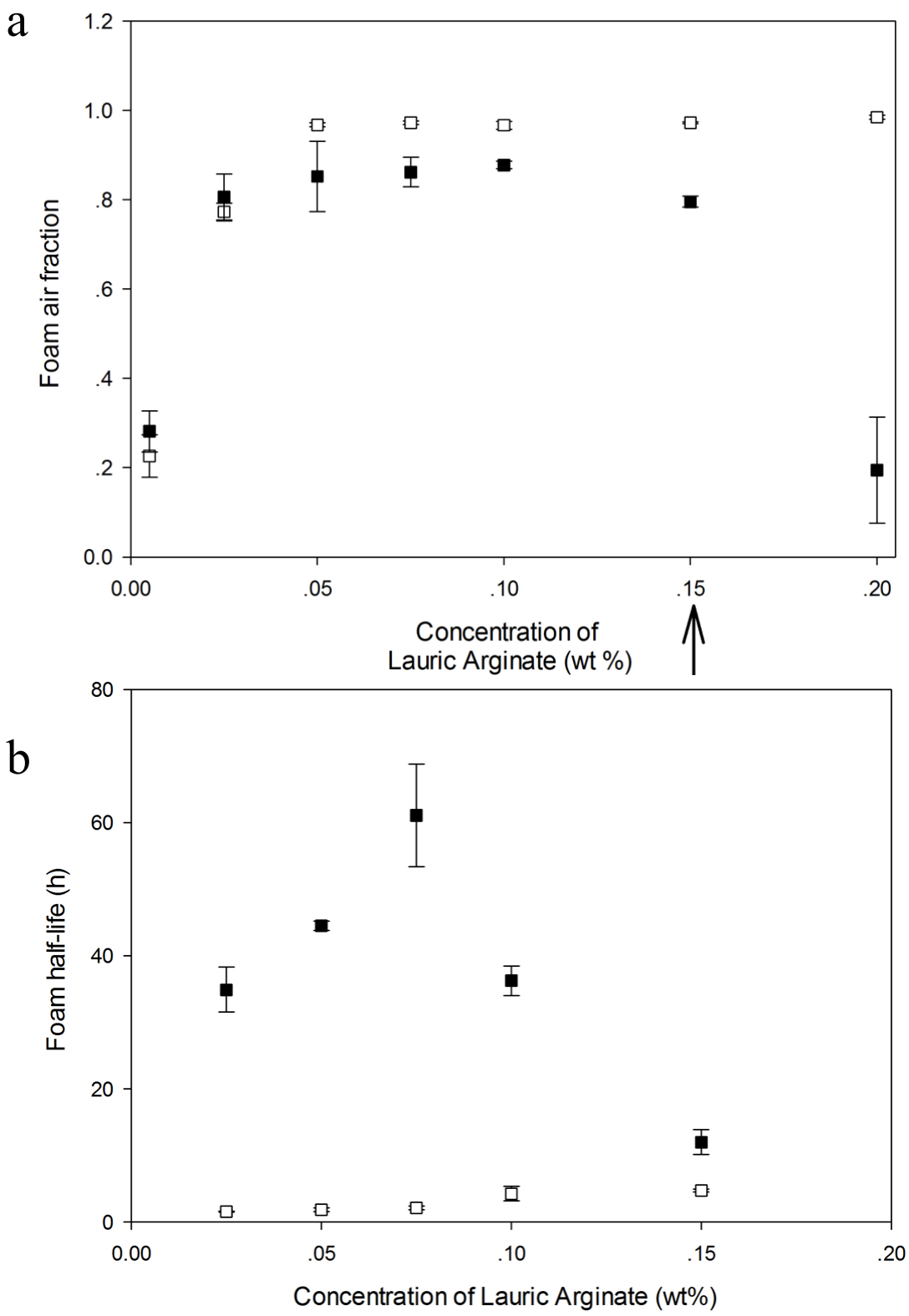


Figure 5.9: (a) Foam air fraction measurements for aerated κC-LA complexes (■) and pure LA solutions (□), as a function of LA concentration. Arrow indicates the CMC of LA. (b) Foam half-life measurements for aerated κC-LA complexes (■) and pure LA solutions (□), as a function of LA concentration.

5.3.5 Foam stability mechanism

Firstly, the location of particles in the foams was examined using optical and confocal microscopy to investigate the surface-activity of the modified κC particles. The bubbles formed upon aerating pure LA solutions were also imaged for comparison; these bubbles were spherical with smooth interfaces (Figure 5.10a). In contrast, foams produced with κC-LA complexes (at all LA concentrations) consisted of bubbles that appeared non-spherical and had a structured surface (Figure 5.10b). This is indicative of bubbles stabilised by adsorbed particles (Cui et al., 2010). The micrograph in Figure 5.10c of aerated κC with 0.075% LA further supports this, as a layer of particulate entities can be seen at the surface of bubbles with tails protruding into the continuous phase. Both micrographs (Figure 5.10b and Figure 5.10c) also demonstrate the presence of particles in the continuous phase that had not adsorbed to the interface. The particles appeared quite different to those imaged in Figure 5.4a before complexation and aeration (longer and thinner in shape), it is possible that some κC:LA aggregation occurred due to insufficient K^+ ions for gelation. To provide further information on the coverage of bubble interfaces, confocal microscopy was used. Particles were dyed with rhodamine B and appear green in the micrographs (Figure 5.10d). A layer of particles can be seen on bubble interfaces providing high coverage. Particles can also be seen in the continuous phase. Microscopy was used to study all aerated complexes; some adsorption of particles at bubble interfaces was seen in all cases, verifying the ability to surface-activate κC particles through surfactant binding. However, it was difficult to quantify the magnitude of particle coverage using microscopy. Therefore, the change in bubble size over time was studied to analyse the effectiveness of particle coverage.

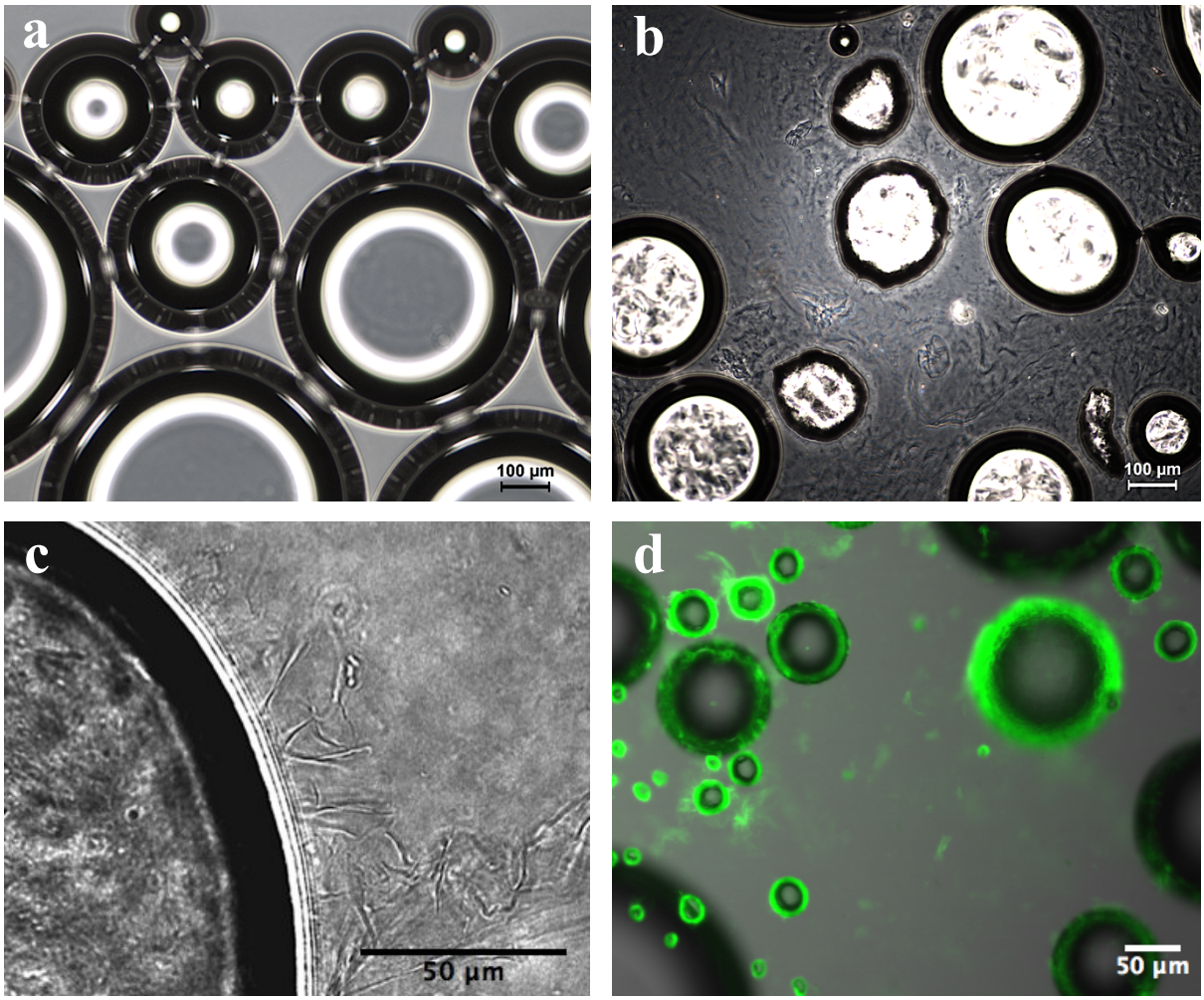


Figure 5.10: (a) Optical micrograph of aerated 0.2% LA solution. (b) optical micrograph of aerated 1 wt% κC + 0.075% LA fluid gel complexes. (c) Optical micrograph of aerated 1 wt% κC + 0.075% LA fluid gel complexes at a higher magnification. (d) Confocal micrograph of aerated 1 wt% κC + 0.075% LA fluid gel complexes dyed with rhodamine B.

It has been well reported that particles adsorbed to a/w interfaces provide a barrier to coarsening of the gas phase (Binks & Horozov, 2005; Dickinson, 2010). The structure of these foams including bubble size over time was therefore recorded using a high resolution camera. Mean bubble area as a function of time for the first 4 h after aeration was plotted for each foam (Figure 5.11a). The initial mean bubble area (MBA) was similar for all foams (~7000 μm^2), which corresponds to a bubble radius of ~12 µm. The MBA increased with time in all cases, due to disproportionation. This is where smaller

bubbles shrink in size and larger bubbles grow due to the difference in their internal Laplace pressure. The foam consisting of κC particles and 0.025% LA displayed the highest rate of disproportionation (MBA ~ 70000 μm^2 after 4 h). Upon increasing LA concentration to 0.05% and 0.075%, the smallest increase in MBA was observed (~20000 μm^2 after 4 h) and upon further increasing LA to 0.1% and 0.15%, the rate of disproportionation subsequently increased again (~40000 μm^2 after 4 h). These changes in disproportionation rates suggest differences in interfacial viscoelasticity, perhaps caused by a difference in stability mechanisms. It appears that at the lowest concentration of LA (0.025%), the foam is surfactant stabilised and therefore more vulnerable to disproportionation. At 0.05% and 0.075% LA, there is sufficient surfactant to coat the surface of the particles and foams are consequently particle stabilised. The interfacial viscoelasticity is high and the interface is protected against disproportionation. Above 0.075%, the rate of disproportionation begins to increase again. This suggests a change in dominant stability mechanism from particle stabilised to surfactant-stabilised. This cannot be due to the formation of a surfactant bilayer and consequent change in particle charge as is common with these systems (discussed in Section 3.4). It is therefore possible that there was a barrier to adsorption for some of the particles. Deleurence et al. (2014) studied the effect of particle aggregation by de-coupling the effects of ζ-potential and particle charge (i.e. they varied the sign of the ζ-potential without changing the contact angle over a large range of surfactant concentration). They found that foam properties were controlled by the flocculation state and the shear energy applied to produce the foam. Large aggregates did not adsorb spontaneously at the interface because of their size, however, when large shear energy was used to produce the foams, a very stable foam was formed. Adsorption of particles occurs if the time for adsorption, t_A is considerably

less than the time for interface creation, t_{CR}. Both times depend on shear energy but the ratio does not. The ratio t_A/t_{CR} scales as a/d, where a is the diameter of the particles and d is the diameter of the bubbles. Large aggregates in the order of 100 μm could therefore not adsorb as t_A/t_{CR}=10. The size of bubbles in this study were initially ~ 12 μm (Figure 5.11a). Therefore, when aggregates reached ~ 120 μm in diameter, adsorption would have been hindered. Above 0.075% LA, aggregates greater than 100 μm in size were observed by optical microscopy, which continued to increase in size with LA concentration (as discussed in Section 3.2). These would have been unable to adsorb to the interface, which explains the trend seen in Figure 5.11a. The interface would have been stabilised by free surfactant monomers, as well as those particles small enough to adsorb (the number of which would have decreased with increasing LA concentration). It is important to note that both the particulate nature and the shape of the complexes require further understanding; if gelation was not complete before the addition of LA, it is hypothesised that additional κC sulphate groups would have interacted with LA upon mixing, resulting in further aggregation of κC:LA (and less LA at the surface) and therefore a different adsorption mechanism to particle adsorption. A higher aggregation state and a lower availability of LA may have also inhibited adsorption.

As well as particles being present at a/w interfaces, microscopy highlighted their presence in the continuous phase i.e. foam channels and nodes. Liquid drainage of the bulk phase was therefore measured to assess how it related to foam stability. Liquid content, calculated using conductivity data, is shown for each foam after 4 h as a fraction of initial content (Figure 5.11b). The trend is similar to that observed for foam half-life. The particle stabilised foams (0.05% LA and 0.07% LA) displayed little change in liquid

content after 4 h. Whereas, a decrease was measured for 0.025%, 0.1% and 0.15% LA (surfactant-stabilised foams). This demonstrates that when particles adsorbed to the interface, their resistance to liquid drainage as well as disproportionation increased. In addition, the interaction and aggregation between particles would have helped to strengthen this barrier through the formation of a particle network between air bubbles (Binks, 2002; Dickinson et al., 2004; Gonzenbach et al., 2006). However, when foams were surfactant stabilised, the classical drainage equation is applicable (Koehler, Hilgenfeldt, & Stone, 2000; Saint-Jalmes, Zhang, & Langevin, 2004). Despite higher viscosity of the continuous phase upon increasing LA concentration (Figure 5.7a), liquid drainage was controlled by the change in stability mechanism.

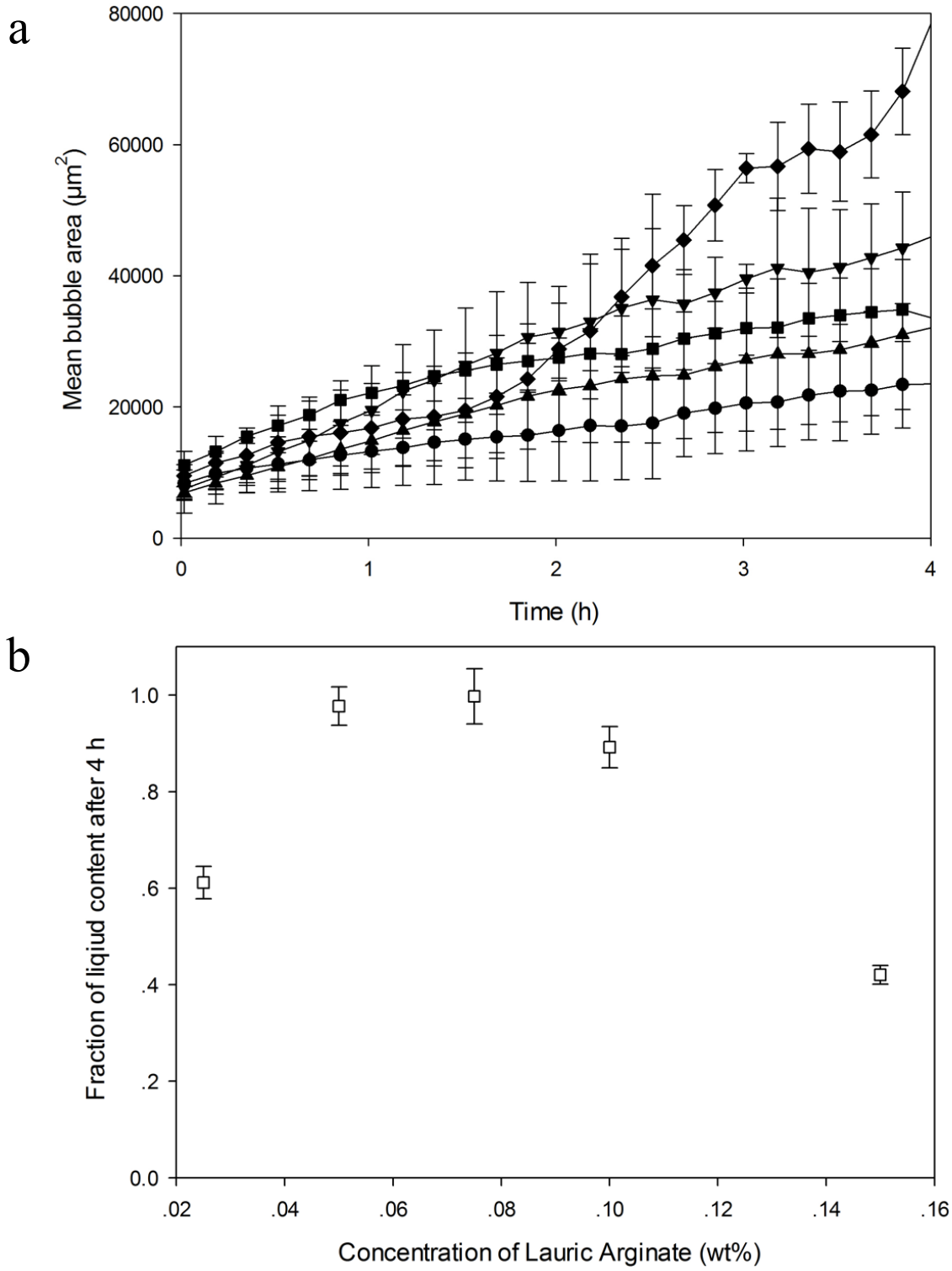


Figure 5.11: (a) Mean bubble area of aerated κC-LA complexes as a function of time after aeration, LA concentrations of 0.025% (◆), 0.05% (●), 0.075% (▲), 0.1% (▼) and 0.15% (■). (b) Fraction of liquid content remaining 4 h after aeration in aerated κC-LA complexes as a function of LA concentration. Measurements were recorded at sensor 3 in a Krüss foam column (positioned half way down the foam).

5.3.6 κC fluid gels with non-ionic surfactant

In order to confirm this change in surface-activity of kappa carrageenan upon binding to LA, the foaming properties of kappa carrageenan mixed with a non-ionic surfactant, Tween 20, were studied. Following the same procedure as LA, a diluted 1% κC fluid gel was prepared and mixed with Tween 20 at various concentrations. Firstly, their ability to incorporate air was determined using foam air fraction measurements and compared to pure surfactant solutions (Figure 5.12a). As the CMC of Tween 20 is quite low (0.0074 wt% (Mittal, 1972)), which is typical of non-ionic surfactants, it was used at concentrations above this in order to increase foamability. The foam air fraction of pure surfactant solutions increased with Tween 20 concentration until it plateaued at around 0.98 (Figure 5.12a). Foam air fractions of κC and Tween 20 mixed solutions followed a similar trend but, as with κC and LA fluid gel solutions, they were slightly below those of pure Tween 20 due to increased viscosity. Foam half-lives were then measured and plotted as a function of Tween 20 concentration in Figure 5.12b. No increase in stability was observed upon addition of κC to Tween 20 solutions; both systems were stable for only 1-4 h at all concentrations. In addition, the bubbles were spherical and non-textured (Figure 5.12b inset), confirming that there was no adsorption of particles at the interface or interaction between κC and Tween 20.

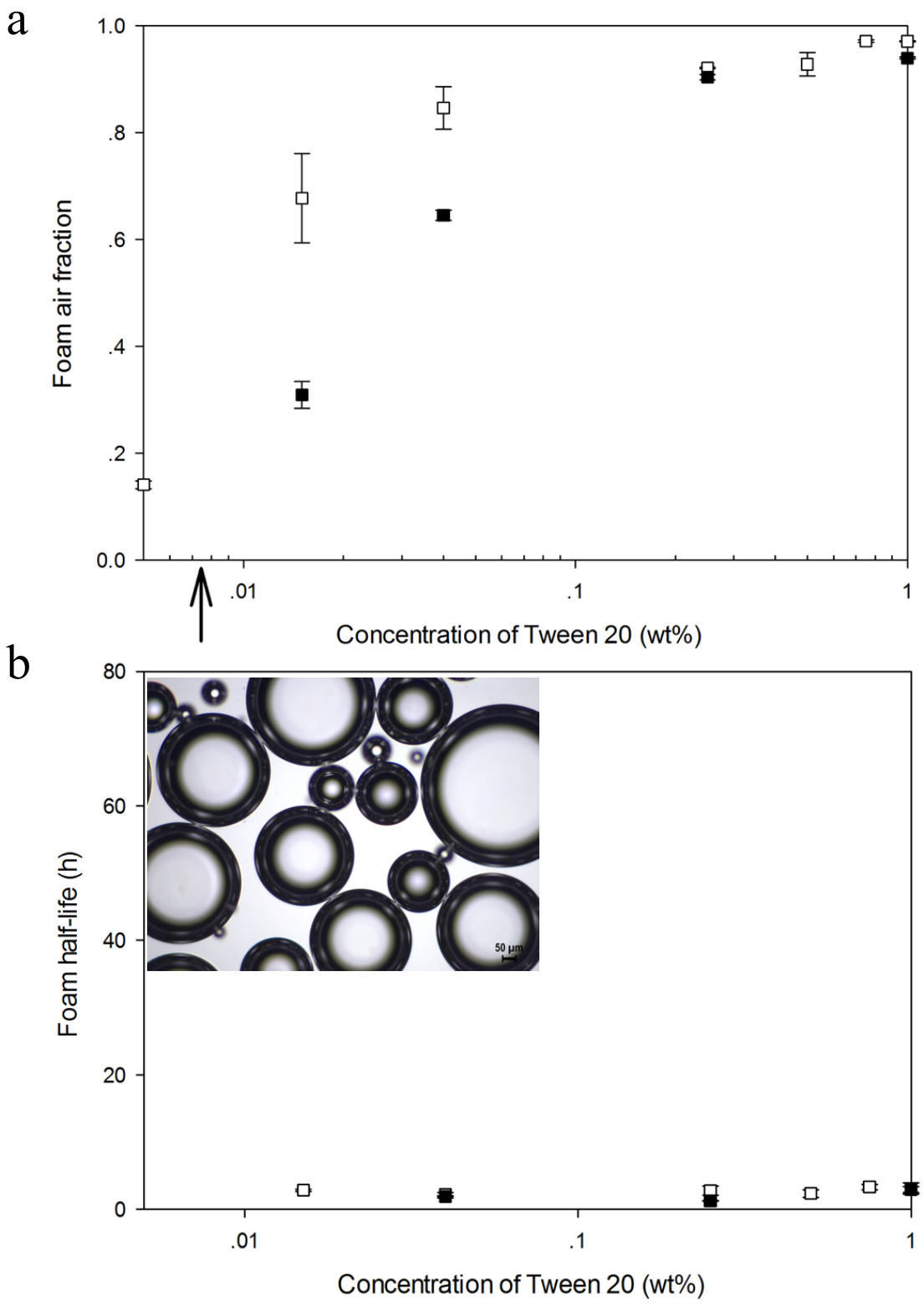


Figure 5.12: (a) Foam air fraction measurements and (b) foam half-life measurements for 1 wt% κC + Tween 20 fluid gel complexes (■) and pure Tween 20 solutions (□), as a function of Tween 20 concentration. Arrow in (a) indicates the CMC of Tween 20. (b) Inset is an optical micrograph of aerated 1 wt% κC + 0.075% Tween 20 fluid gel.

5.4 Conclusions

This research has built upon work by Bonnaud et al. (2010) who characterised an electrostatic interaction between food-grade cationic surfactant, lauric arginate, with negatively charged carrageenan in solution but did not explore their surface properties or ability to stabilise the a/w interface. In this work, the electrostatic interaction was facilitated between microgel particles of kappa carrageenan and LA. Turbidity, ζ-potential and rheological measurements were used to characterise the complexes, in particular their aggregation behaviour, which showed similar patterns to those observed by Bonnaud et al. (2010). The ability of complexes to lower surface tension was similar to that of pure surfactant solutions, however foams were over 10 times more stable in all cases. Foam half-life peaked at an intermediate concentration of LA (0.075% LA). This peak was attributed to a change in stability mechanism from surfactant stabilisation to particle stabilisation, where the most stable foams exhibited a smaller increase in mean bubble size over time (slower disproportionation rate), as well as a slower liquid drainage rate. The adsorbed particles therefore provided sufficient interfacial elasticity to considerably slow these mechanisms, helped also by the interaction and aggregation between particles. However, at higher LA concentrations, extensive aggregation limited their ability to adsorb to the interface and foam stability decreased as surfactant stabilisation once again dominated. Similar particle-surfactant systems have been limited by the formation of a surfactant bilayer on the surface of particles, changing their hydrophobicity (Cui et al., 2010; Guillermic et al., 2009; Liu et al., 2010). A surfactant bilayer did not form in this system, suggesting that by optimising the size of particles and aggregates, greater foam stability can be reached.

In addition, further work is required to investigate the extent of gelation within κC particles; as no additional K^+ ions were included, the final stage of gelation (helix aggregation) may not have completed under shear. This would have resulted in further aggregation of κC:LA as more of the κC sulphate groups would have been available for interaction not just those exposed at the surface of particles. The effect of this aggregation compared to discrete particles on foam stability would be an interesting future area to explore.

Nevertheless, this work helps to expand the existing knowledge of *in-situ* modification of hydrophilic particles for foam stabilisation, in particular work by Binks et al., (2017) who extended this method to the food industry. This is the first time that a surfactant has been used to surface-activate kappa carrageenan particles facilitating their adsorption to a/w interfaces. This provides a simple method to functionalise one of the most commonly used polysaccharides in the food industry, providing a more versatile ingredient for food microstructure design. For example, these particles have the potential to mimic fat droplets in whipped products, in terms of both texture and their role in stabilising the structure.

LIST OF REFERENCES

Asker, D., Weiss, J., & McClements, D. J. (2009). Analysis of the Interactions of a Cationic Surfactant (Lauric Arginate) with an Anionic Biopolymer (Pectin): Isothermal Titration Calorimetry, Light Scattering, and Microelectrophoresis. Langmuir, 25(1), 116-122. doi:10.1021/la803038w

Benford, D., Harrison, R., Larsen, J., & DiNovi, M. (2009). Safety Evaluation of Certain Food Additives: Ethyl Lauroyl Arginate. World Health Organization, Geneva.

Binks, B. P. (2002). Particles as surfactants - similarities and differences. Current Opinion in Colloid & Interface Science, 7(1–2), 21-41. doi:http://dx.doi.org/10.1016/S1359-0294(02)00008-0

Binks, B. P., & Horozov, T. S. (2005). Aqueous foams stabilized solely by silica nanoparticles. Angewandte Chemie International Edition, 44(24), 3722-3725.

Binks, B. P., Muijlwijk, K., Koman, H., & Poortinga, A. T. (2017). Food-grade Pickering stabilisation of foams by in situ hydrophobisation of calcium carbonate particles. Food Hydrocolloids, 63, 585-592. doi:http://dx.doi.org/10.1016/j.foodhyd.2016.10.002

Bonnaud, M., Weiss, J., & McClements, D. J. (2010). Interaction of a food-grade cationic surfactant (lauric arginate) with food-grade biopolymers (pectin, carrageenan, xanthan, alginate, dextran, and chitosan). Journal of Agricultural and Food Chemistry, 58(17), 9770-9777.

Cui, Z. G., Cui, Y. Z., Cui, C. F., Chen, Z., & Binks, B. P. (2010). Aqueous Foams Stabilized by in Situ Surface Activation of $CaCO_3$ Nanoparticles via Adsorption of Anionic Surfactant. Langmuir, 26(15), 12567-12574. doi:10.1021/la1016559

de Carvalho, W., & Djabourov, M. (1997). Physical gelation under shear for gelatin gels. Rheologica Acta, 36(6), 591-609.

Deleurence, R., Parneix, C., & Monteux, C. (2014). Mixtures of latex particles and the surfactant of opposite charge used as interface stabilizers–influence of particle contact angle, zeta potential, flocculation and shear energy. Soft Matter, 10(36), 7088-7095.

Dickinson, E. (2010). Food emulsions and foams: Stabilization by particles. Current Opinion in Colloid & Interface Science, 15(1–2), 40-49. doi:http://dx.doi.org/10.1016/j.cocis.2009.11.001

Dickinson, E., Ettelaie, R., Kostakis, T., & Murray, B. S. (2004). Factors controlling the formation and stability of air bubbles stabilized by partially hydrophobic silica nanoparticles. Langmuir, 20(20), 8517-8525.

Fernández Farrés, I., Moakes, R. J. A., & Norton, I. T. (2014). Designing biopolymer fluid gels: A microstructural approach. Food Hydrocolloids, 42(3), 362-372. doi:http://dx.doi.org/10.1016/j.foodhyd.2014.03.014

Gabriele, A., Spyropoulos, F., & Norton, I. T. (2009). Kinetic study of fluid gel formation and viscoelastic response with kappa-carrageenan. Food Hydrocolloids, 23(8), 2054-2061.

Gabriele, A., Spyropoulos, F., & Norton, I. T. (2010). A conceptual model for fluid gel lubrication. Soft Matter, 6(17), 4205-4213.

Garrec, D. A., Guthrie, B., & Norton, I. T. (2013). Kappa carrageenan fluid gel material properties. Part 1: Rheology. Food Hydrocolloids, 33(1), 151-159.

Gonzenbach, U. T., Studart, A. R., Tervoort, E., & Gauckler, L. J. (2006). Stabilization of foams with inorganic colloidal particles. Langmuir, 22(26), 10983-10988.

Guillermic, R.-M., Salonen, A., Emile, J., & Saint-Jalmes, A. (2009). Surfactant foams doped with laponite: unusual behaviors induced by aging and confinement. Soft Matter, 5(24), 4975-4982.

Hunter, T. N., Pugh, R. J., Franks, G. V., & Jameson, G. J. (2008). The role of particles in stabilising foams and emulsions. Advances in Colloid and Interface Science, 137(2), 57-81.

Koehler, S. A., Hilgenfeldt, S., & Stone, H. A. (2000). A generalized view of foam drainage: experiment and theory. Langmuir, 16(15), 6327-6341.

Lesov, I., Tcholakova, S., & Denkov, N. (2014). Factors controlling the formation and stability of foams used as precursors of porous materials. Journal of Colloid and Interface Science, 426, 9-21. doi:https://doi.org/10.1016/j.jcis.2014.03.067

Liu, Q., Zhang, S., Sun, D., & Xu, J. (2010). Foams stabilized by Laponite nanoparticles and alkylammonium bromides with different alkyl chain lengths.

Colloids and Surfaces A: Physicochemical and Engineering Aspects, 355(1-3), 151-157.

Mittal, K. (1972). Determination of CMC of polysorbate 20 in aqueous solution by surface tension method. Journal of Pharmaceutical Sciences, 61(8), 1334-1335.

Moakes, R., Sullo, A., & Norton, I. (2015). Preparation and characterisation of whey protein fluid gels: The effects of shear and thermal history. Food Hydrocolloids, 45, 227-235.

Morris, E., Rees, D. A., & Robinson, G. (1980). Cation-specific aggregation of carrageenan helices: domain model of polymer gel structure. Journal of Molecular Biology, 138(2), 349-362.

Murphy, R. W., Farkas, B. E., & Jones, O. G. (2016). Dynamic and viscoelastic interfacial behavior of β-lactoglobulin microgels of varying sizes at fluid interfaces. Journal of Colloid and Interface Science, 466, 12-19.

Norton, I. T., Foster, T., & Brown, R. (1998). The science and technology of fluid gels. In Williams, P. A., & Phillips G. O. (Eds.), Gums and Stabilisers for the Food Industry, (Vol. 9, pp. 259-268): Royal Society of Chemistry, Cambridge.

Saint-Jalmes, A. (2006). Physical chemistry in foam drainage and coarsening. Soft Matter, 2(10), 836-849.

Saint-Jalmes, A., Zhang, Y., & Langevin, D. (2004). Quantitative description of foam drainage: Transitions with surface mobility. The European Physical Journal E, 15(1), 53-60.

Chapter 6: CONCLUSIONS AND FUTURE RECOMMENDATIONS

Detailed conclusions were given at the end of each results chapter. The current chapter summarises the overall outcomes of the thesis and proposes recommendations to build upon the work presented.

6.1 Conclusions

The aim of this research was to understand and design hydrocolloid particles for the creation of fat-free aerated products. The focus was directed towards gaining understanding, on a microstructural level, of the performance of fluid gels in foams. Agar fluid gels were prepared and characterised, in particular their material properties were correlated to their properties when aerated in order to find a predictor for foam stability. Furthermore, the impact of sugar addition was investigated and the effect of processing method on particle size was exploited to help further understand the mechanism of foam stability. In the final chapter, the potential to hydrophobically modify and therefore surface activate kappa carrageenan fluid gel particles, was explored. The main conclusions from the results chapters are summarised in the following sections.

6.1.1 The formation and aeration of agar/Tween20 fluid gels

- **Agar/Tween 20 fluid gels were prepared using a pin stirrer and their foam properties characterised.**

  Agar fluid gels were prepared at various concentrations and characterised. A non-ionic surfactant, Tween 20, was incorporated into agar fluid gels without altering their rheological or material properties but allowing foam production.

- **Foam half-life was directly dependent upon fluid gel yield stress and can therefore be predicted.**

Upon increasing the concentration of agar in agar/Tween 20 fluid gels, foam half-life increased gradually with increased yield stress until a sharp rise was observed. This was attributed to the yield stress of the suspending fluid becoming larger than the gravitational stress inside the foam channels, resulting in a reduction in drainage. Yield stress was manipulated by changing the concentration of agar, which increased both the particle modulus and volume fraction. When fluid gels were highly concentrated, increasing the particle modulus continued to increase the yield stress of the fluid gel and, in turn, foam half-life.

- **The advantage of fluid gels compared to weak biopolymer gels is their ability to recover when sheared.**

  Fluid gels exhibit lower thixotropy compared to weak biopolymer gels of the same viscosity, indicating higher structural recovery. Fluid gel particles have the ability to absorb any stress applied to them; the fluid gel properties are therefore regained as interactions are re-established. Conversely, once the quiescently set gel was exposed to shear, the gel network was broken and the structure lost.

- **The extent of quiescent ordering impacts foam stability; pin stirrer T_{exit} is therefore important.**

  Manipulating the exit temperature of agar fluid gels during production allowed a relationship between quiescent ordering and foam stability to be established, where greater quiescent ordering in the fluid gel (at a T_{exit} approaching T_m) reduced its stability upon aeration, due to less structural recovery in the system.

6.1.2 Understanding the addition of sugar in agar/Tween 20 fluid gels

- **Gelation kinetics play a key role in particle formation and size.**

The size of fluid gel particles decreased with increasing sugar concentration due to a higher solution viscosity entering the pin stirrer favouring helix nucleation and inhibiting the growth process.

- **The addition of sugar altered the fluid gel material properties.**

  Increasing the concentration of each sugar up to 50% increased particle rigidity (Young's modulus), shear viscosity, G' and yield stress. All sugars at 60% somewhat inhibited gelation as the glass transition of sugar was approached, fluid gel shear viscosity and G' were considerably higher, due to the conversion of an overall brittle agar gel network to a more rubbery-like structure.

- **Foam half-life was dependent on fluid gel yield stress**.

  Foam half-life was directly influenced by fluid gel yield stress, which supports the results from the previous chapter. In both studies, yield stress was enhanced through increased particle modulus and particle interaction. However, the first example of influencing such parameters by changing solvent availability through the addition of sugar is reported here.

- **Particle size controls the rate of liquid drainage in dilute systems.**

  When fluid gels were diluted, particles were confined in foam channels to such an extent that particle size influenced the rate of liquid drainage. Initially, larger particles were more effective at reducing liquid drainage than smaller particles. However, due to a similar confinement parameter, the particle exclusion transition occurred at a similar time, resulting in a similar time of foam collapse.

6.1.3 The hydrophobic modification of kappa carrageenan fluid gel particles

- **Kappa carrageenan particles were successfully modified.**

An electrostatic interaction between negatively charged kappa carrageenan particles and a positively charged surfactant, lauric arginate, was facilitated and characterised.

- **Particles were surface-activated and therefore adsorbed at the a/w interface, improving foam stability.**

  An intermediate concentration of surfactant resulted in the lowest rate of disproportionation and liquid drainage in foams due to optimum adsorption to bubble interfaces. At higher concentrations of surfactant, large aggregates formed which were unable to adsorb at the interfaces.

6.2 Recommendations for future work

- **Utilise advances made in particle imaging to further understand fluid gel systems.**

  During this study, agar fluid gel particles were visualised using phase contrast optical microscopy. Visualisation of polysaccharide fluid gel particles has not been achieved to this standard for a number of years and the shape of particles observed here has not been previously seen. Therefore, a more in depth study into the effect of processing parameters (e.g. shear rate and cooling rate) and formulation changes (e.g. hydrocolloid concentration, pH, type of salt, salt concentration) on particle size would benefit the overall understanding of fluid gel preparation. Furthermore, these studies should be expanded to fluid gels of different origins e.g. kappa carrageenan and gellan, which have not yet been satisfactory visualised.

- **Visualise the flow of water through foam channels during drainage to clarify the role of particles in the mechanism of foam stability.**

  From Chapters 3 and 4, it is clear that overall foam stability (foam half-life) was dependent upon fluid gel rheology; a higher yield stress of the continuous phase

increased foam stability by reducing the mobility of the continuous phase suspending the bubbles. It is thought that water initially drained through the foam until particles were confined in foam channels. This confinement increased the concentration and viscoelasticity of the particle network, which helps to reduce drainage. Visualisation of this restriction of flow inside the foam channels would strengthen this argument. This could potentially be measured using a type of particle image velocimetry (PIV) where the flow can be illustrated by tracking the particles of interest or other tracking particles. In addition, work in Chapter 4 revealed that when diluted (low volume fraction) fluid gels were aerated, the size of particles influenced the rate of liquid drainage, specifically larger particles were more effective at reducing liquid drainage than smaller particles. However, this did not appear to affect overall foam half-life due to similar timing of the *particle exclusion transition* initiated by a similar confinement parameter i.e. ratio of particle to channel size. It would be valuable to investigate the volume fraction at which particle aggregation decreases to the extent that individual particle size and shape become influential to the foam stability mechanism. Investigating the role of particles further would help to advance the understanding built from the work in this thesis. Isolating variables such as: particle size, size distribution, particle stiffness, volume fraction, yield stress and measuring liquid drainage, as well as visualising the particles inside the foam channels, would help to complete this objective.

- **Optimisation of particle and aggregate size for adsorption at the a/w interface.** Intermediate concentrations of LA were optimum for surface-activation of particles and their adsorption to bubble interfaces providing the lowest disproportionation rate. At low concentrations, it was hypothesised that there was insufficient surfactant to

coat the surfaces of particles, whilst at higher concentrations large aggregates formed which were unable to adsorb at the interfaces. Therefore, microgel shape and size should be optimised for particle adsorption. For example, Murphy, Farkas, and Jones (2016) reported the ability of smaller microgel particles to adsorb to an interface and increase interfacial elasticity more quickly. In order to measure changes in microgel and monolayer characteristics during adsorption and equilibration, Langmuir compression and atomic force microscopy (AFM) could be used. The measured change in surface pressure as microgel-stabilised a/w interfaces are compressed on a Langmuir trough provides information on the adsorption rate. These monolayers can then be imaged using AFM allowing the structure to be visualised. In addition, further work is required to investigate the extent of gelation within κC particles; as no additional K^+ ions were included, the final stage of gelation (helix aggregation) may not have completed under shear. This would have resulted in further aggregation of κC:LA as more of the κC sulphate groups would have been available for interaction not just those exposed at the surface of particles. The effect of this aggregation compared to discrete particles on foam stability would be an interesting future area to explore.

- **Potential modification and surface-activation of other polysaccharide fluid gels.**
  The potential surface-activation of other polysaccharides (both anionic with cationic surfactants and cationic with anionic surfactants) should be explored to utilise this efficient method of modification.
- **Investigate the sensory perception of these aerated fluid gels.**
  Fluid gels were chosen for this study because of their previously cited ability to mimic fat droplets in emulsion systems (Norton & Norton, 2010). This thesis focused on the

structural properties of fluid gels when aerated and how their microstructure could be modified to improve foam stability. The next part of this work should investigate the relationship between the microstructure and sensory perception. The effect of the continuous phase (hydrocolloid type, particle size, volume fraction, particle modulus) and foam properties, such as air fraction and bubbles size distribution, on sensory perception should be investigated. For example, previous studies have shown that fluid gels with different particle rigidity display distinctive tribological behaviour despite exhibiting similar rheological properties (Garrec, 2013). This is therefore expected to influence textural and sensory perception.

- **Understand interactions and behaviour of fluid gels with other food ingredients.** In order to build these fluid gel systems into food products, the addition of further ingredients is necessary. Interactions between agar/kappa carrageenan and these other ingredients therefore requires understanding. For instance, preservatives are often used to give products a longer shelf-life. Potassium sorbate is a common preservative used in these types of products. However, the potassium ions are likely to affect hydrocolloid gelation, in particular the gelation mechanism of kappa carrageenan, where monovalent ions are required for helix aggregation. Furthermore, these types of products are typically maintained at neutral to acidic pH. The pH environment will also affect the gelation of fluid gels and their stability. For example, gelation of kappa carrageenan cannot occur at pH values below 4.3, due to autohydrolysis (Hoffmann, Russell, & Gidley, 1995). Once gelled, the sulphate-bound potassium ions provide stability at low pH. Nevertheless, long exposure to low pH or high temperatures can cause structure breakdown and should be avoided. Likewise, agar is also vulnerable

to hydrolysis at low pH, but only if extensively heated below pH 5.5 (Phillips & Williams, 2009).

LIST OF REFERENCES

Garrec, D. (2013). Understanding Fluid Gels and Hydrocolloid Tribology. University of Birmingham, eThesis.

Hoffmann, R. A., Russell, A., & Gidley, M. (1995). Molecular weight distribution of carrageenans: Characterisation of commercial stabilisers and effect of cation depletion on depolymerisation. Gums and Stabilisers for the Food Industry, 137-150.

Murphy, R. W., Farkas, B. E., & Jones, O. G. (2016). Dynamic and viscoelastic interfacial behavior of β-lactoglobulin microgels of varying sizes at fluid interfaces. Journal of Colloid and Interface Science, 466, 12-19.

Norton, J. E., & Norton, I. T. (2010). Designer colloids—towards healthy everyday foods? Soft Matter, 6(16), 3735-3742.

Phillips, G. O., & Williams, P. A. (2009). Handbook of Hydrocolloids: Elsevier.